

Supplementary Information

Discovery of the first genome-wide significant risk loci for attention-deficit/hyperactivity disorder

Table of Contents

Supplementary Methods and Results	4
Detailed description of individual samples	4
iPSYCH, Denmark.....	4
Samples from the Psychiatric Genomics Consortium (PGC)	6
Parent-offspring trio samples	6
CHOP, USA	6
IMAGE-I, Europe.....	6
PUWMa, USA	7
Toronto, Canada.....	8
Case-control samples	9
Barcelona, Spain.....	9
Beijing, China.....	9
Bergen, Norway.....	10
Cardiff, UK.....	10
Germany	11
IMAGE-II, Europe & USA	12
Yale-Penn, USA.....	13
Replication samples	14
DeCODE, ADHD diagnoses from medical records.....	14
23andMe, self-reported ADHD diagnoses	15
EAGLE, ADHD symptom scores.....	16
QIMR, ADHD rating scale	17
Bioinformatics pipeline for quality control and association analyses.....	18
Pre-imputation quality control	19
Genotype imputation.....	19
Relatedness and population stratification.....	19
GWAS and meta-analysis	21
Defining independent genome-wide significant loci.....	22
Evaluating putative secondary signals.....	23
Correlation of secondary signals with their respective lead index variants	23
Conditional association analysis	24
Bayesian credible set analysis	24
Credible set estimation method	24
Variants considered for credible set analysis	26
Credible set results in PGC and iPSYCH data.....	26
Functional annotation of variants in credible set	27
Gene-based association analysis	29
Exome-wide association of single genes with ADHD.....	29

Gene-wise association of candidate genes for ADHD	30
Gene-set analyses	30
Hypothesis free gene set analyses	30
<i>FOXP2</i> downstream target gene set analysis.....	31
Highly constrained gene set analysis.....	31
LD Score intercept evaluation	32
Genetic correlations between PGC and iPSYCH ADHD samples	33
Genetic correlation between PGC case-control and trio samples.....	33
Polygenic risk scores for ADHD	34
Polygenic risk score prediction in iPSYCH samples.....	34
Polygenic risk score prediction in PGC samples.....	36
Leave-one-out analysis across cohorts.....	37
SNP heritability	37
Partitioning heritability by functional annotation and cell type.....	38
Genetic correlations of ADHD with other traits	40
Replication analysis in external cohorts.....	40
Sign test.....	41
Replication of effect sizes for top loci	43
Genetic correlation analysis of replication cohorts.....	44
Meta-analysis and heterogeneity test with each replication cohort	46
Meta-analysis across replication cohorts	49
Winner's curse correction for effect sizes.....	49
Method for meta-analysis of continuous and dichotomous ADHD measures	50
Basic genetic model for latent-scale phenotypes	51
Defining independent genetic factors.....	52
Effects of individual variants.....	53
GWAS test statistics for β_j	55
Test of β_{ij} in GWAS of dichotomous Y_1	57
Test of β_{1j} in GWAS of continuous Y_2	59
Meta-analysis for β_{1j} from GWAS of dichotomous Y_1 and continuous Y_2	62
Notes on Implementation	63
Supplementary Tables.....	66
Supplementary Table 1. Samples included in the GWAS meta-analyses of diagnosed ADHD.....	66
Supplementary Table 2. Conditional Analysis of Secondary GWAS Signals.....	68
Supplementary Table 3. Heritability and genetic correlations for PGC ADHD samples.....	69
Supplementary Table 4. SNP heritability of ADHD.....	70
Supplementary Table 5. Genetic correlations of ADHD with other selected traits.....	70
Supplementary Table 6. Summary of Bayesian Credible Set Results	72
Supplementary Table 7. Biological function of potential ADHD risk genes located in genome-wide significantly associated loci.....	73
Supplementary Table 8. Results from MAGMA gene-based association with ADHD.....	78
Supplementary Table 9. Enrichment analysis of gene sets related to <i>FOXP2</i> downstream target genes	79
Supplementary Table 10. Enrichment analysis for a set of highly constrained genes.....	79
Supplementary Table 11. Results from MAGMA gene-based association of ADHD candidate genes.....	80
Supplementary Table 12. Sign test results for each replication cohort.....	80
Supplementary Table 13. Results for significant ADHD loci in each replication cohort	81
Supplementary Table 14. Comparison of profile of genetic correlations for the ADHD GWAS and 23andMe.....	82
Supplementary Figures	84
Supplementary Figure 1. Genotyping iPSYCH-ADHD sample, main steps and sample loss.....	84
Supplementary Figure 2. Q-Q plot from test for heterogeneity between Chinese and European ancestry cohorts in the ADHD GWAS meta-analysis.....	85
Supplementary Figure 3a1 – 3n1. Forest plots for index SNPs in gws loci	85

Supplementary Figure 3a2 – 3n2. Regional association plots for index SNPs in gws loci.....	86
Supplementary Figure 4. Manhattan plot from ADHD European GWAS meta-analysis.....	101
Supplementary Figure 5. Manhattan plot from test for heterogeneity between studies/waves in the ADHD GWAS meta-analysis	102
Supplementary Figure 6. Q-Q plot from test for heterogeneity between all samples/waves in the ADHD GWAS meta-analysis.....	103
Supplementary Figure 7. ADHD PRS stratified by case-control status and PGC study	104
Supplementary Figure 8. Odds ratios by PRS within deciles in target groups	105
Supplementary Figure 9. Odds ratios within target groups in iPSYCH	106
Supplementary Figure 10. PRS-based odds ratios within each study/wave.....	107
Supplementary Figure 11a – 11b. Q-Q plot from GWAS meta-analyses	108
Supplementary Figure 12. Partitioning of h^2 by functional annotations	110
Supplementary Figure 13. Partitioning of h^2 by tissue-group annotations.....	111
Supplementary Figure 14. Partitioning of h^2 by tissue-specific H3K4Me1 annotations	113
Supplementary Figure 15a – 15d. Gene-based association, regional association plots	114
Supplementary Figure 16. Comparison of estimated effect sizes from deCODE.....	117
Supplementary Figure 17. Comparison of estimated effect sizes from 23andMe.....	118
Supplementary Figure 18. Distribution of 1000 Genomes Phase 3 European LD Scores	119
Supplementary Figure 19. Shrinkage factor for \tilde{Z}_{2j} with varying I_j	120
Supplementary Figure 20. Relative effective sample size \tilde{N}_{2j} with varying I_j	121
Supplementary Figure 21. Manhattan plot of results from meta-analysis of ADHD+23andMe	122
Supplementary Figure 22. Manhattan plot of results from meta-analysis of ADHD+EAGLE/QIMR.....	123
Supplementary Figure 23. Q-Q plot from test for heterogeneity between ADHD GWAS meta-analysis and 23andMe	124
Supplementary Figure 24. Manhattan plot from test for heterogeneity between ADHD GWAS meta-analysis and 23andMe.....	125
Supplementary Figure 25. Q-Q plot from test for heterogeneity between ADHD GWAS meta-analysis and EAGLE/QIMR.....	126
Supplementary Figure 26. Manhattan plot from test for heterogeneity between ADHD GWAS meta-analysis and EAGLE/QIMR	127

References.....	128
------------------------	------------

Supplementary Note	138
---------------------------------	------------

Additional acknowledgements	138
-----------------------------------	-----

Supplementary Methods and Results

Detailed description of individual samples

iPSYCH, Denmark

A brief overview of the included samples can be found in Supplementary Table 1.

Since 1981 dried blood spot samples (Guthrie cards) from all newborn babies in Denmark have been stored in the Danish Newborn Screening Biobank (DNSB) at Statens Serum Institute (SSI). Samples from this nationwide biobank can be linked with the comprehensive Danish register system through the unique personal identification number (CPR-number), which is assigned to all live-born babies in Denmark. The CPR-number is stored in the Danish Civil Registration System (DCRS)¹ and is used in all contacts with the public sector, including all hospital contacts.

The iPSYCH-ADHD sample is a nationwide population based case-cohort sample selected from a baseline birth cohort comprising all singletons born in Denmark between May 1, 1981, and December 31, 2005, who were residents in Denmark on their first birthday and who have a known mother (N = 1,472,762). Cases were diagnosed by psychiatrists at in- or out-patient clinics, predominantly the latter according to ICD10 (F90.0 diagnosis code), identified using the Danish Psychiatric Central Research Register² (DPCRR). The DPCRR includes data on all people admitted to a psychiatric hospital for assessment, treatment, or both in Denmark since 1969 as well as people who attended psychiatric outpatient services since 1995. Diagnoses were given in 2013 or earlier for individuals at least 1 year old. Individuals with a diagnosis of moderate to severe mental retardation (ICD10 code F71-F79) were excluded. Controls were randomly selected from the same nationwide birth cohort and not diagnosed with ADHD (F90.0) or moderate-severe mental retardation (F71-F79). For both cases and controls all other comorbid diagnoses, except moderate-severe mental retardation, were allowed.

DNA was extracted from dried blood spot samples and whole genome amplified in triplicates as described previously^{3,4}. Genotyping was performed at the Broad Institute of Harvard and MIT (Cambridge, MA, USA) using Illumina's Beadarrays (PsychChip; Illumina, CA, San Diego, USA) according to the manufacturer's protocols. Genotypes were a result of merging callsets from three different calling algorithms (GenCall, Birdseed and Zcall). GenCall⁵ and Birdseed⁶ was used to call genotypes with minor allele frequency (MAF) > 0.01 and zCall⁷ was used to call genotypes with MAF < 0.01. The merging was done after pre-QC on individual call sets.

Processing of DNA, genotyping and genotype calling as well as imputing of genotypes of the iPSYCH-ADHD sample were carried out as a part of the genotyping of the full iPSYCH sample, which in total consists of around 79,492 individuals, including around 54,249 cases diagnosed with at least one of six mental disorders (schizophrenia, bipolar disorder, depression, ADHD, anorexia or autism spectrum disorder) and 26,248 randomly selected population controls (25,243 did not have any of the six psychiatric disorders investigated in iPSYCH). For the study of ADHD individuals with an ADHD diagnosis were exclude among the controls (N = 413). The data processing was done in 23 waves of approximately 3,500 individuals each. In order to control for potential batch effects, we included "wave" as a covariate in the regression models of all downstream analyses when relevant. Following genotyping all data processing, quality control, and downstream analyses were performed at secured servers in Denmark at the GenomeDK high performance-computing cluster (<http://genome.au.dk>). Overview of number samples in the iPSYCH study in the various steps, from identification in the registers to high quality genotypes included in the meta-analysis, can be found in Supplementary Figure 1.

The study was approved by the Danish Data Protection Agency and the Scientific Ethics Committee in Denmark.

Samples from the Psychiatric Genomics Consortium (PGC)

Parent-offspring trio samples

CHOP, USA

The CHOP (Children's Hospital of Philadelphia) ADHD trio sample (2,064 trios) were recruited from pediatric and behavioural health clinics in the Philadelphia area⁸ and included children aged 6–18 years from families of European with an ADHD diagnosis following the K-SADS (Schedule for Affective Disorders and Schizophrenia for School-Age Children; Epidemiologic Version) interview. Exclusion criteria were prematurity (<36 weeks), intellectual disability, major medical and neurological disorders, pervasive developmental disorder, psychoses and major mood disorders. Participants were assayed on the Illumina Infinium II HumanHap550 BeadChip (Illumina, San Diego, CA, USA) as previously described. The study was approved by The Children's Hospital of Philadelphia Institutional Review Board.

IMAGE-I, Europe

The IMAGE-I (International Multisite ADHD Genetics Project) trio samples^{9,10} were collected using a common protocol with centralized training and reliability testing of raters and centralized data management. Family members were Caucasians of European origin from countries in and around Europe including Belgium, Germany, Ireland, the Netherlands, Spain, Switzerland, and the United Kingdom, and Israel. At the IMAGE sites, parents of children were interviewed with the Parental Account of Childhood Symptom (PACS), a semi-structured, standardized, investigator-based interview developed as an instrument to provide an objective measure of child behaviour. Both parents and teachers completed the respective versions of the Conners ADHD rating scales and the Strengths and Difficulties Questionnaire (SDQ). Exclusion criteria were autism, epilepsy, IQ<70, brain disorders and any genetic or medical disorder associated with externalizing behaviours that

might mimic ADHD. Genotyping was conducted at Perlegen Sciences using their 600K genotyping platform, comprising approximately 600,000 tagging SNPs designed to be in high linkage disequilibrium with untyped SNPs for the three HapMap populations. The study was approved by the Institutional Review Board (IRB) or Ethical Committee at each site.

PUWMa, USA

The PUWMa (Pfizer-funded study from the University of California, Los Angeles (UCLA), Washington University, and Massachusetts General Hospital (MGH)) trio samples¹¹ were collected independently at those three sites using similar but slightly different methods.

309 families were recruited from clinics at MGH with children aged 6-17 years. Psychiatric assessments were made with the K-SADS-E. Exclusion criteria were major sensorimotor handicaps (deafness, blindness), psychosis/schizophrenia, autism, inadequate command of the English language, or a Full Scale IQ<80.

At Washington University, 272 families were selected from a population-representative sample identified through birth records of the state of Missouri, for a genetic epidemiologic study of the prevalence and heritability of ADHD. The original sample included 812 complete male and female twin pairs and six individual twins aged 7 to 19 years at the time of interview, identified from the Missouri Family Registry from 1996 to 2002. Families were invited into the study if at least one child exhibited three or more inattentive symptoms on a brief screening interview. Parents reported on their children and themselves, and the youths on themselves, using the Missouri Assessment of Genetics Interview for Children (MAGIC), a semi-structured psychiatric interview. DSM-IV diagnoses of ADHD were based upon parental reports (most of the time, maternal). Exclusion criteria were parent/guardian reported intellectual disability or if the parent/guardian and twins could not speak English.

At UCLA, 156 subjects were drawn from 540 children and adolescents aged 5 to 18 years and 519 of their parents ascertained from 370 families with ADHD-affected sibling pairs. Children and adolescents were assessed using the K-SADS-PL (Present and Lifetime version). Adult parents were assessed using the SADS-LA-IV (Lifetime version), supplemented with the K-SADS Behavioral Disorders module for diagnosis of ADHD and disruptive behavioural disorders. Direct interviews were supplemented with parent and teacher versions of the Swanson, Nolan, and Pelham, version IV (SNAP-IV) rating scale, as well as a parent-completed Childhood Behavior Checklist (CBCL) and Teacher Report Form (TRF). Exclusion criteria were neurological disorder, head injury resulting in concussion, lifetime diagnoses of schizophrenia or autism, or estimated Full Scale IQ<70. For all sites DNA was extracted from blood at each participating institution and Genizon BioSciences Inc. conducted genotyping with funding from Pfizer Inc. Genomic DNA samples from MGH and WASH-U were genotyped using the Illumina Human1M BeadChip (N = 1,057,265 SNPs), whereas the UCLA samples were genotyped using the Illumina Human 1M-Duo array (N = 1,151,846 SNPs). The study was approved by the subcommittee for human subjects of each site.

Toronto, Canada

The Canadian ADHD trio sample¹² was drawn from an outpatient clinic in an urban pediatric hospital and included children aged 6-16 years who were referred for attention, learning and/or behavioural problems. ADHD diagnostic data was obtained from parents and teachers in semi-structured clinical interviews including the Parent Interview for Child Symptoms (PICS) and the Teacher Telephone Interview (TTI). Exclusion criteria were an IQ<80 on both the verbal and the performance subscales of the Wechsler Intelligence Scale for Children (WISC). Samples were genotyped on the Affymetrix Genome-Wide Human SNP Array 6.0 with standard protocols as provided by the manufacturer. The study was approved by the Research Ethics Board of the Hospital for Sick Children, Toronto.

Case-control samples

Barcelona, Spain

The Barcelona sample¹³ comprised 607 ADHD cases. All patients were adults of Caucasian origin, recruited and evaluated at the Hospital Universitari Vall d'Hebron located in Barcelona (Spain). ADHD diagnostic criteria was assessed using the Structured Clinical Interview for DSM-IV and the Conner's Adult ADHD Diagnostic Interview for DSM-IV (CAADID). Impairment was measured with the Clinical Global Impression (CGI), included in the CAADID Part II, and the Sheehan Disability Inventory (SDI). Exclusion criteria were IQ<70, schizophrenia or other psychotic disorders, ADHD symptoms due to mood, anxiety, dissociative or personality disorders, adoption, sexual or physical abuse, birth weight <1.5 kg, and other neurological or systemic disorders that might explain ADHD symptoms. The control sample consisted of 584 unrelated blood donors frequency-matched for gender with the ADHD cases and screened to exclude those with lifetime ADHD symptoms or diagnosis.

Both cases and controls were genotyped on the Illumina HumanOmni1-Quad BeadChip platform. The study was approved by the relevant ethics committee.

Beijing, China

The Beijing, China sample¹⁴ comprised 1,040 ADHD cases aged between 6-16 years of Han Chinese decent. Cases were recruited from the Child and Adolescent Psychiatric Outpatient Department of the Sixth Hospital, Peking University. Clinical diagnoses from a senior child and adolescent psychiatrist were confirmed using the Chinese version of the Clinical Diagnostic Interview Scale. Exclusion criteria were those with major neurological disorders (e.g. epilepsy), schizophrenia, pervasive development disorder, and IQ<70. The 963 control individuals were students from local elementary schools, healthy blood donors from the Blood Center of the First Hospital, Peking University, and healthy volunteers from the institute of Han Chinese decent, screened using the

ADHD Rating Scale-IV (ADHD RS-IV) to exclude ADHD. Additional exclusion criteria were major psychiatric disorders, family history of psychosis, severe physical diseases, and substance abuse.

Both cases and controls were genotyped using the Affymetrix6.0 array at CapitalBio Ltd., Beijing, using the standard Affymetrix protocol.

The study was approved by the Institutional Review Board of the Peking University Health Science Center.

Bergen, Norway

The Bergen, Norway sample¹⁵ consisted of 300 adults with ADHD. Patients recruited through a Norwegian national medical registry, as well as by psychologists and psychiatrists working at out-patient clinics. Information regarding ADHD was obtained following systematic assessment of ADHD diagnostic criteria, developmental history, physical examination, evaluation of comorbidity, and, where possible, information from collateral informants. All gathered information was then sent to one of the expert committees for a definitive diagnostic assessment. There were no formal exclusion criteria. The 205 controls were recruited through the Medical Birth Registry of Norway above the age of 18 years with no known intellectual disability. Cases and controls were genotyped using the Human OmniExpress-12v1-1_B (Illumina, San Diego, CA, USA) platform. Genotyping was performed according to the standard Illumina protocol at Decode facility (Reykjavik, Iceland). The study was approved by the Norwegian Regional Medical Research Ethics Committee West (IRB #3 FWA00009490, IRB00001872).

Cardiff, UK

The Cardiff sample¹⁶ consisted of 727 Caucasian children aged 5-18 years old from Cardiff, Wales (N=510); St. Andrews, Scotland (N=35); and Dublin, Ireland (N=182). All children were recruited from community clinics and were assessed for ADHD using the Child and Adolescent Psychiatric Assessment (CAPA) Parent Version, a semi-structured research diagnostic interview, to assess

psychiatric diagnoses. Pervasiveness of ADHD symptoms (in school) was assessed using the Child ADHD Teacher Telephone Interview or the Conners Teacher Questionnaire. Exclusion criteria were intellectual disability (IQ <70), a major medical or neurological condition (e.g. epilepsy), autistic spectrum disorder, Tourette's syndrome, bipolar disorder, or known chromosomal abnormality. Control participants were obtained from the Wellcome Trust Case Control Consortium–Phase 2. They comprised 3,000 individuals born in the United Kingdom during 1 week in 1958 (the 1958 British Birth Cohort) and 3,000 individuals from the U.K. Blood Services collection (N=5,081 passed QC). The comparison subjects were not screened for psychiatric disorders. ADHD case subjects were genotyped on the Illumina (San Diego) Human660W-Quad BeadChip according to the manufacturer's instructions. Comparison subjects were genotyped by Wellcome Trust Case Control Consortium–Phase2 using the Illumina Human 1.2M BeadChip. The study was approved by the local research ethics committees at each site.

Germany

The German sample¹⁷ comprised 495 patients with ADHD (aged 6–18 years) recruited and phenotypically characterized in six psychiatric outpatient units for children and adolescents (Aachen, Cologne, Essen, Marburg, Regensburg, and Wurzburg). ADHD was assessed using the K-SADS-PL and a German teacher rating scale for ADHD (FBB-HKS). Exclusion criteria were IQ \leq 75, potentially confounding psychiatric diagnoses such as schizophrenia, any pervasive developmental disorder, Tourette's disorder, and primary mood or anxiety disorder, neurological disorders such as epilepsy, a history of any acquired brain damage or evidence of the fetal alcohol syndrome, very preterm birth and/or (f) maternal reports of severe prenatal, perinatal or postnatal complications. The 1,300 adult controls were drawn from three population based epidemiological studies: (a) the Heinz Nixdorf Recall (Risk Factors, Evaluation of Coronary Calcification, and Lifestyle) study 3, (b) PopGen, (c) KORA (Cooperative Health Research in the Region of Augsburg). Ethnicity was assigned to patients

and controls according to self-reported ancestry (all German). The genome-wide genotyping was performed on HumanHap550v3 (Illumina; controls) and Human660W-Quadv1 BeadArrays (Illumina; cases). The study was approved by the ethics committees of all participating hospitals.

IMAGE-II, Europe & USA

The IMAGE-II ADHD case samples¹⁸ included some samples from the original IMAGE project (see IMAGE-I details above) along with samples provided by colleagues at other sites (Cardiff; St. Andrews, Dublin; MGH; Germany; and the Netherlands), using similar but not identical methods. Samples from Dublin and MGH followed the procedures described above for Cardiff and PUWMA, respectively. Case collection for the German and Dutch sites are described below.

In Germany, 351 participants were recruited in order of clinical referral in the outpatient clinics in Wurzburg, Hamburg and Trier. Families were of German, Caucasian ancestry. All children were assessed by full semi-structured interview (Kiddie-Sads-PL-German Version or Kinder-DIPS) and parent and teacher ADHD DSM-IV based rating scales to ensure pervasiveness of symptoms. Exclusion criteria were IQ<80, comorbid autistic disorders or somatic disorders (hyperthyroidism, epilepsy, neurological diseases, severe head trauma etc.), primary affective disorders, Tourette's syndrome, psychotic disorders or other severe primary psychiatric disorders, and birth weight <2000 grams.

At the Dutch site, assessment data are available for 112 subjects aged 3-18 years with DSM-IV ADHD. Most of the sample was collected as part of a sib pair genome-wide linkage study in ADHD¹⁹. Subjects were assessed using the DSM-IV version of the Diagnostic Interview Schedule for Children (DISC-P) with both parents, supplemented by Conners Questionnaires (old versions), the CBCL and TRF. Exclusion criteria were autism, epilepsy, IQ <70, brain disorder, and any genetic or medical disorder associated with externalizing behaviours that might mimic ADHD.

Control samples (1,755 population controls of European ancestry) were assembled from an IRB approved genome-wide association study (GWAS) of myocardial infarction²⁰. Controls were collected from multiple sites in the US and Europe, including Seattle, Washington; Boston, Massachusetts; Gerona, Spain; Malmö, Sweden; and the United Kingdom. Sampling procedures for each cohort have been described previously²⁰. Control participants from the Wellcome Trust Case Control Consortium overlapping with the Cardiff, UK sample (described above) were removed. Cases were genotyped using the Affymetrix 5.0 array at the State University of New York Upstate Medical University, Syracuse using the standard protocol issued by Affymetrix. Controls were genotyped using the Affymetrix 6.0 array. The study was approved by the Institutional Review Board (IRB) or Ethical Committee at each site.

Yale-Penn, USA

The Yale-Penn sample consists of small nuclear families and unrelated individuals (2,020 individuals in 850 families and 6,951 unrelated individuals), collected to study the genetics of substance dependence²¹⁻²³. The case-control subjects were recruited from 2000 to 2013 from substance abuse treatment centers and through advertisements at the University of Connecticut Health Center, Yale University School of Medicine, the Medical University of South Carolina, the University of Pennsylvania, and McLean Hospital. The participants were identified through a family-based and a case-control protocol. Families were ascertained from treatment centers and advertisements that recruited affected sibling pairs (ASPs) meeting Diagnostic and Statistical Manual of Mental Disorders, 4th Edition (DSM-IV) criteria for cocaine or opioid dependence. Other family members of the ASPs were recruited when available, regardless of affection status and unaffected family members were included within the control subjects.

For this study, 182 individuals with ADHD and 1,315 unrelated controls of European ancestry were included. Unrelated individuals with ADHD and controls were selected from the family-based

protocol, with a focus on maximizing the number of ADHD cases retained for the analysis. *DSM-IV* diagnoses of ADHD case status, as well as other major psychiatric traits, were derived from the Semi-Structured Assessment for Drug Dependence and Alcoholism for all participants. Exclusion criteria were a clinical diagnosis of a major psychotic illness (for example, schizophrenia or schizoaffective disorder).

The sample was genotyped using one of two genotyping arrays: (1) the Illumina HumanOmni1-Quad v1.0 microarray containing 988,306 autosomal SNPs (Yale- Penn.1: performed at the Center for Inherited Disease Research (CIDR) and the Yale Center for Genome Analysis), (2) the Illumina Infinium Human Core Exome microarray (Yale-Penn.2 and Yale-Penn.3: performed at the Yale Center for Genome Analysis). The study was approved by the relevant institutional review boards.

Replication samples

DeCODE, ADHD diagnoses from medical records

The Icelandic ADHD cohort ($N = 5,085$) consists of individuals who either have a clinical ADHD diagnosis (mostly ICD10-F90) or who have been prescribed medication specific for ADHD symptoms (ATC-NA06BA, mostly methylphenidate). The Icelandic control individuals ($N = 131,122$) does not contain individuals with a diagnosis of schizophrenia, bipolar disorder, autism spectrum disorder or self-reported ADHD symptoms or diagnosis. All individuals used in the analysis have been chip genotyped, long range phased and genotypes imputed based on the Icelandic dataset as described previously²⁴.

GWAS in the Icelandic sample was performed for top loci with $P < 1 \times 10^{-5}$ (clumped variants with $r^2 < 0.25$) in the primary ADHD GWAS. Results from the Icelandic cohort were matched to the PGC and iPSYCH results based on rs-id and alleles. After filtering, results were available for 123 variants in the Icelandic sample from deCODE Genetics.

23andMe, self-reported ADHD diagnoses

The 23andMe sample consists of individuals who sent saliva samples (using the Oragene kit) to the genetic testing company 23andMe, Inc. and agreed to take part in research and answered questions about their ADHD history as part of a longer survey. All participants provided informed consent and answered surveys online according to 23andMe's human subjects protocol, which was reviewed and approved by Ethical & Independent Review Services, an AAHRPP-accredited institutional review board. As part of the "Your Medical History" survey, they were asked: "Have you ever been diagnosed by a doctor with any of the following psychiatric conditions: Attention deficit disorder (ADD) or Attention deficit hyperactivity disorder (ADHD)?" The response options were: "Yes", "No", "I don't know". A second question asked independently as a "Research Snippet" was: "Have you ever been diagnosed with attention deficit disorder (ADD) or attention deficit hyperactive disorder (ADHD)?" with the response options: "Yes", "No", "I'm not sure". Individuals who gave a positive response to these questions were classed as ADHD cases and controls were those who gave a negative response to these questions. Individuals with discordant responses were excluded.

Research participants were genotyped either on the Illumina HumanHap550k (13,030 controls, 840 cases) or HumanOmniExpress (57,363 controls, 5,017 cases) genotyping platforms by 23andMe. GWAS and imputation were performed separately for data generated by the two platforms. Within each platform, batches of 8,000-9,000 participants were imputed. Results were filtered for average and minimum imputation r^2 to exclude SNPs that showed batch effects. Covariates included in the GWAS by 23andMe were age, sex and the first four principal components to account for population stratification.

For the current study, the GWAS summary statistics were then aligned to the genotyped samples. The 23andMe summary statistics were verified to be consistent with genome build hg19. They were then

matched to the genotype data based on rsid, chromosome and base pair position. For SNPs, reported alleles were required to match the genotype data without a strand flip. For indels and multiallelic variants, alleles reported by 23andMe were evaluated heuristically for consistency with the genotype data and the alleles were matched accordingly (e.g. “I” or “D” alleles reported by 23andMe for indels were matched to the corresponding sequence of alleles for the insertion or deletion included in the genotype data). After alignment, the 23andMe GWAS results for the two platforms were combined in an inverse standard error-weighted meta-analysis to create a single 23andMe results set for use in the replication analyses. In total, 11,198,253 variants were matched from the 23andMe meta-analysis for inclusion in replication analyses.

EAGLE, ADHD symptom scores

The EARly Genetics and Lifecourse Epidemiology (EAGLE) consortium includes population-based birth cohorts from Europe, Australia, and the United States (<http://www.wikigenes.org/e/art/e/348.html>). The consortium focuses on a wide range of phenotypes in childhood including traits related to cognition and behaviour e.g. aggression²⁵, asthma allergy and atopy²⁶ and postnatal growth²⁷. In the study of ADHD symptoms, nine EAGLE cohorts were included with available ADHD symptom scores in childhood (age at measurement <13 years). An overview of the nine cohorts included in the EAGLE meta-analysis is provided in Middeldorp et al.²⁸. In order to assess ADHD symptoms different instruments were used across cohorts, including the Attention Problems scale of the Child Behavior Checklist (CBCL) and the Teacher Report Form (TRF), the Hyperactivity scale of the Strengths and Difficulties Questionnaire (SDQ), and the *DSM-IV* ADHD items as, for example, included in the Conners Rating Scale. For the meta-analysis, one phenotype was selected from each cohort. Based on the phenotype that was most available, school-age ratings were chosen over preschool-age ratings, parent ratings over teacher ratings, and the

measurement instrument with the largest information density was preferred over the other instruments²⁸.

Each of the included cohorts went through their own optimal pre-imputation QC and imputation was done using the March 2012 release of the Genomes Project (phase 1)²⁹. Detailed description of QC, imputation and the analysis procedures for the different cohorts can be found in Middeldorp et al.²⁸. Association analyses were done using linear regression and relevant principal components and subsequently meta-analysed using METAL³⁰. Summary statistics from the meta-analysis of N=17,666 individuals were provided for inclusion in the current study. These results were meta-analysed with results from QIMR as described below for inclusion in the replication analysis.

QIMR, ADHD rating scale

The QIMR (Queensland Institute of Medical Research) sample is drawn from the Brisbane Longitudinal Adolescent Twin Study which between 1992 and 2013 continuously recruited 12-year-old twins and their non-twin siblings from the greater Brisbane region³¹. Participants were recruited by contacting the principals of primary and secondary schools in the greater Brisbane area, media appeals and by word of mouth. It is estimated that approximately 50% of the eligible birth cohort were recruited into the study. The study used a longitudinal design in which participants were followed up at 14 and 16 years of age. In 2009 and 2015 additional cross-sectional follow-ups were conducted with participants over the ages of 19 and 25 respectively.

The phenotypic data used in the current analyses are maternal reports of ADHD symptoms for 2,798 individuals collected using the SWAN questionnaire³² which was introduced to the study protocol in 2010 and was completed during the first clinic visit after this date. The parents of participants who were over 14 years of age when the scale was added to the study were asked to complete the SWAN scale by online questionnaire in 2010.

Participants were genotyped using the Illumina Human610Quad BeadChip (Illumina, San Diego, CA, USA) as previously described. Genotypes were imputed to the 1000 genome references (Phase 3 Release 5) using the University of Michigan Imputation Server³³. Genome-wide association analysis was conducted in RAREMETALWORKER (<http://genome.sph.umich.edu/wiki/RAREMETALWORKER>) to correct for relatedness and included age, sex and ancestry PCs as covariates. The results of an earlier GWAS on a subset of 1,851 individuals were previously described by Ebejer et al.³⁴. Ethical approval for the study was obtained from the QIMR Human Research Ethics Committee.

For the current study, summary statistics from the EAGLE and QIMR meta-analyses were aligned to the genotyped ADHD samples based on rsid and chromosome and base pair location. SNP alleles were required to be concordant without a strand flip. Indels and multiallelic variants with inconclusive matching to the ADHD GWAS were also excluded. After alignment and filtering for allele frequency and imputation quality, the EAGLE and QIMR results for 6,312,392 variants were meta-analysed to get a single genome-wide meta-analysis of ADHD-related behavioural traits. We denote this meta-analysis as EAGLE/QIMR, and focus on it for replication analyses.

Bioinformatics pipeline for quality control and association analyses

Quality control, imputation and primary association analyses were done using the bioinformatics pipeline “Ricopili”, which has been developed by the Psychiatric Genomics Consortium (PGC) Statistical Analysis Group³⁵. The pipeline generates high quality imputed data and performs GWAS and meta-analysis of large genetic data sets. In order to avoid potential study and “wave” effects the eleven PGC samples were processed separately and the iPSYCH sample was processed in 23 separate batches referred to as waves (see sample description above) unless otherwise is stated.

Pre-imputation quality control

Subjects and SNPs were included in the analyses based on the following quality control parameters: SNP call rate > 0.95 (before sample removal), subject call rate > 0.98 (> 0.95 for the iPSYCH samples), autosomal heterozygosity deviation ($| F_{het} | < 0.2$), SNP call rate > 0.98 (after sample removal), difference in SNP missingness between cases and controls < 0.02 , and SNP Hardy-Weinberg equilibrium (HWE) ($P > 10^{-6}$ in controls or $P > 10^{-10}$ in cases).

Genotype imputation

In order to obtain information about non-genotyped markers, we used the pre-phasing software SHAPEIT³⁶ to estimate haplotypes and subsequently IMPUTE2³⁷ for imputing genotypes. Imputing was done in chunks of 3 Mb using default parameters. The imputation reference data consisted of 2,504 phased haplotypes from the 1000 Genomes Project, phase 3 (1KGP3)^{38,39} data (October 2014, 81,706,022 variants, release 20130502). Trio imputation was done with a case-pseudocontrol setup, where a pseudocontrol was defined to each affected offspring using the non-transmitted alleles from the two parents (estimated based on the haplotypes of the parents).

Relatedness and population stratification

Relatedness and population stratification were evaluated using a set of high quality markers (genotyped autosomal markers with minor allele frequency (MAF) > 0.05 , HWE $p > 1 \times 10^{-4}$ and SNP call rate > 0.98), which were pruned for linkage disequilibrium (LD) resulting in a set of ~30,000 pruned markers (markers located in long range LD regions defined by Price et al.⁴⁰ were excluded). This was done separately for each of the PGC samples and on a merged set of genotypes from the 23 iPSYCH waves. In order to identify related individuals an identity by state analysis were performed

using PLINK v1.9^{41,42}, and one individual was excluded in pairs of subjects with $\hat{\pi} > 0.2$ (cases preferred kept over controls).

In order to identify genetic outliers, a principal component analysis (PCA) was performed using smartPCA incorporated in the software Eigensoft⁴³, and the same set of pruned autosomal markers as described above. For the iPSYCH sample a genetic homogenous sample was defined based on a subsample of individuals being Danes for three generations. This subsample was defined using register information about birth country of the individuals, their parents and grandparents, which was required to be Denmark in order to be included in the subsample. The subsample of Danes was used in order to define the center of an ellipsoid based on the mean values of principal component (PC) 1 and PC2. Subsequently PC1 and PC2 for all individuals in the iPSYCH sample were used to define a genetic homogenous population by excluding individuals with PC values greater than six standard deviations from the mean. For the PGC samples genetic outliers were removed based on visual inspection of the first six PCs. PCA including samples from the 1000 Genomes Project was also performed to confirm that the selected individuals matched the ancestry of European reference populations.

PCA was redone after exclusion of genetic outliers. The first 20 principal components were tested for association with the phenotype using logistic regression and their impact on the genome-wide test statistics were evaluated using λ . In the iPSYCH GWAS PC1-4 and significant PCs were included as covariates. For PGC samples, the number of PCs was adjusted based on the cohort's sample size in order to avoid overfitting and to reflect the differential power to capture true population structure by PCA. Specifically, the first five principal components were included as covariates for samples with fewer than 1000 individuals, and the first ten PCs were included for larger samples. Trio samples did not include PCs in the analysis unless strong population structure was evident (i.e. PUWMa). Where

necessary, study specific design covariates were also included (e.g. indicators variables for IMAGE-I sampling centres, alcohol dependence diagnosis for ascertainment in Yale-Penn).

GWAS and meta-analysis

Association analyses using the imputed marker dosages were performed separately for the 11 PGC samples and the 23 waves in iPSYCH by an additive logistic regression model using PLINK v1.9^{41,42}, with the derived principal components and necessary design factors included as covariates as described above (Supplementary Table 1). Adding sex as a covariate to the PGC and iPSYCH samples does not meaningfully alter the meta-analysis results (data not shown).

The meta-analysis included summary statistics from GWASs of the 23 waves in iPSYCH and 11 PGC samples, in total containing 20,183 cases and 35,191 controls. No individual genotypes were used for the meta-analysis. Only SNPs with imputation quality (INFO score) > 0.8 and MAF > 0.01 were included in the meta-analysis. Meta-analysis was performed using an inverse-weighted fixed effects model implemented in the software METAL (<http://csg.sph.umich.edu/abecasis/Metal/>)³⁰. Finally we filtered the GWAS meta-analysis, so only markers which were supported by an effective sample size ($N_{\text{eff}} = 4/(1/N_{\text{cases}} + 1/N_{\text{controls}})$)⁴⁴ greater than 70% were included (8,047,421 markers).

In some of the secondary analyses (e.g. when using LD score regression⁴⁵ and MAGMA⁴⁶ (see below)), information about LD structure in a reference genome reflecting the ancestry of the analysed population is used. Such analyses therefore require results from a GWAS meta-analysis based on a genetic homogenous group reflecting the same ancestry. We therefore performed a GWAS of the iPSYCH samples and the PGC samples with European ancestry (subsequently referred to as European GWAS meta-analysis). In this GWAS meta-analysis the Chinese PGC sample was excluded and the PUWMa sample was replaced with the PUWMa (strict) sample, in which individuals with non-

European genetic ancestry were excluded, resulting in 19,099 cases and 34,194 controls with European ancestry.

The GWAS meta-analysis identified 12 independent genome-wide significant (gws) loci (see Manhattan plot [Figure 1], forest plots [Supplementary Figure 3a1 – 3n1] and regional association plots [Supplementary Figure 3a2 – 3n2]). Independent loci were defined as described below. A more detailed description of potential risk genes located in the identified gws loci can be found in Supplementary Table 7.

In the European GWAS meta-analysis the number of independent gws loci decreased to 11. The gws locus on chromosome 2 (located in *SPAG16*) in the GWAS meta-analysis did not pass the significance threshold when only including individuals with European ancestry (see Manhattan plot, Supplementary Figure 4).

In addition, heterogeneity across studies/waves were tested with the Cochran's Q test and quantified with the I^2 heterogeneity index. No markers demonstrated significant heterogeneity between all cohorts (Supplementary Figures 5 and 6) or between the Chinese and European ancestry cohorts (Supplementary Figure 2).

Defining independent genome-wide significant loci

303 variants reached genome-wide significance ($P < 5 \times 10^{-8}$) in the meta-analysis. We then identified independent loci from these markers based on LD clumping (--clump in PLINK 1.9^{41,42}). Beginning with the most significantly associated variant as the first index variant, we labelled variants as being part of the same locus if they were within 500 kb and correlated with an index variant ($r^2 > 0.2$). Variants not within 500 kb and not correlated with an existing index variant were labelled as a new index variant. Correlations were estimated from European-ancestry populations in the 1000 Genomes

Phase 3 reference panel³⁹. Clumping continued until all variants with $P < 5 \times 10^{-8}$ were either labelled as an index variant or assigned to a locus.

A gws locus was then defined as the physical region containing the identified LD independent index variants and their correlated variants ($r^2 > 0.6$) with $P < 0.001$. Associated loci located less than 400 kb apart were merged. The same process was applied to define independent genome-wide significant loci in subsequent meta-analyses.

Evaluating putative secondary signals

Correlation of secondary signals with their respective lead index variants

Two of the genome-wide significant loci defined by this process in the ADHD meta-analysis include more than one index variant (Supplementary Table 2). In other words, they contain two genome-wide significant variants that are within 500 kb but are not correlated ($r^2 < 0.1$). In this case, we label the less significantly associated index variant as a putative secondary signal and perform additional analyses to evaluate whether the second index variant can be confirmed as independent.

First, we confirmed that the putative secondary signals are not strongly correlated with their respective lead index variants in the current genotype data. The correlation with the index variant was evaluated in (1) imputed best-guess genotype data (hard-called genotypes derived from imputed genotype probabilities, for all variants with an imputation info score > 0.8) from the 11 PGC cohorts, and (2) imputed best-guess genotype data from iPSYCH. For both putative secondary effects, the correlation between the index variant and secondary effect is ($r^2 < 0.1$) in both the PGC and iPSYCH imputed genotype data (Supplementary Table 2). This confirms that the putative secondary signal does not reflect LD structure in the ADHD cohorts that is not well captured by the 1000 Genomes Phase 3 European reference panel³⁹.

Conditional association analysis

The two putative secondary signals were then evaluated by considering analysis conditional on the lead index variant in each locus. In each cohort, logistic regression was performed with the imputed genotype dosage for the lead index variant included as a covariate. All covariates from the primary GWAS (e.g. principal components, site indicators) were also included. The conditional association results were then combined in an inverse-variance weighted meta-analysis.

Neither of the putative secondary signals achieve genome-wide significance in the conditional association analysis (Supplementary Table 2). The decreased significance observed in the conditional analysis reflects modestly attenuated estimates of the odds ratio and increased standard errors compared to the marginal association analysis in the primary GWAS.

Based on the non-significant results for the putative secondary variants in the conditional analyses, we conclude that there is not yet sufficient evidence to confidently label these as independent effects in their respective loci.

Bayesian credible set analysis

In order to refine the genome-wide significant loci, we defined a credible set of variants in each locus using the method described by Maller et al.⁴⁷. Under the assumption that (a) there is one causal variant in each locus, and (b) the causal variant is observed in the genotype data, the credible set can be considered to have a 99% probability of containing the causal variant.

Credible set estimation method

We summarize the method here following the description of Gormley et al.⁴⁸. Briefly, let D be the data including the genotype matrix X with P variants and the vector Y of phenotypes, and let β be the regression model parameters. Define P models A_j where variant j is causal and the remaining

variants are not causal, and define the null model A_0 where no variants are causal. Then by Bayes' rule the probability of model A_j is:

$$\Pr(A_j|D) = \int \Pr(D, \beta|A_j) \cdot \frac{\Pr(A_j)}{\Pr(D)} \cdot d\beta$$

Assuming a flat prior for the model parameters β , the integral can be approximated using the maximum likelihood estimates $\widehat{\beta}_j$, such that

$$\Pr(A_j|D) \approx \Pr(D|A_j, \widehat{\beta}_j) \cdot N^{-\frac{|\beta_j|}{2}} \cdot \frac{\Pr(A_j)}{\Pr(D)}$$

where N is the sample size and $|\beta_j|$ denotes the number of fitted parameters for model A_j . Given the assumption of one causal variant per locus, $|\beta_j|$ is a constant for all A_j . Next, note that the conventional likelihood ratio test of model A_j compared to the null model A_0 is defined as

$$\chi_j^2 \equiv -2 \log \frac{\Pr(D|A_0, \widehat{\beta}_0)}{\Pr(D|A_j, \widehat{\beta}_j)}.$$

Thus by substitution,

$$\Pr(A_j|D) \approx \exp\left(\frac{\chi_j^2}{2}\right) \cdot l_0 \cdot N^{-\frac{|\beta_j|}{2}} \cdot \frac{\Pr(A_j)}{\Pr(D)}$$

with $l_0 = \Pr(D|A_0, \widehat{\beta}_0)$. Given a flat prior for models A_j the latter terms are constant, leaving

$$\Pr(A_j|D) \propto \exp\left(\frac{\chi_j^2}{2}\right).$$

Normalizing across all possible models A_j thus yields

$$\Pr(A_j) \equiv \Pr(A_j|D) / \sum_k \Pr(A_k|D).$$

Finally, the 99% credible set of variants is defined as the smallest set S of models such that

$$\sum_{A_j \in S} \Pr(A_j) \geq .99.$$

If the model assumptions are correctly specified, then this credible set S has a 99% probability of containing the true causal variant.

We implemented this approach using the published R script freely available online

(<https://github.com/hailianghuang/FM-summary>).

Variants considered for credible set analysis

We applied the Bayesian credible set analysis to each of the 12 genome-wide significant loci identified in the primary meta-analysis of ADHD as described above. For each locus, variants within 1MB and in linkage disequilibrium (LD) with correlation $r^2 > 0.4$ to the index variant were considered for inclusion in the credible set.

Because the credible set estimation is conditioned on LD structure, we performed the credible set analysis using the European GWAS meta-analysis to ensure consistent LD structure in the analysed cohorts. Credible sets were also estimated based on both (a) the observed LD in European ancestry PGC datasets, and (b) the observed LD in the iPSYCH dataset.

Observed LD with the index variant in each locus was computed using imputed best-guess genotype data (generated as described previously) with PLINK 1.9 (<https://www.cog-genomics.org/plink2>)⁴².

For the European ancestry PGC datasets, imputed genotype data was merged across cohorts prior to computed LD. For the iPSYCH dataset, imputed genotyped data for the 23 genotyping waves were similarly merged before computing LD.

Credible set results in PGC and iPSYCH data

Bayesian credible sets for each of the 12 genome-wide significant loci are reported in Supplementary Data 2 (A-L). For the majority of the loci (7 of 12), there is no difference between the credible set results based on LD structure in the PGC datasets versus LD from the iPSYCH dataset (Supplementary Table 6). Differences between the credible sets for the remaining loci are modest,

with no more than six non-overlapping variants between the two sets for each locus. The non-overlapping variants also tend to have weak evidence for inclusion in the 99% credible set; of the 19 non-overlapping variants, only six would be included in an 90% credible set (i.e. the smallest set of variants with an 90% probability of containing the true causal variant under the Bayesian model), and only one would be included in an 80% credible set. To be conservative, we define the final credible set as the union of the credible sets estimated from the PGC and iPSYCH LD structure.

Functional annotation of variants in credible set

To evaluate the potential impact of the variants in the credible set for each locus, we consider annotations of predicted functional consequences for those variants based on external reference data.

In particular we evaluate:

- **Functional consequences:** Coding and regulatory consequences of each variant were annotated using the Ensembl Variant Effect Predictor (VEP⁴⁹) for genome build GRCh37 (hg19). Annotated consequences for transcripts without a HGNC gene symbol (e.g. clone-based vega genes) were excluded. Gene names were updated to the current HGNC gene symbol where applicable. For each variant, we summarize (a) annotated genes, excluding “upstream” and “downstream” annotations; (b) genes with an annotated consequence (i.e. excluding intronic annotations); and (c) annotated regulatory regions.
- **Transcription start site (TSS):** We annotate variants within 2kb upstream of the TSS of at least one gene isoform based on Gencode v19⁵⁰.
- **Hi-C interactions:** Variants annotated as physically interacting with a given gene were identified based on Hi-C data from samples of developing human cerebral cortex during neurogenesis and migration⁵¹. Annotations are considered for both the germinal zone (GZ),

primarily consisting of actively dividing neural progenitors, and the cortical and subcortical plate (CP), primarily consisting of post-mitotic neurons.

- Expression quantitative trait loci (eQTLs): SNPs associated with gene expression were annotated using FUMA (<http://fuma.ctglab.nl/>). Annotated eQTLs were identified from GTEx v6⁵² and BIOS⁵³, and filtered for false discovery rate (FDR) $< 1 \times 10^{-3}$ within each dataset. Annotations were updated to current HGNC gene symbols where applicable. For variants with multiple eQTL associations, we summarize the strongest eQTL association (i.e. the association with the lowest P-value) from each dataset.
- Chromatin state: Chromatin states for each variant were annotated based on the 15-state chromHMM analysis of epigenomics data from Roadmap⁵⁴. For each SNP, the most common chromatin state across 127 cell types was annotated using FUMA (<http://fuma.ctglab.nl/>). For all variants, we also annotate the predicted chromatin state in fetal brain. The 15 states are summarized to annotations of active chromatin marks (i.e. Active TSS, Flanking Active TSS, Flanking Transcription, Strong Transcription, Weak Transcription, Genic Enhancer, Enhancer, or Zinc Finger [ZNF] gene), repressive chromatin marks (Heterochromatin, Bivalent TSS, Flanking Bivalent TSS, Bivalent Enhancer, Repressed Polycomb, or Weak Repressed Polycomb), or quiescent.
- CADD: Combined Annotation Dependent Depletion (CADD v1.3⁵⁵) scores were annotated for each SNP using FUMA (<http://fuma.ctglab.nl/>).

Supplementary Data 3 summarizes the observed annotations for the credible set at each locus (see also Supplementary Data 4 for variant-level annotations).

Gene-based association analysis

Exome-wide association of single genes with ADHD

Gene-based association with ADHD was estimated by MAGMA 1.05⁴⁶ using the summary statistics from the European GWAS meta-analysis ($N_{\text{cases}} = 19,099$; $N_{\text{controls}} = 34,194$; Supplementary Table 1). We annotated SNPs to genes within their transcribed regions using the NCBI 37.3 gene definitions provided with MAGMA. We then calculated gene P-values using the SNP-wise mean model in which the sum of $-\log(\text{SNP P-value})$ is used as a test statistic. The gene P-value was calculated using a known approximation of the sampling distribution⁵⁶. MAGMA accounts for gene-size, number of SNPs in a gene and LD between markers. When using summary statistics in estimating gene-based P-values, MAGMA corrects for LD based on estimates from reference data with similar ancestry; for this we used the 1KGP3, European ancestry samples, as the reference³⁹.

In total 20 genes demonstrated significant gene-wise association with ADHD after Bonferroni correction (correction for 17,877 genes; Supplementary Table 8). 11 genes were located in the complex region on chromosome 1 demonstrating strong gws association with ADHD in the single marker GWAS meta-analysis (see regional association plot for this region, Supplementary Figure 3a2). Additional five genes overlapped with loci with gws single markers (*MEF2C*, *FOXP2*, *SORCS3*, *DUSP6* and *SEMA6D*). Four genes (*MANBA*, *CUBN*, *PIDDI*, *CDH8*) not located in single marker gws loci showed significant association (Supplementary Table 8). The LD region around three of the genes (*MANBA*, *CUBN*, *CDH8*) contains only the respective genes, indicating that the gene-based association signals were driven by markers in the genes and were unlikely to be caused by extended LD with markers in neighbouring gene loci (see regional association plots for the four new genes; Supplementary Figure 15a– 15d).

Gene-wise association of candidate genes for ADHD

Prior to the availability of large-scale whole-genome methods and technologies, many candidate genes have been examined in relation to ADHD. Such candidate gene studies frequently fail to replicate⁵⁷ and are likely to have been affected by publication bias, so it is unclear how many of the reported candidate genes are actually robustly associated with ADHD. As such, we set out to examine what the evidence for association is for the most highly studied candidate genes for ADHD, obtained from a recent review⁵⁸, in the current GWAS dataset. Annotated ADHD SNP results were tested for enrichment in each of these candidate genes using MAGMA to obtain overall gene P-values. The results do not show any support for the majority of the candidate genes that have been historically studied in relation to ADHD (Supplementary Table 11). The only exception is *SLC9A9* which shows nominal enrichment.

Gene-set analyses

Hypothesis free gene set analyses

For gene set analyses, we applied MAGMA⁴⁶. The analyses were based on the gene-based *P*-values generated as described above under “Gene-based association analysis”, based on summary statistics from the European GWAS meta-analysis. Those *P*-values were used to analyse sets of genes in order to test for enrichment in association signals in genes belong to specific to biological pathways or processes. MAGMA applies a competitive test to analyse if the genes of a gene set are more strongly associated with the trait than other genes, while correcting for a series of confounding effects such as gene length and size of the gene-set. In the analysis only genes on autosomes, and genes located outside the broad MHC region (hg19:chr6:25-35M) were included in the analysis. We applied no padding around genes. We used the gene names/locations and the European genotype reference panel

provided with the program. For gene sets we used the Gene Ontology⁵⁹ sets curated in MsigDB 6.0⁶⁰ keeping only gene sets with 10-1000 genes. No gene-sets remained significant after correction for multiple testing (Supplementary Data 5).

***FOXP2* downstream target gene set analysis**

Targeted gene set analyses were run in MAGMA to determine whether *FOXP2* downstream target gene sets are enriched in ADHD. Three sets of genes were examined: 1) Putative target genes of *FOXP2* that were enriched in wild type compared to control *FOXP2* knockout mouse brains in ChIP-chip experiments, 2) Genes showing differential expression in wild type compared to *FOXP2* knockout mouse brains, and 3) *FOXP2* target genes that were enriched in either or both basal ganglia (BG) and inferior frontal cortex (IFC) from human fetal brain samples in ChIP-chip experiments. Curated lists of high-confidence genes were obtained from Vernes et al.⁶¹ and Spiteri et al.⁶². Mouse genes were mapped to human orthologues using MGI and NCBI. *FOXP2* was excluded, only 8 genes were present on more than one list and only one gene was present on all three lists (*NRN1*). ADHD SNP results were annotated using MAGMA and used for gene set analyses. Competitive P-values, using a conditional model to correct for confounding due to gene size and gene density were obtained for each gene set. The results showed no evidence of enrichment for any of these gene sets (Supplementary Table 9).

Highly constrained gene set analysis

We assessed whether genes that are intolerant to loss of function and thereby highly evolutionarily constrained are enriched in ADHD. The set of highly constrained genes was defined using a metric for probability of being loss-of-function (LoF) intolerant (pLI) based on the observed and expected protein-truncating variant (PTV) counts within each gene in a very large study of exome data (the

Exome Aggregation Consortium; ExAC)⁶³. Genes with observed <10% of expected PTVs were deemed haploinsufficient or highly constrained. Publically available results based on the full ExAC dataset were downloaded from:

ftp://ftp.broadinstitute.org/pub/ExAC_release/release0.3.1/functional_gene_constraint

Genes with $pLI \geq 0.9$ were selected as the set of highly constrained genes. Annotated ADHD SNP results were tested for enrichment in this gene set in MAGMA using a competitive gene set analysis. Results showed a significant enrichment of this set of genes (see Supplementary Table 10).

LD Score intercept evaluation

A strong deviation from null was observed in the distribution of the test statistics in the quantile-quantile plot (Q-Q plot) of the results from the GWAS meta-analyses (Supplementary Figure 11a – 11b). When using LD score regression it is possible to distinguish the contribution of polygenicity from other confounding factors such as cryptic relatedness and population stratification to the deviation in the distribution of the test statistics⁴⁵. Under this model when regressing the chi-square statistics from GWAS against LD scores (pre-computed LD-scores downloaded from <https://github.com/bulik/ldsc>) for each SNP, the intercept minus one is an estimator for the mean contribution of confounding bias to the inflation in the test statistics. LD score regression analysis of the European GWAS meta-analysis estimated that the intercept was close to one (intercept = 1.04 (SE = 0.01)). Additionally, the ratio (ratio = (intercept-1)/(mean(chi²)-1)), which estimate of the proportion of the inflation in the mean chi-square that the LD Score regression intercept ascribes to causes other than polygenic heritability was estimated to ratio = 0.12 (SE = 0.03), indicating that the strong inflation in the distribution of the test statistics is caused primarily by polygenicity rather than confounding.

Genetic correlations between PGC and iPSYCH ADHD samples

In order to estimate the overlap in shared genetic risk factors between samples, genetic correlations r_g were calculated using LD Score regression⁴⁵. Pre-computed LD scores for HapMap3 SNPs calculated based on 378 phased European-ancestry individuals from the 1000 Genomes Project were used in the analysis (LD scores available on <https://github.com/bulik/ldsc>) and the summary statistics from European GWAS meta-analysis (iPSYCH + PGC European samples) and the PGC European samples²⁸. The r_g estimate was left unbounded in order to obtain unbiased estimates of SE. Only results for markers with an imputation INFO score > 0.90 were included in the analysis. The estimated genetic correlation between iPSYCH and PGC European GWAS was highly significant ($r_g = 1.17$; $SE = 0.2$; $P = 7.98 \times 10^{-9}$) and did not suggest imperfect correlation (i.e. $r_g < 1$) of common genetic risk factors between the studies.

Genetic correlation between PGC case-control and trio samples

The PGC European ancestry dataset consisted of two kinds of association study designs: case-control (Bergen, Cardiff, Germany, IMAGE-II, Spain, Yale-Penn) and trios (CHOP, Canada, IMAGE-I, PUWMA). A previous analysis of the PGC samples showed a genetic correlation of 0.71 ($SE=0.17$) across case-control and trio studies⁶⁴. We repeated this analysis within this newer set of PGC ADHD data.

For each of the PGC studies, best guess genotype data were generated using Ricopili and strictly filtered ($MAF > 0.05$, in addition to previous frequency, imputation quality and other filters). Genotypes were merged together across studies using PLINK. Asymmetric/ambiguous (AT, TA, CG, GC) and duplicate position SNPs were excluded. GCTA⁶⁵ was used to calculate a genomic relationship matrix for all individuals in this merged PGC sample for HapMap-3 SNPs. Analyses were based on 191,466 SNPs. One of each pair of individuals related at the level of 2nd cousins (pi-

hat>0.05) was excluded, preferentially keeping cases; this excluded: N=16 cases and N=91 controls. PCA was performed on the merged, unrelated samples using PLINK. The first 10 principal components as well as binary study/wave indicators were used as covariates for subsequent analyses. Univariate GREML analyses in GCTA were used to estimate SNP- h^2 on the liability scale (assuming a population prevalence of 5%) in the case-control samples and the trio samples separately. The GREML method was used for consistency with the previously published comparison of trio and case-control ADHD cohorts, and to accommodate the smaller sample sizes of the PGC subsets. As in the primary GWAS, trio studies were analysed using a case/pseudo-control design, where the pseudo-control is composed of the un-transmitted chromosomes from the parents of the proband. Bivariate GREML was then used to estimate the genetic correlation across these sub-cohorts.

The genetic correlation between the trio and case-control cohorts was strong and indistinguishable from 1 ($r_g=1.02$, $SE=0.32$), though the standard error remains quite large (Supplementary Table 3). The observed SNP- h^2 estimates were somewhat lower than the overall SNP- h^2 estimated in the primary analyses for the full meta-analysed results, consistent with the somewhat lower SNP- h^2 estimated from the PGC samples compared to iPSYCH (see SNP heritability analysis below).

Polygenic risk scores for ADHD

In addition to the genetic correlation analyses, we performed analyses of polygenic risk scores (PRS) to evaluate the consistency of common genetic effects and their predictive power across cohorts. We specifically considered PRS prediction within the iPSYCH samples, within the PGC cohorts, and in leave-one-out analysis across all cohorts.

Polygenic risk score prediction in iPSYCH samples

For analysis with the iPSYCH sample as the target cohort, the 23 genotyping-waves within the iPSYCH sample were split into five groups, aiming for approximately equal numbers of ADHD cases

within each group. We then conducted two sets of five leave-one-out analyses, with each leave-one-out analysis using four out of five iPSYCH groups as training datasets for estimation of SNP weights and then applying those weights to estimate PRS for the remaining target group⁶⁶. One set of leave-one-out analyses was performed with PGC European samples among the training datasets, while the other was without (only iPSYCH). The meta-analysis of the training samples was conducted using a SNP list filtered for minor allele frequency > 0.01 and an imputation threshold score above 0.8 intersecting across waves. Indels and variants in the extended MHC region (chromosome 6: 25-34 Mb) were also removed. Meta-analysis and “clumping” of significant SNPs was conducted using the Ricopili pipeline³⁵. PRS were then estimated for each target sample using a range of meta-analysis P-value thresholds (5×10^{-8} , 1×10^{-6} , 1×10^{-4} , 1×10^{-3} , 0.01, 0.05, 0.1, 0.2, 0.5, 1.0), multiplying the natural log of the odds ratio of each variant by the allele-dosage (imputation probability) of each variant. Whole genome PRS were obtained by summing values over variants for each individual. For each of the five groups of target samples PRS were normalized (subtracting the mean and dividing by the standard deviation), and the significance of the case-control score difference was tested by standard logistic regression including the first six principal components and a dummy variable indicating genotyping wave as covariates (using the `glm()` function of R 3.2.2). For each target group and for each P-value threshold the proportion of variance explained (i.e. Nagelkerke’s R^2) was estimated, comparing the full model to a reduced model without PRS and covariates only. The mean of the maximum Nagelkerke’s R^2 across P-value thresholds for each group was $R^2 = 0.055$ (SE = 0.055, range 0.047 – 0.06). For the P-value threshold with the highest Nagelkerke’s R^2 , odds ratios for PRS decile groups compared to the lowest decile were estimated for each target group (Supplementary Figure 8) and for the normalized score pooled across groups (Figure 2). Odds ratios were also estimated using logistic regression on the continuous scores for each target group separately

and finally an OR based on all samples was estimated by using the normalized PRS across all groups (Supplementary Figure 9).

Polygenic risk score prediction in PGC samples

Next the predictive utility of PRS was evaluated in the PGC samples. All European ancestry PGC best guess genotype data were merged together and iPSYCH-only summary statistics were used to calculate PRS in the PGC samples, using the approach described above. PRS in the PGC dataset were based on 9,323 clumped SNPs with $P < 0.1$ in the iPSYCH sample. The association between ADHD PRS and case status was significant in the merged PGC sample (OR=1.26 (1.22-1.31), variance explained on the liability scale (R^2) = 0.0103, $P = 2.4E-35$). Figure 2 displays odds ratios for ADHD case status by ADHD PRS decile for the PGC datasets. In the merged dataset, PRS were converted to deciles (where 1 was the lowest decile and 10 was the highest). Deciles 2-10 were then compared to the lowest decile using logistic regression including PCs as covariates. There is a clear pattern of increasing ORs with increasing decile.

To examine variation that could be related to differences in ascertainment of cases and controls within the PGC sample, mean PRS (residualised for PC covariates) were plotted stratified by case status and study (see Supplementary Figure 7). PGC cases had consistently higher PRS than PGC controls in the same study. There is some variation in PRS z-score across cases in different studies, for example with ADHD cases from the Cardiff (UK) sample having particularly high scores. Within controls, individuals within the Yale-Penn study have particularly high PRS; this may be due to this sample's ascertainment for the primary phenotype of substance abuse, with high levels of these problems in both the cases and controls^{21-23,67}. Variation in PRS in controls from different studies may be due to differences in ascertainment (e.g. pseudo-controls, screened or unscreened controls).

Leave-one-out analysis across cohorts

The odds ratio based on PRS over all PGC and iPSYCH waves/studies was also evaluated using a leave-one-study/wave-out approach. First, GWAS analyses of imputed dosage data were run for all samples in each PGC study and iPSYCH wave separately, as described previously, co-varying for relevant PCs. Meta-analyses using METAL³⁰ (with the STDERR scheme) were run excluding one set of summary results at a time, for each combination of studies. For each set of discovery results, LD-clumping was run to obtain a relatively independent set of SNPs, while retaining the most significant SNP in each LD block. The following parameters were applied in PLINK: --clump-kb 500 --clump-r2 0.3 --clump-p1 0.5 --clump-p2 0.5. Asymmetric/ambiguous (AT, TA, CG, GC) SNPs, indels and duplicate position SNPs were excluded. The SNP selection P-value threshold used was $P < 0.1$. The number of clumped SNPs for each study/wave varied from 20596-43427. Polygenic risk scores were calculated for each individual as described above. Scores were derived in best guess genotype data after filtering out SNPs with $MAF < 0.05$ and $INFO < 0.8$. The polygenic risk scores were standardized using z-score transformations. Logistic regression analyses including PCs tested for association of polygenic risk scores with case status. Finally, overall meta-analyses of the leave-one-out analyses were performed (Supplementary Figure 10).

SNP heritability

SNP heritability was estimated using LD score regression⁴⁵ in order to evaluate how much of the variation in the phenotypic trait could be ascribed to common additive genetic variation. Summary statistics from GWAS meta-analyses and pre-computed LD scores (available from <https://github.com/bulik/ldsc>) were used in the analyses. The SNP heritability for ADHD was calculated on the liability scale when using summary statistics from analyses of diagnosed ADHD and assuming a 5% prevalence of ADHD in the population⁶⁸. The SNP heritability (h^2_{SNP}) was

estimated to be 0.216 (SE = 0.014) based on the summary statistics from the European GWAS meta-analysis. LD score regression SNP heritability estimates for the iPSYCH and PGC samples respectively can be found Supplementary Table 4.

In order to evaluate the stability of our heritability estimates we also performed univariate GREML analyses in GCTA. However due to strict restrictions on access to individual genotypes, GREML analyses could only be performed separately in the PGC and iPSYCH cohorts. For each of these datasets, best guess genotype data were generated (hard called genotypes with imputation INFO-score > 0.8) and filtered to include genotypes with MAF>0.05. Asymmetric/ambiguous (AT, TA, CG, GC), multi-allelic and duplicate position SNPs were excluded. For each dataset, a genomic-relationship matrix was calculated, restricted to HapMap-3 SNPs. Analyses were based on the following numbers of SNPs: PGC-only: 191,466 SNPs; iPSYCH-only: 435,086 SNPs. One of each pair of individuals related (π -hat>0.05) was excluded, preferentially keeping cases. In the PGC dataset N=16 cases and N=91 controls were excluded and N=1,439 cases and N=3,170 controls in the iPSYCH dataset. PCA (after LD-pruning and removing SNPs located in long-range LD regions) was performed on the merged, unrelated samples using PLINK, to derive population covariates. The first 10 PCs as well as study/wave indicators were used as covariates in the univariate GREML analyses in GCTA.

Partitioning heritability by functional annotation and cell type

Partitioning of the heritability by functional categories was done using LD score regression and 53 functional overlapping annotations described in Finucane et al.⁶⁹ and the baseline model LD scores, regression weights and allele frequencies based on the 1KGP3 European ancestry samples were downloaded from <https://data.broadinstitute.org/alkesgroup/LDSCORE/>. The summary statistics from the European GWAS meta-analysis were used in the analysis. Enrichment in the heritability of

a functional category was defined as the proportion of SNP heritability explained divided by the proportion of SNPs⁶⁹. Results from analysis of the 24 main annotations (no window around the functional categories) are displayed in Supplementary Figure 12. The analysis revealed significant enrichment in the heritability by SNPs located in conserved regions ($P = 8.49 \times 10^{-10}$; Supplementary Figure 12).

Test for enrichment in the heritability of SNPs located in cell-type-specific regulatory elements was evaluated in two ways. One by using the 220 cell-type-specific annotations that have been grouped into 10 cell-type groups as described in Finucane et al.⁷⁰. These annotations are based on cell-specific histone markers, related to H3K4me1⁷¹, H3K4me3⁷¹, H3K9ac⁷¹ and H3K27ac⁷². The test was done using the summary statistics from the European GWAS meta-analysis and cell-type specific LD scores, baseline model LD scores, regression weights and allele frequencies based on 1KGP3 European ancestry samples available for download at: <https://data.broadinstitute.org/alkesgroup/LDSCORE/>. In the analyses, it was tested if the cell-group specific annotations contributed significantly to the SNP heritability when controlling for the annotations in the full baseline model (the coefficient P-value). The analysis revealed a significant enrichment in the heritability by SNPs located in central nervous system specific enhancers and promoters (enrichment = 2.44, SE=0.35, $P = 5.81 \times 10^{-5}$; Supplementary Figure 13).

Additionally we expanded the cell-type specific heritability analysis by including an annotation based on information about H3K4Me1 imputed gapped peaks excluding the broad MHC-region (chr6:25-35MB), generated by the Roadmap Epigenomics Mapping Consortium^{72,73}. This mark has previously been used with success in identifying significant enrichments in tissues/cells and often in a biologically plausible manner^{71,72}. This analysis identified enrichment in the heritability of SNPs located in specific regulatory elements of nine brain tissues as well as three stem-cell lines (Supplementary Figure 14).

Genetic correlations of ADHD with other traits

The genetic correlation of ADHD with other traits were evaluated using LD Score regression⁴⁵. Correlations with 211 phenotypes were tested using LD Hub (<http://ldsc.broadinstitute.org/ldhub/>)⁷⁴. This estimation was based on summary statistics from the European GWAS meta-analysis and summary statistics from published GWASs. In addition, we tested for genetic correlation with eight phenotypes on our local server: human intelligence⁷⁵, four phenotypes related to education and cognition analysed in samples from the UK-Biobank (college/university degree, verbal-numerical reasoning, memory and reaction time)⁷⁶, insomnia⁷⁷, anorexia nervosa⁷⁸, and correlation with Major Depressive Disorder was tested using GWAS results from an updated analysis of 130,664 cases and 330,470 controls from the Psychiatric Genomics Consortium⁷⁹. In total 219 phenotypes were tested for genetic overlap with ADHD and 43 demonstrated significant correlation after Bonferroni correction ($P < 2.28 \times 10^{-4}$). Detailed information about significant genetic correlations can be found in Supplementary Table 5 and extended results for all phenotypes tested can be found in Supplementary Data 1.

Replication analysis in external cohorts

To replicate the results of the ADHD GWAS meta-analysis we compared the results to analyses of the deCODE, 23andMe, and EAGLE/QIMR cohorts. The sample design of these cohorts and the process for matching their GWAS results to the ADHD GWAS are described under the sample description section. Briefly, the deCODE analysis is based on ICD-10 diagnoses and prescription data from medical records, the 23andMe analysis is based on self-reported history of ADHD diagnosis, and EAGLE/QIMR involve analyses of continuous measures of ADHD-related behavioural traits in the general population. Given the phenotypic differences between these cohorts we evaluated

replication separately for each of these cohorts. The included replication analyses also depended on whether data is available for genome-wide variants (23andMe and EAGLE/QIMR) or only top hits (deCODE) and whether effect sizes are directly comparable to the ADHD GWAS (23andMe and deCODE only).

Taken together, we evaluated replication based on: (a) sign tests of concordance between the ADHD GWAS meta-analysis and each replication cohort; (b) comparison of bias-corrected effect sizes between the ADHD GWAS and the deCODE and 23andMe replication cohorts; (c) genetic correlation between the ADHD GWAS and the 23andMe and EAGLE/QIMR replication cohorts; (d) meta-analysis of the ADHD GWAS meta-analysis results with the results from each replication cohort; and (e) tests of heterogeneity between the ADHD GWAS and each replication cohorts.

Sign test

To evaluate concordance of the direction of effect between the ADHD GWAS and the replication cohorts, we first identified the overlapping SNPs present in the ADHD GWAS and analysis of each of the three replication cohorts (i.e. deCODE, 23andMe, and EAGLE/QIMR). For each replication cohort, the ADHD GWAS results for the intersecting SNPs were then clumped to define independent loci using PLINK 1.9⁴². Given that the previous conditional analysis was unable to conclusively confirm putative independent signals in the loci defined with LD $r^2 > 0.1$ within 500 kb of the index variant, we apply more conservative clumping parameters to ensure independence for the sign test ($r^2 > 0.05$ within 1 Mb) and merge index variants within 1 Mb. This clumping was performed for all variants with $P < 1 \times 10^{-4}$ in the ADHD GWAS (or $P < 1 \times 10^{-5}$ for the deCODE replication) using 1000 Genomes Phase 3 data on European ancestry populations as reference.

After clumping, sign tests were performed to compare the loci from the ADHD GWAS meta-analysis to each replication cohort. Specifically, for loci passing a given P-value threshold in the ADHD

GWAS meta-analysis, we tested the proportion with a concordant direction of effect in the replication cohort (π) using a one sample test of the proportion with Yates' continuity correction⁸⁰ against a null hypothesis of $\pi = 0.50$ (i.e. the signs are concordant between the two analyses by chance) in R⁸¹. This test was evaluated separately for concordance in deCODE, 23andMe, and EAGLE/QIMR for loci passing P-value thresholds of $P < 5 \times 10^{-8}$ (i.e. genome-wide significant loci), $P < 1 \times 10^{-7}$, $P < 1 \times 10^{-6}$, $P < 1 \times 10^{-5}$, and $P < 1 \times 10^{-4}$ in the ADHD GWAS meta-analysis. We note that the number of clumped loci at each P-value threshold varies depending on the availability of results for variants in each replication cohort. For example, the genome-wide significant variants ($P < 5 \times 10^{-8}$) from the chromosome 4 locus in the ADHD GWAS (index variant: rs28411770) are all absent in the 23andMe results, thus the sign test is limited to the other 11 loci.

Sign test results for each replication cohort are reported in Supplementary Table 12. Sign concordance between each of the three replication cohorts and the ADHD GWAS was significantly greater than would be expected by chance ($P < 0.0167 = 0.05/3$ replication cohorts) for nominally associated loci from the ADHD GWAS ($P < 1 \times 10^{-6}$). Power of the sign test at stricter P-value thresholds is limited by the number of loci at that level in the ADHD GWAS, but the sign test remained significant for EAGLE/QIMR which was sign concordant for all loci with $P < 1 \times 10^{-7}$ in the ADHD GWAS. Sign concordance was generally strongest in EAGLE/QIMR, followed by deCODE and 23andMe, though 23andMe showed stronger sign concordance for loci with $P < 1 \times 10^{-5}$ in the ADHD GWAS.

Focusing on the genome-wide significant loci ($P < 5 \times 10^{-8}$) for the ADHD GWAS, 11 of the 12 loci show sign concordance in at least 2 of the 3 replication cohorts (Supplementary Table 13). Eight of the 12 loci were sign concordant in all available replication results for either the index variant or a proxy variant in the locus. The weakest sign concordance was observed for the chromosome 16 locus (rs212178, *LINC01572*), which was only sign concordant in EAGLE/QIMR with discordant estimates observed from deCODE and 23andMe. Sign discordant estimates were also observed for

the chromosome 1 (index variant rs11420276, *PTPRF/ST3GAL3*) and chromosome 15 (rs281324, *SEMA6D*) loci in 23andMe, and for the chromosome 2 locus (rs9677504, *SPAG16*) in deCODE.

Replication of effect sizes for top loci

Although the sign test provides a useful check of concordance for direction of effect in the replication samples, it does not consider replication of the magnitude of the effect. For the deCODE and 23andMe replication cohorts that included GWAS of ADHD status from various sources, we anticipate that the true effect sizes should be similar to, though not necessarily identical to, the effect size for ADHD as defined in the current meta-analysis. Therefore, we looked at the replication of the effect sizes of the top loci in the ADHD GWAS in the replication cohorts.

Specifically, for each of deCODE and 23andMe we identified clumped loci that are nominally associated ($P < 1 \times 10^{-6}$) with ADHD in the primary ADHD GWAS. We then regressed the effect size in the replication cohort (i.e. the log odds ratio) on the estimated effect size from the ADHD GWAS after adjustment for winner's curse (described below). For this regression, we oriented all variants in the direction of the risk increasing allele estimated from the ADHD GWAS, constrained the intercept term to zero, and weighed the variants proportional to the inverse of their squared standard error from the ADHD GWAS. If the included variants are all truly associated with ADHD with the same true population effect size in the ADHD GWAS and replication cohorts (i.e. regardless of the phenotyping measure for ADHD status) then the expected slope of this regression is one. On the other hand, if all SNPs are truly null in the ADHD GWAS and the replication cohorts then the expected slope of this regression is zero.

Comparison of effects sizes from the ADHD GWAS to the deCODE cohort suggests good but imperfect replication of top loci (Supplementary Figure 16). The deCODE effect size estimates are significantly correlated with the adjusted ADHD GWAS betas (slope = 0.664, SE=.154, $P=1.2 \times 10^{-4}$)

but this slope is also significantly less than 1 ($P=0.0178$). The estimated effect of rs9677504 (*SPAG16* locus) is a visible outlier in this comparison, following the discordant direction of association as noted in the sign test results. Omitting this effect size the regression increases the slope but is not sufficient to eliminate the significant difference from one (slope = 0.710, SE=0.149, $P = 0.030$ for comparison to slope=1).

Comparison of effect sizes with 23andMe follows a similar trend, but with somewhat weaker overall strength of replication (Supplementary Figure 17). Regressing 23andMe estimates of effect size on the adjusted ADHD GWAS effect sizes yields a slope of 0.417 (SE=0.117), which is significantly greater than zero ($P=1.11 \times 10^{-3}$) and significantly less than one ($P=9.52 \times 10^{-6}$). This lower slope compared to the deCODE replication is consistent with the weaker sign test results. The comparison of effect sizes also emphasizes the strong discordance at rs112984125 (*ST3GAL3/PTPRF*) and rs212178 (*LINC01572*). Removing those two loci from the regression increases the slope to 0.538 (SE=0.102, $P=3.86 \times 10^{-5}$ for slope less than 1).

Genetic correlation analysis of replication cohorts

Genetic correlation of the ADHD GWAS with the 23andMe and EAGLE/QIMR results was computed using LD score regression⁴⁵ with pre-computed European ancestry LD scores following the same procedure as described above for other genetic correlation analyses. Genetic correlation could not be computed for deCODE since results were only available for top loci from the ADHD GWAS.

The estimated genetic correlation between the 23andMe and the ADHD GWAS was large and significant ($r_g = 0.653$, SE = 0.114, $P = 1.11 \times 10^{-8}$), but also significantly less than 1 (one-sided $P=1.17 \times 10^{-3}$). Genetic correlation analysis with EAGLE/QIMR suggest a stronger overlap ($r_g = 0.970$, SE = 0.207, $P = 2.66 \times 10^{-6}$) with a genetic correlation not significantly different from one (one-sided

$P = 0.442$). These results are both consistent with sign test results, where both 23andMe and EAGLE/QIMR show significant concordance with the ADHD GWAS, with EAGLE/QIMR showing the most consistent results. The moderate but highly significant genetic correlation observed with 23andMe is also consistent with the moderate slope in the replication of effect sizes for top loci from the ADHD GWAS.

To further explore the moderate genetic correlation between the 23andMe results and the ADHD GWAS we evaluated the genetic correlation between 23andMe and traits from LD Hub (<http://ldsc.broadinstitute.org/ldhub/>)⁷⁴. The goal of this analysis is to potentially identify differences in the profile of genetic correlation of these studies to other traits, with the expectation that such differences may highlight domains where the 23andMe and ADHD GWAS results are particularly different. We focus this comparison on a curated set of 28 phenotypes with at least nominal ($P < 0.01$) evidence of genetic correlation with either the ADHD GWAS or 23andMe, with the set of phenotypes selected to emphasize domains of interest for ADHD while reducing the number of closely related traits.

Genetic correlation results for the 23andMe and ADHD GWAS with the 28 selected phenotypes are reported in Supplementary Table 14. To evaluate the magnitude of the observed differences in r_g we consider both the absolute difference (i.e. $|r_{g,ADHD} - r_{g,23andMe}|$) and the test of an approximate Z score for this difference:

$$Z = \frac{r_{g,ADHD} - r_{g,23andMe}}{\sqrt{SE_{ADHD}^2 + SE_{23andMe}^2}}$$

The denominator is motivated by the expected standard error of the difference between the two means under the assumption that the samples are not correlated. In the context of mean differences this approximation may be expected to be conservative when the r_g estimates are positively correlated. We do not expect this to be an ideal formal test for the difference between two genetic correlations as estimated by LD score regression, and therefore emphasize the importance of caution in

interpreting the precise results. Nevertheless, it does offer a useful benchmark for evaluating the magnitude of the difference between the r_g estimates in the context of the uncertainty in those values. Comparison of the r_g results for the ADHD GWAS and 23andMe identifies some striking differences. Most notably, the 23andMe GWAS shows little to no genetic correlation with college completion ($r_g=0.056$, compared to $r_g=-0.54$ for the primary ADHD GWAS; $P=1.1 \times 10^{-9}$ for difference) and only limited correlation to childhood IQ ($r_g=-0.22$ vs. $r_g=-0.41$ in ADHD, $P=2.46 \times 10^{-1}$) and educational attainment ($r_g=-0.20$ vs. $r_g=-0.53$ in ADHD, $P=1.8 \times 10^{-7}$). The genetic correlation with age of first birth is also strongly attenuated in 23andMe ($r_g=-0.33$ vs. $r_g=-0.61$ in ADHD, $P=6.3 \times 10^{-4}$), while results for the other reproductive phenotypes are more similar. The 23andMe GWAS also shows evidence of weaker genetic correlations with the weight-related phenotypes, most notably class 1 obesity ($r_g=0.11$, vs. $r_g=0.29$ in ADHD, $P=0.024$) and childhood obesity ($r_g=-0.025$, vs $r_g=0.22$ in ADHD, $P=0.036$). The one domain where 23andMe exhibits a trend toward stronger genetic correlations is schizophrenia ($r_g=0.27$, vs. $r_g=0.12$ in ADHD, $P=0.053$) and bipolar disorder ($r_g=0.29$, vs. $r_g=0.095$ in ADHD, $P=0.09$), these differences are not significant with the approximated Z score. There is a corresponding trend towards weaker genetic correlation with depressive symptoms compared to the ADHD GWAS, but it is also not significant with the current test ($r_g=0.30$, vs. $r_g=0.45$ in ADHD, $P=0.24$).

Meta-analysis and heterogeneity test with each replication cohort

For the replication analysis, we considered meta-analyses of the ADHD GWAS results with each of the three replication cohorts. The 23andMe and deCODE cohorts were each meta-analysed with the ADHD GWAS using conventional inverse variance-weighted meta-analyses. For EAGLE/QIMR, meta-analysis was performed using a modified sample size-based weighting method (see detailed description of methods below). For each of these three meta-analyses, we evaluated results for the

genome-wide significant loci from the ADHD GWAS and identified new loci reaching nominal genome-wide significance ($P < 5 \times 10^{-8}$, unadjusted for number of replication cohorts). In addition, we considered Cochran's Q test of heterogeneity, computing the 1 degree of freedom test for heterogeneity between the ADHD GWAS and each replication cohort.

Meta-analysis of the discovery ADHD GWAS with deCODE (hereafter ADHD+deCODE) yields 10 genome-wide significant loci (Supplementary Data 6). Of these loci 5 were significant in the ADHD GWAS, leaving 7 loci that were significant in the ADHD GWAS but are not significant after meta-analysis with the deCODE replication cohort: rs1222063 (chr. 1, intergenic), rs9677504 (chr. 2, *SPAG16*), rs4858241 (chr. 3, *SGOI-ASI*), rs4916723 (chr. 5, *LINC00461*), rs74760947 (chr. 8, *LINC01288*), rs281324 (chr. 15, *SEMA6D*), and rs212178 (chr. 16, *LINC01572*). None of these loci show genome-wide significant heterogeneity between the ADHD GWAS and deCODE, though in many cases there is nominal evidence ($P < .05$) of heterogeneity. The remaining 5 loci significant in the ADHD+deCODE replication meta-analysis are novel: rs1592757 (chr. 5, Refseq gene *LOC105379109*), rs28452470 (chr. 7, *CADPS2*), rs10956838 (chr. 8, intergenic), rs4275621 (chr. 11, intergenic), and rs1848160 (chr. 11, intergenic).

The replication meta-analysis with 23andMe (hereafter ADHD+23andMe) identified 10 genome-wide significant loci (Supplementary Data 6, Supplementary Figure 21). Three of these loci were novel: rs30266 (chr. 5, Refseq gene *LOC105379109*), rs62250537 (chr. 3, *CADM2*), and rs2243638 (chr. 13, *RNF219-ASI*). The chromosome 5 locus is the same region identified by the ADHD+deCODE meta-analysis. The other 7 genome-wide significant loci in ADHD+23andMe match loci from the discovery GWAS. The remaining 4 of the 12 genome-wide significant loci from the ADHD GWAS meta-analysis were no longer significant after meta-analysing with 23andMe: rs281324 (chr15, *SEMA6D*), rs212178 (chr16, *LINC01572*), rs4916723 (chr5, *LINC00461*), rs74760947 (chr8, *LINC01288*). The final significant locus from the ADHD GWAS, rs28411770

(chr4, *PCDH7*), is not present in the 23andMe results. Cochran's Q test of heterogeneity identified genome-wide significant heterogeneity between the ADHD GWAS and the 23andMe GWAS in the top locus on chromosome 1 from the ADHD GWAS (Supplementary Figure 23-24). The strongest evidence for discordance was at rs12410155 (*ST3GAL3*), with an estimated odds ratio of 1.111 ($P = 3.63 \times 10^{-13}$) in the ADHD GWAS, compared to an odds ratio of 0.954 ($P = 0.0244$) in the 23andMe analysis (heterogeneity $P = 2.28 \times 10^{-9}$, $I^2 = 97.2$).

Lastly, meta-analysis of the ADHD GWAS with EAGLE/QIMR (ADHD+EAGLE/QIMR) produced 15 genome-wide significant loci (Supplementary Data 6, Supplementary Figure 22). All 12 of the genome-wide significant loci from the ADHD GWAS remain significant in the ADHD+EAGLE/QIMR meta-analysis, consistent with the sign concordance at all 12 loci. The three additional significant loci are located on chromosome 7 (rs1443749, *CADPS2*), chromosome 10 (rs9665567, intergenic) and chromosome 13 (rs7997529, *RNF219-AS1*). The chromosome 7 locus is concordant with the locus reaching genome-wide significance in ADHD+deCODE, and the chromosome 13 locus similarly matches the significant locus from ADHD+23andMe. No significant heterogeneity was observed between the EAGLE/QIMR and ADHD GWAS meta-analyses (Supplementary Figure 25-26), consistent with the strong genetic correlation between the two studies. Overall, 4 of the 12 significant loci from the ADHD GWAS are significant in all three of these replication meta-analyses: index variants rs11420276 (chr. 1, *ST3GAL3/PTPRF*), rs5886709 (chr. 7, *FOXP2*), rs11591402 (chr. 10, *SORCS3*), and rs1427829 (chr. 12, intergenic). The remaining loci are all significant in at least one of the replication meta-analyses. In addition, 3 novel loci reach genome-wide significance in two of these replication meta-analyses: index variants rs1592757/rs30266 (chr. 5, Refseq *LOC105379109*), rs28452470/rs1443749 (chr. 7, *CADPS2*), and rs2243638/rs9574218 (chr. 13, *RNF219-AS1*).

Meta-analysis across replication cohorts

We finally consider meta-analysis with all available data. Because replication results from deCODE are only available for top loci from the primary ADHD GWAS we are unable to estimate heritability and genetic correlation with EAGLE/QIMR to calibrate the meta-analysis weights as used for the other EAGLE/QIMR analyses (described below). Since we consequently cannot perform a meta-analysis simultaneously including both deCODE and EAGLE/QIMR, we instead separately evaluate the replication meta-analysis of all case/control cohorts (i.e. ADHD+deCODE+23andMe, omitting EAGLE/QIMR) and the replication meta-analysis of all genome-wide studies (i.e. ADHD+23andMe+EAGLE/QIMR, omitting deCODE).

Results for the ADHD+deCODE+23andMe and ADHD+23andMe+EAGLE/QIMR replication meta-analyses are generally consistent with the meta-analyses for each replication cohort (Supplementary Data 6). Two new loci – located near *MAD1L1* (chr. 7) and *TM6SF2* (chr. 19) – nominally reach genome-wide significance in ADHD+23andMe+EAGLE/QIMR before consideration of multiple testing for the replication meta-analyses. No additional loci are nominated by the ADHD+deCODE+23andMe meta-analysis. Of the 12 significant loci in the ADHD GWAS, three are not significant in either of these pooled replication meta-analyses, primarily due to poor support for the locus in 23andMe: rs281324 (chr15, *SEMA6D*), rs212178 (chr16, *LINC01572*), and rs74760947 (chr8, *LINC01288*).

Winner’s curse correction for effect sizes

To evaluate replication of the ADHD GWAS effect sizes it is necessary to account for the bias from the “winner’s curse” in looking at only top loci nominally associated with ADHD. To correct for this bias, we compute posterior estimates for the expected value of β_j for each SNP given the observed

GWAS estimate and a spike-and-slab prior as described by Okbay et al.⁸² Briefly, we assume that marginal SNP effects follow the spike-and-slab distribution

$$\beta_j \sim \begin{cases} 0 & \text{with probability } \pi \\ N(0, \tau^2) & \text{otherwise} \end{cases}$$

where β_j is standardized for MAF such that τ^2 corresponds to average variance explained per SNP.

Following this model, we estimate $\hat{\pi}$ and $\hat{\tau}^2$ via maximum likelihood with the observed $\hat{\beta}_j$ from the ADHD GWAS. We then compute the posterior probability that each SNP is null $\hat{\pi}_j$. The posterior estimate of β_j corrected for winner's curse is then given by

$$\hat{\beta}_{adj,j} = (1 - \hat{\pi}_j) \frac{\hat{\tau}^2}{\hat{\tau}^2 + \hat{s}_j^2} \hat{\beta}_j$$

where \hat{s}_j^2 is the squared standard error of $\hat{\beta}_j$ from the ADHD GWAS. As implied by this formula, the resulting $\hat{\beta}_{adj,j}$ corrected for winner's curse will be shrunk towards zero proportional to the probability that SNP j is null and the degree of uncertainty in its effect size as indicated by the standard error.

Method for meta-analysis of continuous and dichotomous ADHD measures

In order to integrate the EAGLE/QIMR data with the current analysis, we need to define a framework for comparing the GWAS of (continuous) measures of ADHD-related behaviour to the ADHD GWAS meta-analysis of (dichotomous) clinical diagnosis of ADHD.

As a starting point, motivated by the strong genetic correlation between the EAGLE/QIMR results and the ADHD GWAS meta-analysis, we could consider a conventional sample size-weighted meta-analysis of Z scores. Such an analysis however would not account for: (a) differences in power for continuous vs. dichotomous phenotypes, (b) differences in power from ascertainment on the dichotomous phenotype, (c) differences in the relative strength of overall genetic association (e.g.

SNP heritability) for the phenotype measures, or (d) imperfect correlation between the continuous ADHD-related behaviours measured in EAGLE/QIMR and clinical diagnosis of ADHD, with the matter being the phenotype of interest for the current study.

Therefore, we instead define a basic model for the genetic relationship between clinical diagnosis of ADHD and continuous ADHD-related behaviours that allows us to derive modified sample size-based weights that account for these factors. These weights should be better calibrated to provide a statistically efficient meta-analysis of the EAGLE/QIMR results with the ADHD GWAS.

Basic genetic model for latent-scale phenotypes

We begin by defining a joint model for the genetics of the two phenotypes. Let Y_1 be the observed dichotomous phenotype and Y_2 be the observed continuous phenotype. For dichotomous phenotype Y_1 , we assume there exists some latent continuous liability θ_1 such that

$$Y_1 = \begin{cases} 0, & \theta_1 < \tau_1 \\ 1, & \theta_1 \geq \tau_1 \end{cases}$$

where τ_1 is a threshold corresponding to the population prevalence K of Y_1 consistent with the standard liability threshold model⁸³. For convenience, assume that θ_1 is standardized with mean zero and unit variance. Similarly, let θ_2 denote the continuous phenotype Y_2 normalized to have mean 0 and unit variance in the population.

We describe a model for the genetics of the latent continuous phenotypes θ_1 and θ_2 before returning to the impact of the observed scale for each phenotype. Let g_1 and e_1 be genetic and environment components of θ_1 , respectively, and let g_2 and e_2 be corresponding components of θ_2 such that

$$\begin{bmatrix} \theta_1 \\ \theta_2 \end{bmatrix} = \begin{bmatrix} g_1 \\ g_2 \end{bmatrix} + \begin{bmatrix} e_1 \\ e_2 \end{bmatrix}$$

$$E \left(\begin{bmatrix} \theta_1 \\ \theta_2 \end{bmatrix} \right) = E \left(\begin{bmatrix} g_1 \\ g_2 \end{bmatrix} \right) = E \left(\begin{bmatrix} e_1 \\ e_2 \end{bmatrix} \right) = \begin{bmatrix} 0 \\ 0 \end{bmatrix}$$

$$\text{Cov}\left(\begin{bmatrix} g_1 \\ g_2 \\ e_1 \\ e_2 \end{bmatrix}\right) = \begin{bmatrix} h_1^2 & \rho_g & 0 & 0 \\ \rho_g & h_2^2 & 0 & 0 \\ 0 & 0 & \epsilon_1^2 & \rho_e \\ 0 & 0 & \rho_e & \epsilon_2^2 \end{bmatrix}$$

Note that we assume that not only are genetics and environment uncorrelated within phenotype (i.e. $\text{Cov}(g_1, e_1) = \text{Cov}(g_2, e_2) = 0$), but also between phenotypes ($\text{Cov}(g_1, e_2) = \text{Cov}(g_2, e_1) = 0$). Since θ_1 and Y_2^* are each defined to have unit variance, it follows that $\epsilon_1^2 = 1 - h_1^2$, $\epsilon_2^2 = 1 - h_2^2$, and ρ_g and ρ_e are the genetic and environmental covariances, respectively. The genetic correlation between the latent phenotypes θ_1 and θ_2 can then be defined as $r_g \equiv \text{cor}(g_1, g_2) = \rho_g / \sqrt{h_1^2 h_2^2}$.

Defining independent genetic factors

We next seek to specify the covariance of g_1 and g_2 in terms of two independent factors f_1 and f_2 . This transformation serves two purposes. First, for modeling the effects of individual SNPs it will allow us to define independent effects on f_1 and f_2 . Second, if we specify that g_1 depends only on f_1 while g_2 may depend on both f_1 and f_2 , then it will be possible to focus on the factor f_1 that determines the genetic component g_1 for Y_1 separate from any independent factors f_2 that contribute to Y_2 only. Separating these factors therefore allows us to move towards the goal of defining a scheme for meta-analysis that focuses only on genetic effects for the dichotomous phenotype (i.e. clinical ADHD diagnosis) while discounting any independent genetic effects that are only relevant to the continuous phenotype (i.e. ADHD-related behaviours).

The desired transformation is given by the inverse of the Cholesky decomposition of the covariance matrix for g_1 and g_2 , which yields

$$\begin{bmatrix} f_1 \\ f_2 \end{bmatrix} \equiv \begin{bmatrix} \frac{1}{\sqrt{h_1^2}} & 0 \\ -r_g & 1 \end{bmatrix} \begin{bmatrix} g_1 \\ g_2 \end{bmatrix}.$$

It can then be shown that

$$\text{Cov}\left(\begin{bmatrix} f_1 \\ f_2 \end{bmatrix}\right) = \begin{bmatrix} 1 & 0 \\ 0 & 1 \end{bmatrix},$$

and $E(f_1) = E(f_2) = 0$. By substitution for g_1 and g_2 , the latent phenotypes are related to these factors by

$$\begin{aligned} \theta_1 &= \left(\sqrt{h_1^2}\right) f_1 + e_1 \\ \theta_2 &= \left(r_g \sqrt{h_2^2}\right) f_1 + \left(\sqrt{1 - r_g^2} \sqrt{h_2^2}\right) f_2 + e_2. \end{aligned}$$

Effects of individual variants

The above model fully specifies the overall genetic components of the two phenotypes, but does not model the contribution of any specific variant. We now define the effects of individual variants so that we can work towards describing the GWAS results for each phenotype and the desired meta-analysis in terms of parameters for a given variant.

To consider effects for a given variant, let γ_{1j}^* be the causal effect of variant j on f_1 , and let γ_{2j}^* be the corresponding effect on f_2 . Then

$$\begin{aligned} f_1 &= \sum_j \gamma_{1j}^* x_j \\ f_2 &= \sum_j \gamma_{2j}^* x_j, \end{aligned}$$

where x_j is the standardized genotype of variant j . We denote these causal effects as γ to distinguish them from marginal effects β , and use the * superscript here to indicate that these are effect sizes on the latent genetic components f_1 and f_2 as opposed to the standardized phenotypes. The corresponding causal effects on θ_1 and θ_2 are

$$\gamma_{1j} = \sqrt{h_1^2} \gamma_{1j}^*$$

$$\gamma_{2j} = \left(r_g \sqrt{h_2^2}\right) \gamma_{1j}^* + \left(\sqrt{1 - r_g^2} \sqrt{h_2^2}\right) \gamma_{2j}^*$$

respectively.

The marginal effect on f_1 and f_2 will depend not only on the variant's causal effect, but on the causal effect of other variants in LD with x_j . We define the corresponding marginal effects β_j^* as

$$\beta_{1j}^* = (X_j' X_j)^{-1} X_j' \mathbf{X} \boldsymbol{\gamma}_1^* = \sum_k \gamma_{1k}^* r_{jk}$$

$$\beta_{2j}^* = (X_j' X_j)^{-1} X_j' \mathbf{X} \boldsymbol{\gamma}_2^* = \sum_k \gamma_{2k}^* r_{jk}$$

where $r_{jk} = \text{cov}(x_j, x_k)$ and $\boldsymbol{\gamma}_1^*$ and $\boldsymbol{\gamma}_2^*$ are column vectors with elements γ_k^* for all k . As with γ^* , the superscript denotes these β_j^* as effect sizes on the latent genetic components f_1 and f_2 .

To get marginal effect sizes on the phenotypes, we can denote

$$f_{1,-j} = f_1 - \beta_{1j}^* x_j$$

$$f_{2,-j} = f_2 - \beta_{2j}^* x_j$$

to indicate f_1 and f_2 with the full marginal effect of x_j removed, so that we can then express the phenotypes in terms of the marginal effect of variant j as

$$\begin{aligned} \theta_1 &= (f_{1,-j} + \beta_{1j}^* x_j) \sqrt{h_1^2} + e_1 \\ &= (\beta_{1j}^* \sqrt{h_1^2}) x_j + (\sqrt{h_1^2}) f_{1,-j} + e_1 \end{aligned}$$

$$\begin{aligned} \theta_2 &= (r_g \sqrt{h_2^2}) (f_{1,-j} + \beta_{1j}^* x_j) + \left(\sqrt{h_2^2(1 - r_g^2)}\right) (f_{2,-j} + \beta_{2j}^* x_j) + e_2 \\ &= \left[\beta_{1j}^* (r_g \sqrt{h_2^2}) + \beta_{2j}^* \left(\sqrt{h_2^2(1 - r_g^2)}\right) \right] x_j + (r_g \sqrt{h_2^2}) f_{1,-j} + \left(\sqrt{h_2^2(1 - r_g^2)}\right) f_{2,-j} + e_2 \end{aligned}$$

Therefore, given θ_1 , θ_2 and x_j are all standardized and x_j , $f_{1,-j}$, $f_{2,-j}$, e_1 , and e_2 are all independent except for $cov(e_1, e_2) = \rho_e$,

$$\begin{aligned}\beta_{1j} &= cor(x_j, \theta_1) = \beta_{1j}^* \sqrt{h_1^2} \\ \beta_{2j} &= cor(x_j, \theta_2) = \beta_{1j}^* \left(r_g \sqrt{h_2^2} \right) + \beta_{2j}^* \left(\sqrt{h_2^2 (1 - r_g^2)} \right)\end{aligned}$$

These are the standardized marginal effect of variant j on each phenotype (defined on the latent liability scale in the case of the dichotomous phenotype Y_1). We denote them as β_j because they are the effects of interest for the GWASs of θ_1 and θ_2 .

GWAS test statistics for β_j

Given the above parameterization, we can now focus on the behaviour of the test statistics from the GWAS of each phenotype. These test statistics are of primary interest since they are the intended input for the desired meta-analysis across the two phenotypes. In particular, we are focused on defining the relationship between these test statistics and β_{1j} , the effect of variant j on the dichotomous phenotype, so that we can calibrate meta-analysis of the observed Z scores to test the null hypothesis $\beta_{1j} = 0$.

Before discussing the test statistics for the observed phenotypes however, it is instructive to describe test statistics for a hypothetical GWAS of the latent phenotypes (θ_1 and θ_2), as a foundation evaluating the impact of e.g. dichotomizing θ_1 to a case/control phenotype. If both θ_1 and θ_2 were observed, we could define Z scores for the standardized effects β_j as

$$\begin{aligned}Z_{\theta,1j} &= \sqrt{N_1} \hat{\beta}_{1j} \\ &= \sqrt{N_{1j}} \beta_{1j} + \sqrt{N_{1j}} \delta_{1j} \\ Z_{\theta,2j} &= \sqrt{N_2} \hat{\beta}_{2j} \\ &= \sqrt{N_{2j}} \beta_{2j} + \sqrt{N_{2j}} \delta_{2j}\end{aligned}$$

where $\hat{\beta}_j$ is the observed GWAS estimate of β_j , N_j is the sample size of the data used to estimate $\hat{\beta}_j$, and δ_j is the corresponding sampling error of the estimate.

$$\delta_{1j} \sim N\left(0, \frac{1}{N_{1j}} \text{var}\left[\left(\sqrt{h_1^2}\right)f_{1,-j} + e_1\right]\right)$$

$$\delta_{2j} \sim N\left(0, \frac{1}{N_{2j}} \text{var}\left[\left(r_g \sqrt{h_2^2}\right)f_{1,-j} + \left(\sqrt{h_2^2(1-r_g^2)}\right)f_{2,-j} + e_2\right]\right)$$

Assuming the marginal effect of any given variant is small, we can approximate $f_{1,-j} \approx f_1$ and

$f_{2,-j} \approx f_2$, giving

$$\begin{aligned}\delta_{1j} &\sim N\left(0, \frac{1}{N_{1j}} [h_1^2 + \epsilon_1^2]\right) \\ &\sim N\left(0, \frac{1}{N_{1j}}\right) \\ \delta_{2j} &\sim N\left(0, \frac{1}{N_{2j}} [r_g^2 h_2^2 + (1-r_g^2)h_2^2 + \epsilon_2^2]\right) \\ &\sim N\left(0, \frac{1}{N_{2j}} [h_2^2 + \epsilon_2^2]\right) \\ &\sim N\left(0, \frac{1}{N_{2j}}\right)\end{aligned}$$

based on f and e being independent, $\text{var}(f) = 1$, $\text{var}(e) = \epsilon^2$, and $h^2 + \epsilon^2 = 1$. To the extent that $f \neq f_{-j}$, then this is an overestimate of the variance of δ_j since $\text{var}(f_{-j}) \leq 1$. Returning to the Z scores defined previously, this gives

$$Z_{\theta,1j} \sim N(\sqrt{N_{1j}}\beta_{1j}, 1)$$

$$Z_{\theta,2j} \sim N(\sqrt{N_{2j}}\beta_{2j}, 1)$$

which have the desired standard normal distribution when $\beta_j = 0$. We can also express these in terms of the latent effects β_j^*

$$Z_{\theta,1j} \sim N(\sqrt{N_{1j}h_1^2}\beta_{1j}^*, 1)$$

$$\begin{aligned}
Z_{\theta,2j} &\sim N\left(r_g\sqrt{N_{2j}h_2^2}\beta_{1j}^* + \sqrt{N_{2j}h_2^2(1-r_g^2)}\beta_{2j}^*, 1\right) \\
&\sim N\left(\sqrt{N_{2j}h_2^2}[r_g\beta_{1j}^* + \sqrt{1-r_g^2}\beta_{2j}^*], 1\right)
\end{aligned}$$

We now consider how the actual observed Z statistics for each phenotype will differ from these idealized tests of association with the latent phenotypes.

Test of β_{ij} in GWAS of dichotomous Y_1

For the dichotomous phenotype (i.e. ADHD diagnosis) we do not observe the latent liability θ_1 , and thus we cannot compute $Z_{\theta,1j}$. Instead the GWAS results come from logistic regression of the observed phenotype Y_1 . The statistical properties of Z_{2j} will be affected by two key features of GWAS with case/control phenotypes: dichotomization and ascertainment. For dichotomization, recall that

$$\beta_{1j} = \text{cor}(x_j, \theta_1)$$

It has been shown that dichotomizing one variable attenuates the correlation such that if x and Y are approximated as bivariate normal

$$\text{cor}(x_j, Y_1) \approx \frac{\phi(\Phi^{-1}[K])}{\sqrt{K(1-K)}} \text{cor}(x_j, \theta_1)$$

where K is the prevalence of $Y_1 = 1$ after dichotomization, and $\phi(\cdot)$ and $\Phi^{-1}(\cdot)$ are the density function and inverse of the cumulative density function of the standard normal distribution, respectively^{84,85}.

With respect to case/control ascertainment, we note that the power of logistic regression is approximately proportional to $\sqrt{P^*(1-P^*)}$, where P^* is the probability $Y = 1$ at the mean liability in the sample⁸⁶. Given a symmetric distribution of liability, $P^* \approx P$ where P is the sample proportion

of cases. Therefore, power for the analysis in an ascertained sample differs from power in a population sample with the sample size by a factor of $\sqrt{P(1-P)}/\sqrt{K(1-K)}$.

Putting together these adjustments for dichotomization and ascertainment, we adopt the approximation

$$Z_{1j} \sim N\left(\frac{\phi(\Phi^{-1}[K])}{\sqrt{K(1-K)}} \frac{\sqrt{P(1-P)}}{\sqrt{K(1-K)}} \sqrt{N_{1j}} \beta_{1j}, 1\right)$$

Importantly, we note that this adjustment mirrors the conversion between observed scale heritability and liability scale heritability derived by Lee et al⁸⁷.

$$h_{obs}^2 = h_{liab}^2 \frac{(\Phi^{-1}[K])^2}{K(1-K)} \frac{P(1-P)}{K(1-K)}$$

Indeed, noting that

$$\beta_{1j} = \beta_{1j}^* \sqrt{h_1^2}$$

we can equate

$$\begin{aligned} E(Z_{1j}) &= \frac{\phi(\Phi^{-1}[K])}{\sqrt{K(1-K)}} \frac{\sqrt{P(1-P)}}{\sqrt{K(1-K)}} \sqrt{N_{1j}} \beta_{1j} \\ &= \frac{\phi(\Phi^{-1}[K])}{\sqrt{K(1-K)}} \frac{\sqrt{P(1-P)}}{\sqrt{K(1-K)}} \sqrt{N_{1j}} \beta_{1j}^* \sqrt{h_1^2} \\ &= \sqrt{N_{1j}} \sqrt{h_1^2 \frac{(\Phi^{-1}[K])^2}{K(1-K)} \frac{P(1-P)}{K(1-K)}} \beta_{1j}^* \\ &= \sqrt{N_{1j}} \sqrt{h_{1,obs}^2} \beta_{1j}^* \end{aligned}$$

which highlights the parallel between the observed Z_{1j} , the test the effect of variant j on the observed scale, and the corresponding $Z_{\theta,1j}$ testing on the latent scale.

Finally, we can define an effective sample size adjustment for N_1

$$\tilde{N}_{1j} \equiv N_{1j} \frac{P(1-P) \phi(\Phi^{-1}[K])^2}{[K(1-K)]^2}$$

so that the approximate distribution of Z_{1j} from logistic regression of the dichotomous phenotype can be expressed as

$$Z_{1j} \sim N\left(\sqrt{\tilde{N}_{1j}}\beta_{1j}, 1\right)$$

This formulation, with Z_{1j} following a standard normal distribution conditional on (adjusted) sample size and the effect of interest (β_{1j}), is central to allowing the desired meta-analysis.

Test of β_{1j} in GWAS of continuous Y_2

For the continuous phenotype Y_2 , the observed Z scores are computed from conventional linear regression of the observed phenotype. The observed phenotype only differs from the latent θ_2 by a linear transformation to center and scale to unit variance. Thus, since Z scores are invariant linear transformations of the phenotype,

$$Z_{2j} = Z_{\theta,2j}$$

But unlike the dichotomous phenotype analysis, the GWAS of Y_2 is a test of $\beta_{2j} = 0$ rather than $\beta_{1j} = 0$. For the current analysis, our primary interest is in the latter test to identify effects β_{1j} of each variant on the dichotomous phenotype of ADHD diagnosis. The residual effects from f_2 in β_{2j}^* that are unique to the continuous trait (population measures of ADHD-related behavior) are of less relevance, and given a high r_g are anticipated to have a limited contribution even to the continuous measure (proportional to $\sqrt{1 - r_g^2}$).

For that reason, we adopt a random effects framework for β_{2j}^* , and treat them as nuisance parameters. Specifically, we assume that the causal effect sizes

$$\gamma_{2j}^* \sim N\left(0, \frac{1}{M}\right)$$

where M is the total number of variants j . This is equivalent to the standard infinitesimal random effects model used by^{45,88}, but specified here in terms of γ_{2j}^* on the latent scale of f_2 prior to scaling by h_2^2 for the phenotype. For the marginal effects

$$\beta_{2j}^* = \sum_k \gamma_{2k}^* r_{jk}$$

we additionally assume that γ_{2k}^* and r_{jk} are independent, meaning that the causal effect size of variant k is independent of its LD with other variants. This leads to

$$\beta_{2j}^* \sim N\left(0, \sum_k \frac{1}{M} r_{jk}^2\right)$$

$$\beta_{2j}^* \sim N\left(0, \frac{1}{M} l_j\right)$$

where we note that

$$l_j = \sum_k r_{jk}^2$$

is the LD score of variant j as defined by Bulik-Sullivan et al⁴⁵.

Returning to the Z score, we note that the previous expression for Z_{2j}^* is now a conditional distribution given a particular value of β_{2j}^* .

$$Z_{2j} | \beta_{2j}^* \sim N\left(\sqrt{N_{2j} h_2^2} \left[r_g \beta_{1j}^* + \sqrt{1 - r_g^2} \beta_{2j}^*\right], 1\right)$$

Substituting $\beta_{1j} = \beta_{1j}^* \sqrt{h_1^2}$ as the actual parameter of interest and marginalizing over β_{2j}^* as a random effect yields

$$Z_{2j} \sim N\left(r_g \sqrt{N_{2j} h_1^2 h_2^2} \beta_{1j}, 1 + (1 - r_g^2) \frac{N_{2j} h_2^2}{M} l_j\right)$$

To construct the intended meta-analysis for genetics effects on the diagnosis of ADHD, we want to have a test statistic that has a standard normal distribution under the null hypothesis $\beta_{1j} = 0$. Although Z_{2j} is normally distributed with mean zero under that null hypothesis, it's variance is inflated if Y_2 is heritable (i.e. $h_2^2 > 0$) and is not completely genetically correlated with Y_1 (i.e. $r_g < 1$). We note that inflation proportional to $N_{2j}h_2^2l_j/M$ is consistent the expected values derived by Bulik-Sullivan et al.⁴⁵ To obtain a statistic with the desired distribution, we define a new modified Z score

$$\tilde{Z}_{2j} = \text{sign}(r_g) \cdot \frac{Z_{2j}}{\sqrt{1 + (1 - r_g^2) \frac{N_{2j}h_2^2}{M} l_j}}$$

which is distributed as

$$\tilde{Z}_{2j} \sim N \left(\frac{|r_g| \sqrt{N_{2j}h_2^2/h_1^2}}{\sqrt{1 + (1 - r_g^2) \frac{N_{2j}h_2^2}{M} l_j}} \beta_{1j}, 1 \right)$$

Including $\text{sign}(r_g)$ in this definition of \tilde{Z}_{2j} ensures that its expected value has the same sign as β_{1j} . We note that $|\tilde{Z}_{2j}| \leq |Z_{2j}|$ since $[1 + (1 - r_g^2) N_{2j}h_2^2l_j/M] \geq 1$ by definition for the involved quantities. Therefore \tilde{Z}_{2j} can be interpreted as a more conservative estimate for inference about β_{1j} that has been attenuated from the raw observation proportional to the potential for genetic effects on the continuous phenotype to be unique to that phenotype rather than shared with the dichotomous outcome (i.e. $[1 - r_g^2]h_2^2$).

Lastly, if we define adjusted N_2 as

$$\tilde{N}_{2j} \equiv N_{2j} \frac{r_g^2 h_2^2 / h_1^2}{1 + (1 - r_g^2) N_{2j} h_2^2 l_j / M}$$

then the distribution of the modified test statistic can be expressed as

$$\tilde{Z}_{2j} \sim N\left(\sqrt{\tilde{N}_{2j}}\beta_{1j}, 1\right)$$

We note that the multiplication by $\text{sign}(r_g)$ in defining \tilde{Z}_{2j} ensures that it's distribution involves the positive root of \tilde{N}_{2j} and matches the sign of β_{1j} in expectation. The resulting statistic provides a clear parallel to Z_{1j} for the dichotomous phenotype, and sets up the meta-analysis of the two Z scores.

Meta-analysis for β_{1j} from GWAS of dichotomous Y_1 and continuous Y_2

Summarizing the above derivations, we have now established a framework for the GWAS results of dichotomous phenotype Y_1 and continuous phenotype Y_2 , respectively, where we can approximate

$$Z_{1j} \sim N\left(\sqrt{\tilde{N}_{1j}}\beta_{1j}, 1\right)$$

$$\tilde{Z}_{2j} \sim N\left(\sqrt{\tilde{N}_{2j}}\beta_{1j}, 1\right)$$

where

$$\tilde{Z}_{2j} = \text{sign}(r_g) \cdot \frac{Z_{2j}}{\sqrt{1 + (1 - r_g^2)N_{2j}h_2^2 l_j/M}}$$

$$\tilde{N}_{1j} = N_{1j} \frac{P(1 - P) \phi(\Phi^{-1}[K])^2}{[K(1 - K)]^2}$$

$$\tilde{N}_{2j} = N_{2j} \frac{r_g^2 h_2^2 / h_1^2}{1 + (1 - r_g^2) N_{2j} h_2^2 l_j / M}$$

From this form, we have a pair of Z statistics for β_{1j} with corresponding (adjusted) sample sizes.

This is sufficient to then proceed with a conventional sample size-weighted meta-analysis⁸⁹.

$$Z_{j,meta} = \frac{\sqrt{\tilde{N}_{1j}}Z_{1j} + \sqrt{\tilde{N}_{2j}}\tilde{Z}_{2j}}{\sqrt{\tilde{N}_{1j} + \tilde{N}_{2j}}}$$

Expanding the numerator makes it clear that the adjusted sample size weights corresponds to weighting each Z proportional to the observed heritability and then balancing by genetic correlation.

$$Z_{j,meta} = \frac{\sqrt{N_{1j} \frac{P(1-P)\phi(\Phi^{-1}[K])^2}{[K(1-K)]^2}}Z_{1j} + \sqrt{N_{2j} \frac{r_g^2 h_2^2/h_1^2}{1 + (1-r_g^2)N_{2j}h_2^2 l_j/M}}\tilde{Z}_{2j}}{\sqrt{\tilde{N}_{1j} + \tilde{N}_{2j}}}$$

$$Z_{j,meta} \propto \sqrt{h_{1,obs}^2} \sqrt{N_{1j}} Z_{1j} + |r_g| \sqrt{h_2^2} \sqrt{N_{2j}} \frac{\tilde{Z}_{2j}}{\sqrt{1 + (1-r_g^2)N_{2j}h_2^2 l_j/M}}$$

We use these weights to implement the meta-analysis of the GWAS of ADHD-related behaviour from EAGLE/QIMR with GWAS of ADHD diagnoses.

Notes on Implementation

It may be noted that \tilde{Z}_{2j} , \tilde{N}_{1j} , and \tilde{N}_{2j} are computed from both observed values (Z_{1j} , Z_{2j} , N_{1j} , N_{2j} , and P) and unknown population parameters (K , r_g^2 , h_1^2 , h_2^2 , l_j , and M). Sensible estimates for each of these population parameters can be obtained as described below and plugged into the expression for the weights. Importantly, estimation error in K , r_g^2 , h_1^2 , h_2^2 , l_j , and M is only expected to affect the efficiency (i.e. power) of the meta-analysis. For a fully null variant (i.e. $\beta_{1j}^* = \beta_{2j}^* = 0$), Z_{1j} and Z_{2j} both have standard normal distributions, and since they are independent any weighted combination of these Z scores will also follow the null distribution. Suboptimal weights will only affect the power of the meta-analysis when the null hypothesis does not hold. In addition, since we use \tilde{Z}_{2j} in place of

\tilde{Z}_{2j} and $|\tilde{Z}_{2j}| \leq |Z_{2j}|$, the test of $Z_{j,meta}$ will be conservative when there is no genetic effect specific to the continuous phenotype (i.e. $\beta_{2j}^* = 0$).

With this reassurance, we obtain estimates of K , r_g^2 , h_1^2 , h_2^2 , l_j , and M as follows:

- Estimates of K can be derived from the literature. We use $K = .05$ for the prevalence of ADHD here and throughout this paper⁹⁰.
- Estimates of r_g^2 , h_1^2 and h_2^2 are computed from the GWAS results using LD score regression⁴⁵. For meta-analysis with the ADHD GWAS, we use the European ADHD GWAS to estimate these parameters in order to ensure that the population ancestry is matched between the input GWAS for ADHD, EAGLE/QIMR, and the European reference panel used for computing LD scores.
- For M , we utilize the value $M = 5,961,159$ corresponding to LD scores computed from 1000 Genomes Project Phase 3 data on individuals of European ancestry³⁹. These LD scores have been described previously⁶⁹ and are publically available for download at: <http://data.broadinstitute.org/alkesgroup/LDSCORE/>
- We estimate $l_j = 124.718$, the mean LD score of common HapMap3 SNPs as computed from 1000 Genomes Project Phase 3 data on individuals of European ancestry (as above). We use this value for two reasons: (a) using a single value is convenient and allows meta-analysis for all variants in the GWAS, including variants that may not be present in the precomputed LD scores from the 1000 Genomes Project reference data; and (b) we can demonstrate that the value of l_j has a trivial impact on the derived meta-analysis weights when the sample sizes, heritabilities, and genetic correlation are at the levels observed in the current study.

To demonstrate this final point, we consider the relative difference in \tilde{Z}_{2j} and \tilde{N}_{2j} conditional on a range of possible values of l_j with fixed values of N_{1j} , N_{2j} , and P and fixed estimates of K , r_g^2 , h_1^2 , h_2^2 , and M . First, we observe that the >99.5% of 1000 Genomes LD scores have values between 0 and 1000 (Supplementary Figure 24); variants with higher LD scores are predominantly from known regions of long-range LD (e.g. the MHC region⁴⁰). Then we show that for LD scores in this range the value of $\sqrt{1 + (1 - r_g^2)N_{2j}h_2^2 l_j/M}$, the term used to adjust the magnitude of Z_{2j} to account for polygenic effects specific to the second phenotype, is minimally affected by the value of l_j conditional on the estimates of r_g^2 , N_{2j} , and h_2^2 , observed in the current study (Supplementary Figure 19). The impact of l_j on the relative effective sample size \tilde{N}_{2j} is also limited, with the weight effectively unchanged for values of l_j between 0 and 1000 (Supplementary Figure 20).

We note however that the limited effect of l_j on the shrinkage parameter and the relative effective sample size is conditional on the estimated values for the other parameters in the current study.

Specifically, l_j contributes to the meta-analysis weights through the term $\sqrt{1 + (1 - r_g^2)N_{2j}h_2^2 l_j/M}$.

When r_g is large (e.g. $r_g = .97$ for the ADHD GWAS and EAGLE/QIMR) and N_{2j} and h_2^2 are modest (e.g. $N_{2j} = 20,464$ and $h_2^2 = .064$ for EAGLE/QIMR) the potential contribution of l_j to the value of this term is limited. On the other hand, if the genetic correlation is further from 1 (e.g. $r_g = .7$) or the GWAS of the continuous phenotype is better powered (e.g. $N_{2j} = 40,000$ and $h_2^2 = .16$) then the influence of l_j on the meta-analysis weights becomes non-negligible (Supplementary Figures 18-19). Thus, although the parameters for the current study enable the convenient use of mean l_j for all variants, this simplification cannot be expected to hold for all studies.

Supplementary Tables

Supplementary Table 1. Samples included in the GWAS meta-analyses of diagnosed ADHD

Samples marked in bold are included in the GWAS meta-analysis. The European GWAS meta-analysis excludes samples marked with “*” and PUWMa (strict) is used in place of PUWMa. For each cohort, the number of cases and controls and the percentage of females (“% F”) among each group is reported. The age group of ADHD cases (children or adults) is given. Principal components (“PCs”) and other covariates used in each GWAS are indicated. “Literature” lists previously published studies including the ADHD cohort.

Sample	Cases	% F cases	Controls	% F controls	Age Group	Sample design	Ancestry	Covariates	Genotyping chip	Literature
Lundbeck Foundation Initiative for Integrative Psychiatric Research (iPSYCH)										
iPSYCH-ADHD, Denmark	14584	26.6%	22492	49.2%	Children & adults	Case-control	European	PCs	PsychChip	New
Psychiatric Genomics Consortium (PGC)										
Barcelona, Spain	572	30.20%	425	23.50%	Adults	Case-control	European	PCs	Illumina Omni1-Quad	Ribases et al. ⁹¹ , Sanchez-Mora et al. ¹³
Beijing, China*	1012	15.70%	925	37.80%	Children	Case-control	Han Chinese	PCs	Affymetrix 6.0	Yang et al. ¹⁴
Bergen, Norway	295	53.60%	202	60.90%	Adults	Case-control	European	PCs	Illumina OmniExpress-12v1	Zayats et al. ¹⁵
Cardiff, UK	721	12.90%	5081	49.40%	Children	Case-control	European	PCs	Illumina 660K (cases) & Illumina 1.2M (controls)	Stergiakouli et al. ¹⁶
CHOP, USA	262	24.40%	262	24.40%	Children	Trios	European	None	Illumina 550K	Elia et al. ⁸ , Neale et al. ¹⁰
Germany	487	19.30%	1290	49.10%	Children	Case-control	European	PCs	Illumina 660K (cases) & Illumina 550v3 (controls)	Hinney et al. ¹⁷
IMAGE-I	700	12.10%	700	12.10%	Children	Trios	European	Site	Perlegen 600K	Neale et al. ^{9,10}

IMAGE-II	624	18.60%	1755	50.00%	Children	Case-control	European	PCs	Affymetrix 5.0 & Affymetrix 6.0	Neale et al. ¹⁰
PUWMa*	635	35.70%	635	35.70%	Children	Trios	Diverse (USA)	PCs	Illumina 1M-Duo	Mick et al. ¹¹ , Neale et al. ¹⁰
PUWMa (strict)	563	35.90%	563	35.90%	Children	Trios	European	PCs	Illumina 1M-Duo	
Toronto, Canada	109	24.80%	109	24.80%	Children	Trios	European	None	Affymetrix 6.0	Lionel et al. ¹²
Yale-Penn	182	30.20%	1315	42.20%	Adults	Case-control	European	PCs, alcohol dependence diagnosis	Illumina HumanOmni1-Quad & Illumina Infinium Human Core Exome	Gelernter et al. ²¹⁻²³ (studies of substance use disorders)

Supplementary Table 2. Conditional Analysis of Secondary GWAS Signals

Linkage disequilibrium (r^2) computed between the putative secondary effect variant and the index variant in individuals of European ancestry from the 1000 Genomes Project (1KG), and imputed genotypes in the merged PGC and iPSYCH cohorts (20,183 cases and 35,191 controls). Two-sided P-values from meta-analysis using an inverse-variance weighted fixed effects model based on results from logistic regression with the imputed genotype dosage for the lead index variant included as a covariate together with covariates from the primary GWAS. Odds ratio (OR) and standard error (SE) of the secondary variant reported for the primary GWAS and conditional on the corresponding index variant.

Variant	CHR	BP	Index Var.	r^2 with Index Variant			Marginal Association			Conditional Association		
				1KG	PGC	iPSYCH	OR	SE	P	OR	SE	P
rs3952787	1	44323244	rs11420276	0.054	0.046	0.064	1.085	0.015	3.49×10^{-8}	1.063	0.015	6.02×10^{-5}
rs304132	5	88215594	rs4916723	0.051	0.059	0.091	0.925	0.014	4.23×10^{-8}	0.939	0.015	2.03×10^{-5}

Supplementary Table 3. Heritability and genetic correlations for PGC ADHD samples

Univariate and bivariate heritability estimates for PGC ADHD samples stratified by study design type (case-control vs. parent-offspring trios). The estimated SNP heritability (SNP-h^2) of each subset and the genetic correlation (r_g) between the two sets are reported with their respective standard errors (SE). Heritability estimates are reported on the liability scale assuming a 5% population prevalence of ADHD.

Cohort	N cases	N controls	SNP- h^2 (SE)	r_g (SE)
PGC case-control	2871	9983	0.138 (0.019)	1.02 (0.32)
PGC trios	1628	1629	0.081 (0.045)	

Supplementary Table 4. SNP heritability of ADHD

Estimated SNP heritability (h^2) and standard error (SE) using LD score regression (ldsc) and univariate GREML analysis in GCTA. Estimates are reported on the liability scale assuming a 5% population prevalence of ADHD. Only PGC European samples (Eur samples) were included. NA = not available.

Sample	N cases	N controls	h^2 (ldsc)	SE (ldsc)	h^2 (GCTA)	SE (GCTA)
iPSYCH	14,584	22,492	0.26	0.02	0.187	0.008
PGC (Eur samples)	4,515	11,702	0.12	0.03	0.104	0.013
iPSYCH+PGC (Eur samples)	19,099	34,194	0.22	0.01	NA	NA

Supplementary Table 5. Genetic correlations of ADHD with other selected traits

Genetic correlation (r_g) and its standard error (SE) is estimated using LD score regression and summary statistics from the European GWAS meta-analysis (iPSYCH + PGC European samples (Eur samples), (19,099 cases, 34,194 controls) and summary statistics from published GWASs of other selected traits. Two-sided P-values represents tests for the difference of the genetic correlations from zero. Correlations significant after Bonferroni correction are presented in the table (correction for 219 tests). Extended table with results for all 219 phenotypes can be found in Supplementary Data 1). Four significant results are omitted in this table as they were based on analyses of populations with mixed ancestry (Body fat and Coronary artery disease) and large overlap in samples already represented in other analyses (Years of schooling 2013 and 2014), results for correlation with these traits can be found in Supplementary Data 1.

Trait	Trait type	N	r _g	SE	P-value
Childhood IQ ⁹²	Cognition/education	17,989	-0.411	0.082	5.09 x 10 ⁻⁷
Years of schooling ⁸²	Cognition/education	328,917	-0.535	0.028	1.44 x 10 ⁻⁸⁰
College completion ⁹³	Cognition/education	126,559	-0.538	0.046	3.30 x 10 ⁻³¹
Human intelligence ⁷⁵	Cognition/education	78,308	-0.407	0.039	7.03 x 10 ⁻²⁶
UKB college/university degree ⁷⁶	Cognition/education	111,114	-0.520	0.038	5.60 x 10 ⁻⁴²
UKB verbal–numerical reasoning ⁷⁶	Cognition/education	36,035	-0.360	0.050	5.58 x 10 ⁻¹³
Neuroticism ⁹⁴	Personality	170,911	0.264	0.046	1.02 x 10 ⁻⁸
Depressive symptoms ⁹⁴	Psychiatric	161,460	0.446	0.050	7.00 x 10 ⁻¹⁹
Subjective well being ⁹⁴	Psychiatric	298,420	-0.283	0.048	3.73 x 10 ⁻⁹
Major depressive disorder ⁷⁹	Psychiatric	461,134	0.424	0.033	7.38 x 10 ⁻³⁸
PGC cross-disorder analysis ⁹⁵	Psychiatric	61,220	0.266	0.046	5.58 x 10 ⁻⁹
Anorexia nervosa ⁷⁸	Psychiatric	14,477	-0.244	0.065	1.62 x 10 ⁻⁴
Body mass index ⁹⁶	Weight related	123,865	0.258	0.032	1.68 x 10 ⁻¹⁵
Waist circumference ⁹⁷	Weight related	224,459	0.269	0.034	2.20 x 10 ⁻¹⁵
Hip circumference ⁹⁷	Weight related	254,459	0.160	0.034	2.13 x 10 ⁻⁶
Waist-to-hip ratio ⁹⁸	Weight related	254,459	0.304	0.036	1.16 x 10 ⁻¹⁷
Overweight ⁹⁷	Weight related	158,855	0.275	0.036	1.73 x 10 ⁻¹⁴
Obesity class 1 ⁹⁷	Weight related	98,697	0.285	0.036	1.81 x 10 ⁻¹⁵
Obesity class 2 ⁹⁷	Weight related	75,729	0.320	0.046	5.10 x 10 ⁻¹²
Obesity class 3 ⁹⁷	Weight related	50,364	0.338	0.067	4.05 x 10 ⁻⁷
Extreme BMI ⁹⁷	Weight related	16,068	0.254	0.052	9.31 x 10 ⁻⁷
Childhood obesity ⁹⁹	Weight related	13,848	0.216	0.046	3.29 x 10 ⁻⁶
Type 2 Diabetes ¹⁰⁰	Glycemic	149,821	0.185	0.047	7.80 x 10 ⁻⁵
HDL cholesterol ¹⁰¹	Lipids	99,900	-0.217	0.042	2.44 x 10 ⁻⁷
Triglycerides ¹⁰¹	Lipids	96,598	0.159	0.040	6.49 x 10 ⁻⁵
Ever vs never smoked ¹⁰²	Smoking behaviour	74,035	0.478	0.059	4.33 x 10 ⁻¹⁶
Cigarettes smoked per day ¹⁰²	Smoking behaviour	68,028	0.451	0.103	1.07 x 10 ⁻⁵
Former vs Current smoker ¹⁰²	Smoking behaviour	41,969	-0.344	0.086	6.74 x 10 ⁻⁵
Lung cancer ¹⁰³	Cancer	56,697	0.390	0.063	6.35 x 10 ⁻¹⁰
Lung cancer (all) ¹⁰⁴	Cancer	27,209	0.368	0.071	2.53 x 10 ⁻⁷
Squamous cell lung cancer ¹⁰³	Cancer	56,697	0.549	0.135	4.57 x 10 ⁻⁵
Age of first birth ¹⁰⁵	Reproductive	251,151	-0.612	0.037	3.70 x 10 ⁻⁶¹
Number of children ever born ¹⁰⁵	Reproductive	343,072	0.421	0.051	8.51 x 10 ⁻¹⁷
Age at Menopause ⁵⁹	Reproductive	69,360	-0.161	0.042	1.50 x 10 ⁻⁴
Mothers age at death ¹⁰⁶	Aging	52,776	-0.432	0.087	6.48 x 10 ⁻⁷
Fathers age at death ¹⁰⁶	Aging	63,775	-0.298	0.066	7.19 x 10 ⁻⁶
Parents age at death ¹⁰⁶	Aging	45,627	-0.376	0.091	3.51 x 10 ⁻⁵
Insomnia ⁷⁷	Sleep	113,006	0.421	0.064	3.85 x 10 ⁻¹¹
Rheumatoid Arthritis ¹⁰⁷	Autoimmune	103,638	0.162	0.042	1.32 x 10 ⁻⁴

Supplementary Table 6. Summary of Bayesian Credible Set Results

For each genome-wide significant locus (denoted with the chromosome [CHR] and base pair [BP] position of the index variant), the number of variants that are the in the 99% credible set computed based on linkage disequilibrium (LD) in the PGC European cohorts (4,515 cases 11,702 controls), the 99% credible set computed based on LD in the iPSYCH data (14,584 cases 22,492 controls), and their overlap (19,099 cases, 34,194 controls).

CHR	Index Variant	BP	Number of Variants in Credible Set		
			PGC only	iPSYCH only	Both sets
1	rs11420276	44184192	0	0	96
12	rs1427829	89760744	0	0	13
16	rs212178	72578131	0	3	21
4	rs28411770	31151456	0	0	53
10	rs11591402	106747354	0	0	87
8	rs74760947	34352610	0	1	13
2	rs9677504	215181889	0	0	23
5	rs4916723	87854395	0	0	67
7	rs5886709	114086133	5	0	63
3	rs4858241	20669071	1	5	44
15	rs281324	47754018	0	0	43
1	rs1222063	96602440	0	4	4

Supplementary Table 7. Biological function of potential ADHD risk genes located in genome-wide significantly associated loci

Literature review of biological function, mutational constraint, tissue-specific expression, and relevant phenotypic associations for genes affiliated with the 12 loci significantly associated with ADHD. Mutational constraint is indexed by the estimated probability of loss-of-function intolerance (pLI) reported by the Exome Aggregation Consortium (ExAC; release 0.3.1)⁶³.

Chr	Gene	Index SNP	P-value	Function of encoded product	pLI	Tissue specificity	ADHD-related phenotype associations
1	<i>ST3GAL3</i>	rs11420276	2.14 x 10 ⁻¹³	ST3 Beta-Galactoside Alpha-2,3-Sialyltransferase 3 (<i>ST3GAL3</i>), encodes a membrane protein (ST3Gal III) that adds sialic acid to the terminal site of glycolipids or glycoproteins. ST3Gal III may play an important role in brain development as the human brain is especially enriched in sialic acid-containing glycolipids (termed gangliosides) ¹⁰⁸⁻¹¹⁰ and in mice <i>St3gal2</i> and <i>St3gal3</i> were found to be responsible for nearly all the terminal sialylation of brain gangliosides ¹¹¹ as well as playing an important role for normal cognition ¹⁰⁹ . Gangliosides are known to modulate Ca(2+) homeostasis and signal transduction in neurons ^{112,113} .	0.57	This gene is expressed in several tissues including neurons ¹⁰⁹ .	Mutations in this gene have been associated with autosomal recessive mental retardation ¹¹⁰ and early infantile epileptic encephalopathy ¹¹⁴ . DNA methylation at sites annotated to <i>ST3GAL3</i> were reported capable to differentiate individuals with high and low ADHD symptomatology ratings ¹¹⁵ . Variants in <i>ST3GAL3</i> have also been associated with educational attainment ⁸² .
1	<i>PTPRF</i>	rs3001723	3.62 x 10 ⁻¹⁰	Homo sapiens protein tyrosine phosphatase, receptor type, F (<i>PTPRF</i>). <i>PTPRF</i> encodes the leukocyte common antigen-related (LAR) receptor PTP which is present in neurons expressing	1.00	This gene is expressed in several tissues including neurons ¹¹⁷ .	Gws association of genetic markers in <i>PTPRF</i> with schizophrenia has been found ³⁵ . Gws association of genetic markers in <i>PTPRF</i> with educational attainment has been found in a study of

				TrkB, and LAR is associated with caveolae and regulates survival and neurite outgrowth ¹¹⁶ . The LAR receptor is present in neurons expressing TrkB, which is receptor for the brain-derived neurotrophic factor (BDNF), and it has been demonstrated that LAR, through its interaction with TrkB can affect the neurotrophic activity of BDNF ¹¹⁷ .			individuals from the UK Biobank (N=112,151) ⁷⁶ . Overexpression of the LAR receptor encoded by <i>PTPRF</i> may contribute to insulin resistance ¹¹⁸ .
1	Intergenic	rs1222063	3.07 x 10 ⁻⁸	Not applicable.	n/a	Not applicable.	Not applicable.
2	<i>SPAG16</i>	rs9677504	1.39 x 10 ⁻⁸	Homo sapiens sperm associated antigen 16 (<i>SPAG16</i>). <i>SPAG16</i> encodes two major proteins that associate with the microtubular backbone of sperm tails and the nucleus of postmeiotic germ cells ^{119,120} .	0.00	Highly expressed in testis, but also detected throughout many tissues including brain, spinal cord, pituitary ovary, esophagus, thyroid, vagina, tibial nerve, bladder (http://www.gtexportal.org/home/gene/ENSG00000144451.14)	Studies have suggested that SPAG16 may play a role in multiple sclerosis ^{121,122} .
3	Intergenic	rs4858241	1.74 x 10 ⁻⁸	Not applicable.	n/a	Not applicable.	Not applicable.
4	<i>PCDH7</i>	rs28411770	1.15 x 10 ⁻⁸	Homo sapiens protocadherin 7 (<i>PCDH7</i>). This gene belongs to the protocadherin gene family, a subfamily of the cadherin superfamily. It encodes an integral membrane protein that is thought to function in cell-cell recognition and calcium-dependent adhesion ^{123,124} and plays an important role in neuron development ¹²⁵ .	n/a	The gene is expressed in several brain regions especially the thalamus, cerebral cortex and brainstem circuits ¹²⁶ .	Variants in <i>PCDH7</i> have been significantly associated with generalised epilepsy in GWAS ¹²⁷ . <i>PCDH7</i> is a target gene for <i>MECP2</i> ¹²⁸ and <i>MECP2</i> mutations causes Rett syndrome, which is a neurodevelopmental disorder characterized by loss of speech, microcephaly, seizures, and mental retardation (http://omim.org/entry/312750).

5	<i>LINC00461</i>	rs4916723	1.58 x 10 ⁻⁸	Homo sapiens long intergenic noncoding RNA 461 (<i>LINC00461</i>), also known as visual cortex-expressed gene (Visc). The locus is conserved across diverse mammals, but mouse knockouts of the Visc-2 transcript do not exhibit any clear anatomical phenotype ¹²⁹ .	n/a	Primarily expressed in the brain ⁵² (https://www.gtexportal.org/home/gene/LINC00461). In mice, it's strongly localized in the cortex and sites of neurogenesis during neurodevelopment and continuing into adulthood ¹²⁹ .	Variants in <i>LINC00461</i> have been associated with educational attainment ⁸² .
5	<i>MEF2C</i> / <i>MEF2C-AS1</i>	rs304132	4.22 x 10 ⁻⁸	Homo sapiens myocyte enhancer factor 2C (<i>MEF2C</i>). <i>MEF2C</i> encodes a member of the MADS box transcription factors, which binds to the conserved MADS box sequence motif ¹³⁰ . <i>MEF2C</i> is important for normal neuronal function by regulating neuronal proliferation, differentiation, survival and synapse development ¹³¹⁻¹³³ . Plays a role in hippocampal-dependent learning and memory, possibly by controlling the number of excitatory synapses ^{132,134} .	0.00	<i>MEF2C</i> is expressed in brain especially the frontal cortex, cortex and skeletal muscle (http://www.gtexportal.org/home/gene/MEF2)	Mutations and deletions in <i>MEF2C</i> have been associated with severe mental retardation, stereotypic movements, epilepsy, lack of speech and cerebral malformation (http://omim.org/entry/613443). GWAS studies have identified genome-wide significant association of variants in loci implicating <i>MEF2C</i> with Alzheimer's disease ¹³⁵ , depression ¹³⁶ and schizophrenia ³⁵ . <i>Mef2c</i> knockout mice have demonstrated autism like behaviours ^{131,133} , and individuals with <i>MEF2C</i> deletions have been found to display autism like traits ^{137,138} .
7	<i>FOXP2</i>	rs5886709	1.66 x 10 ⁻⁸	Homo sapiens forkhead box P2 (<i>FOXP2</i>). This gene encodes a member of the forkhead/winged-helix (FOX) family of transcription factors. <i>FOXP2</i> is involved in e.g. synapse formation and neural mechanisms mediating the development of speech and language and learning related to linguistic issues ¹³⁹⁻¹⁴¹ . It influences a large number of downstream gene targets ^{62,139,142} with	1.00	<i>FOXP2</i> is expressed in both fetal and adult human brain ^{143,144} .	Deletions in <i>FOXP2</i> may cause speech-language disorder 1 (SPCH1) inherited in an autosomal dominant manner. The disorder is characterized by abnormal development of several brain areas critical for both orofacial movements and sequential articulation ^{142,145} (http://omim.org/entry/602081). Candidate gene analysis previously suggested tentative evidence for association between <i>FOXP2</i> and ADHD ¹⁴⁶ . Variants in <i>FOXP2</i> have also

				potential regional or tissue-specific differences in activity ⁶² .			been associated with educational attainment ⁸² , and age of having a child ¹⁰⁵ .
8	<i>LINC01288</i>	rs74760947	1.35 x 10 ⁻⁸	Homo sapiens long intergenic non-protein coding RNA 1288 (<i>LINC01288</i>). No additional information available.	n/a	No information available.	No information available.
10	<i>SORCS3</i>	rs11591402	1.34 x 10 ⁻⁸	Homo sapiens sortilin-related VPS10 domain containing receptor 3 (<i>SORCS3</i>). This gene encodes a transmembrane receptor that is a member of the vacuolar protein sorting 10 receptor family ¹⁴⁷ . <i>SORCS3</i> is involved in signalling and intracellular sorting ¹⁴⁸ important for neuronal development and synaptic plasticity ^{149,150} .	0.33	Expressed in both the prenatal and adult brain regions ¹⁵⁰ (http://www.gtexportal.org/home/gene/SORCS3)	Rare CNVs overlapping <i>SORCS3</i> have been suggested to be involved in ADHD ¹² . Decreased expression of <i>SORCS3</i> in brains from patients with Alzheimer's disease compared to controls has been found ¹⁵¹ . GWAS studies have demonstrated strong association of variants in <i>SORCS3</i> with schizophrenia (however not gws) ³⁵ and gws association with depression ¹³⁶ .
12	<i>DUSP6</i>	rs1427829	1.82 x 10 ⁻⁹	Homo sapiens dual specificity phosphatase 6 (<i>DUSP6</i>). The protein encoded by <i>DUSP6</i> is a member of the dual specificity protein phosphatase subfamily ¹⁵² . <i>DUSP6</i> (also referred to as mitogen kinase phosphatase 3 (<i>MKP-3</i>)) is involved in negative regulation of mitogen-activated protein kinases (MAPKs) by acting as a dual phosphatase that dephosphorylate MAPKs at both threonine and tyrosine residues and thereby inactivate them ¹⁵³ . <i>DUSP6</i> is a cytoplasmic enzyme which has preference for extracellular signal-regulated MAPKs ¹⁵³⁻¹⁵⁵ . MAPKs are components of highly conserved signal transduction pathways, responding to a wide variety of extracellular and intracellular stimuli, and they are	0.91	Generally expressed at low levels in the brain (http://gtexportal.org/home/gene/DUSP6) and is strongly regulated during development ¹⁵⁸ .	Rare mutations in <i>DUSP6</i> may lead to congenital hypogonadotropic hypogonadism ¹⁶² (http://omim.org/entry/602748). <i>DUSP6</i> may play a role in Hirschsprung's disease, due to decreased expression ¹⁶³ . <i>DUSP6</i> have been found in reduced levels in Alzheimer brains ¹⁶⁴ . Additionally, <i>MKP-3</i> may play a critical role in cancer development ^{165,166} .

				involved in e.g. embryogenesis, cellular proliferation and differentiation ¹⁵⁶⁻¹⁵⁸ . Additionally <i>MKP-3</i> has been suggested to play a role in regulating neurotransmitter homeostasis, as increased <i>MKP-3</i> was found to reduce depolarization-dependent release of dopamine in rat PC12 cells, possibly through a down regulation of <i>Cacna1c</i> ¹⁵⁹ . It has been suggested that <i>MKP-3</i> stabilizes the dopamine transporter in the presynaptic dopaminergic neuron ¹⁶⁰ . <i>MKP-3</i> is upregulated by methamphetamine ¹⁶¹ .			
15	<i>SEMA6D</i>	rs281324	2.68 x 10 ⁻⁸	Homo sapiens sema domain, transmembrane domain (TM), and cytoplasmic domain, (semaphorin) 6D (<i>SEMA6D</i>). The product encoded by this gene is a transmembrane semaphoring which play role in maintenance and remodelling of neuronal connections ¹⁶⁷ . <i>Sema6D</i> acts as ligand for PlexinA1 which is involved in critical steps of neuronal development in the spinal cord ¹⁶⁸ as well as cardiac development ^{169,170} .	1.00	Expressed in adult brain, spinal cord, and fetal brains ¹⁶⁷ .	Variants in <i>SEMA6D</i> have been associated with educational attainment ⁸² .
16	<i>LINC01572</i>	rs212178	7.68 x 10 ⁻⁹	Homo sapiens long intergenic non-protein coding RNA 1572 (<i>LINC01572</i>). No additional information available.	n/a	No information available.	No information available.

Supplementary Table 8. Results from MAGMA gene-based association with ADHD

Genes demonstrating significant gene-wise association with ADHD after Bonferroni correction in the MAGMA⁴⁶ analysis (based on summary statistics from the European GWAS meta-analysis, 19,099 cases; 34,194 controls). Chromosome (CHR), number of SNPs in the genes (N SNPS) and number of relevant parameters used in the model (N PARAM), two-sided association P-values (P) are shown. Chromosome band location of the associated gene and the chromosome band location of the nearest gws single marker are shown. Genes marked in bold are not overlapping with loci with gws single markers.

Gene	CHR	N SNPS	N PARAM	P	Location of Gene	Location of nearest gws marker
<i>ST3GAL3</i>	1	483	57	7.38×10^{-12}	1p34.1	1p34.1
<i>KDM4A</i>	1	71	28	2.15×10^{-11}	1p34.1	1p34.1
<i>PTPRF</i>	1	226	60	5.68×10^{-10}	1p34.2	1p34.2
<i>SZT2</i>	1	87	25	8.47×10^{-9}	1p34.2	1p34.2
<i>TIE1</i>	1	30	15	2.01×10^{-8}	1p34.2	1p34.2
<i>MPL</i>	1	13	6	3.33×10^{-8}	1p34.2	1p34.2
<i>CDC20</i>	1	5	5	6.34×10^{-8}	1p34.2	1p34.2
<i>HYI</i>	1	5	4	3.28×10^{-7}	1p34.2	1p34.2
<i>SLC6A9</i>	1	60	31	7.58×10^{-7}	1p34.1	1p34.1
<i>ELOVL1</i>	1	3	3	1.26×10^{-6}	1p34.2	1p34.2
<i>CCDC24</i>	1	6	5	2.12×10^{-6}	1p34.1	1p34.1
<i>MANBA</i>	4	203	55	6.00×10^{-8}	4q24	4p15.1(<i>PCDH7</i>)
<i>MEF2C</i>	5	320	54	3.19×10^{-8}	5q14.3	5q14.3
<i>FOXP2</i>	7	812	110	5.50×10^{-7}	7q31.1	7q31.1
<i>SORCS3</i>	10	1823	106	2.18×10^{-9}	10q25.1	10q25.1
<i>CUBN</i>	10	1172	167	1.59×10^{-7}	10p13	10q25.1 (<i>SORCS3</i>)
<i>PIDD1</i>	11	27	12	5.30×10^{-7}	11p15.5	NA
<i>DUSP6</i>	12	20	8	2.24×10^{-9}	12q21.33	12q21.33
<i>SEMA6D</i>	15	1458	138	2.63×10^{-10}	15q21.1	15q21.1
<i>CDH8</i>	16	764	79	4.67×10^{-8}	16q21	16q22.2 (<i>LINC01572</i>)

Supplementary Table 9. Enrichment analysis of gene sets related to *FOXP2* downstream target genes

Competitive gene set analysis of each set of *FOXP2* target genes performed using MAGMA⁴⁶ (based on summary statistics from the European GWAS meta-analysis, 19,099 cases, 34,194 controls). For each gene set, the number of genes (N Genes), raw and semi-standardized (Std.) regression coefficients, and corresponding standard error (SE) are and two-sided association P-values (P) are reported.

Gene Set	N Genes	Beta	Beta (Std.)	SE	P
Mouse brain (ChIP-chip)	219	0.016	0.002	0.06	0.39
Mouse brain (knockout)	243	0.034	0.004	0.055	0.27
Human brain (ChIP-chip)	258	-0.094	-0.011	0.053	0.96

Supplementary Table 10. Enrichment analysis for a set of highly constrained genes

Competitive gene set analysis of highly constrained genes (pLI > 0.9) performed using MAGMA⁴⁶ (based on summary statistics from the European GWAS meta-analysis, 19,099 cases; 34,194 controls). The number of genes (N Genes), raw and semi-standardized (Std.) regression coefficients, and corresponding standard error (SE) and two-sided association P-value (P) is reported.

Gene Set	N Genes	Beta	Beta (Std.)	SE	P
Highly constrained genes	2932	0.062	0.023	0.018	2.60 x10 ⁻⁴

Supplementary Table 11. Results from MAGMA gene-based association of ADHD candidate genes

MAGMA⁴⁶ analysis (based on summary statistics from the European GWAS meta-analysis, (19,099 cases, 34,194 controls) of previously reported candidate genes for ADHD from a recent review⁵⁸. Number of SNPs in the genes (N SNPS), number of relevant parameters used in the model (N PARAM) and two-sided association P-values (P) are shown.

Gene symbol	Entrez ID	N SNPS	N PARAM	Z	P
<i>SLC9A9</i>	285195	1609	129	3.395	3.40 x10 ⁻⁴
<i>DRD5</i>	1816	4	2	-1.374	0.92
<i>SLC6A3</i>	6531	101	12	-0.975	0.84
<i>HTR1B</i>	3351	3	1	2.246	0.012
<i>DRD4</i>	1815	5	2	-0.192	0.58
<i>NOS1</i>	4842	410	30	1.088	0.14
<i>GIT1</i>	28964	21	5	0.77	0.22
<i>SLC6A4</i>	6532	67	12	-0.021	0.51
<i>SNAP25</i>	6616	180	25	-0.512	0.7

Supplementary Table 12. Sign test results for each replication cohort

Test of whether the proportion of loci with estimated effects in the same direction as the ADHD GWAS (π) is greater than expected by chance. Sample size: deCODE 5,085 cases and 131,122 controls; 23andMe 5,857 cases and 70,393 controls; QIMR 2,798 individuals/EAGLE 17,666 individuals. Values in bold are nominally significant after Bonferroni correction ($P < 0.0167$) for testing in 3 replication cohorts at a given P-value threshold in the ADHD GWAS meta-analysis.

P Threshold	deCODE Concordance			23andMe Concordance			EAGLE/QIMR Concordance		
	# Loci	π	P	# Loci	π	P	# Loci	π	P
5.00E-08	12	0.833	0.0193	11	0.727	0.1133	12	1.000	2.44E-04
1.00E-07	14	0.786	0.0287	13	0.615	0.2905	14	1.000	6.10E-05
1.00E-06	37	0.73	0.00382	36	0.722	0.00567	34	0.824	9.76E-05
1.00E-05	99	0.636	0.00432	99	0.747	4.25E-07	98	0.694	7.81E-05
1.00E-04	--	--	--	326	0.607	6.28E-05	301	0.641	5.51E-07

Supplementary Table 13. Results for significant ADHD loci in each replication cohort

GWAS results from deCODE (5,085 cases; 131,122 controls), 23andMe (5,857 cases; 70,393 controls), and EAGLE/QIMR (QIMR 2,798 individuals/EAGLE 17,666 individuals) for the genome-wide significant loci identified in the ADHD GWAS (20,183 cases; 35,191 controls). Replication is tested for the index variant from the ADHD GWAS, or for a proxy variant when the index variant is not present in the replication cohort. Proxy variants are identified by linkage disequilibrium (LD) clumping of the ADHD GWAS results using European ancestry samples from the 1000 Genomes Project after restricting to variants present in the replication cohort. No proxy variant is available for rs28411770. Effects (Z or odds ratio [OR]) that are sign concordant with the ADHD GWAS are indicated in bold. Two-sided P-values from logistic regression (deCODE), from inverse standard error-weighted meta-analysis (iPSYCH/PGC, 23andMe) and from linear regression and subsequent meta-analysis (EAGLE/QIMR).

Variant		chr	Effect Allele	LD to Index	iPSYCH/PGC		DeCODE		23andMe		EAGLE/QIMR	
Index	Proxy				OR	P	OR	P	OR	P	Z	P
rs11420276	--	1	G	--	1.113	2.14E-13	1.006	8.23E-01	--	--	--	--
rs11420276	rs112984125		A	0.98	0.899	3.58E-13	--	--	1.044	4.01E-02	-1.540	1.24E-01
rs1222063	--	1	A	--	1.101	3.07E-08	1.006	7.97E-01	--	--	0.522	6.02E-01
rs1222063	rs2391769		A	0.093	0.927	3.96E-08	1.013	6.01E-01	0.957	3.20E-02	-0.501	6.16E-01
rs9677504	--	2	A	--	1.124	1.39E-08	0.938	1.33E-01	1.068	3.52E-02	0.160	8.73E-01
rs4858241	--	3	T	--	1.082	1.74E-08	1.017	4.75E-01	1.016	4.44E-01	1.259	2.08E-01
rs28411770	--	4	T	--	1.090	1.15E-08	1.017	7.05E-01	--	--	0.398	6.91E-01
rs4916723	--	5	A	--	0.926	1.58E-08	0.976	2.92E-01	0.989	5.88E-01	-2.752	5.93E-03
rs5886709	--	7	G	--	1.079	1.66E-08	1.049	4.06E-02	1.045	2.62E-02	--	--

rs5886709	rs10262192	A	0.955	1.076	2.89E-08	--	--	1.045	2.57E-02	1.639	1.01E-01	
rs74760947	--	8	A	--	0.835	1.35E-08	0.996	9.28E-01	0.955	3.90E-01	-0.870	3.84E-01
rs11591402	--	10	A	--	0.911	1.34E-08	0.955	9.40E-02	0.957	6.27E-02	-1.175	2.40E-01
rs1427829	--	12	A	--	1.083	1.82E-09	1.021	3.63E-01	1.036	6.97E-02	0.418	6.76E-01
rs281324	--	15	T	--	0.928	2.68E-08	0.988	6.06E-01	1.007	7.05E-01	-1.659	9.72E-02
rs212178	--	16	A	--	0.891	7.68E-09	1.012	7.32E-01	1.030	3.80E-01	-1.044	2.96E-01

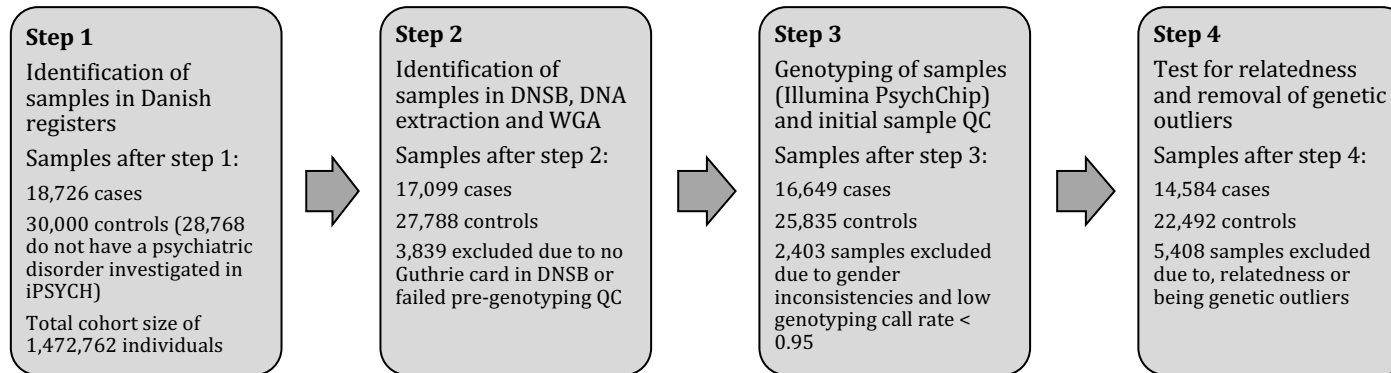
Supplementary Table 14. Comparison of profile of genetic correlations for the ADHD GWAS and 23andMe

Comparison of genetic correlation (r_g) results, including block jack-knife standard errors (SE), of each GWAS with 28 selected traits from LD Hub (<http://ldsc.broadinstitute.org/ldhub/>). For each trait, the absolute difference between the 23andMe (5,857 cases; 70,393 controls) and ADHD GWAS (19,099 cases, 34,194 controls) r_g estimates is reported, along with the approximate pooled standard error and corresponding approximate P value from testing the difference between the two r_g means. P values for the difference reaching nominal significance ($P < .05$) are indicated in italics, and Bonferroni-corrected significant P values ($P < 0.05/28 = 1.8 \times 10^{-3}$) are indicated in bold. References and sample sizes for each trait are the same as Supplementary Table 5.

Trait	Category	ADHD GWAS			23andMe			Difference		
		r_g	SE	P	r_g	SE	P	$ r_1-r_2 $	SE	P
College completion	Cognition/education	-0.538	0.046	3.30E-31	0.056	0.086	5.13E-01	0.594	0.097	1.07E-09
Years of schooling 2016	Cognition/education	-0.535	0.028	1.44E-80	-0.199	0.058	6.00E-04	0.336	0.064	1.84E-07
Childhood IQ	Cognition/education	-0.411	0.082	5.09E-07	-0.219	0.144	1.27E-01	0.192	0.165	2.46E-01
Neuroticism	Personality	0.264	0.046	1.02E-08	0.145	0.090	1.08E-01	0.120	0.101	2.38E-01
Schizophrenia	Psychiatric	0.122	0.036	7.00E-04	0.275	0.070	8.95E-05	0.153	0.079	5.30E-02

Bipolar disorder	Psychiatric	0.095	0.055	8.05E-02	0.293	0.103	4.60E-03	0.198	0.117	9.10E-02
Subjective well being	Psychiatric	-0.283	0.048	3.73E-09	-0.146	0.102	1.53E-01	0.137	0.113	2.26E-01
Depressive symptoms	Psychiatric	0.446	0.050	7.00E-19	0.300	0.114	8.80E-03	0.146	0.125	2.44E-01
PGC cross-disorder analysis	Psychiatric	0.266	0.046	5.58E-09	0.286	0.104	6.00E-03	0.020	0.113	8.61E-01
Obesity class 1	Weight related	0.285	0.036	1.81E-15	0.108	0.070	1.26E-01	0.178	0.079	2.43E-02
Childhood obesity	Weight related	0.216	0.046	3.29E-06	-0.025	0.105	8.10E-01	0.241	0.115	3.61E-02
Waist-to-hip ratio	Weight related	0.304	0.036	1.16E-17	0.154	0.073	3.38E-02	0.150	0.081	6.30E-02
Birth weight	Weight related	-0.132	0.039	8.00E-04	0.012	0.079	8.79E-01	0.144	0.088	1.03E-01
Body mass index	Weight related	0.258	0.032	1.68E-15	0.132	0.075	8.06E-02	0.126	0.082	1.25E-01
Overweight	Weight related	0.275	0.036	1.73E-14	0.183	0.077	1.72E-02	0.092	0.085	2.81E-01
Type 2 Diabetes	Glycemic	0.185	0.047	7.80E-05	0.058	0.100	5.64E-01	0.127	0.110	2.51E-01
Triglycerides	Lipids	0.159	0.040	6.49E-05	0.048	0.065	4.58E-01	0.111	0.076	1.47E-01
HDL cholesterol	Lipids	-0.217	0.042	2.44E-07	-0.131	0.082	1.11E-01	0.086	0.092	3.54E-01
Former vs Current smoker	Smoking behaviour	-0.344	0.086	6.74E-05	-0.132	0.157	4.00E-01	0.212	0.179	2.37E-01
Ever vs never smoked	Smoking behaviour	0.478	0.059	4.33E-16	0.340	0.108	1.60E-03	0.139	0.123	2.58E-01
Cigarettes smoked per day	Smoking behaviour	0.451	0.103	1.07E-05	0.343	0.149	2.08E-02	0.108	0.181	5.50E-01
Lung cancer	Cancer	0.390	0.063	6.35E-10	0.139	0.113	2.18E-01	0.251	0.129	5.15E-02
Squamous cell lung cancer	Cancer	0.549	0.135	4.57E-05	0.393	0.180	2.86E-02	0.156	0.224	4.88E-01
Age of first birth	Reproductive	-0.612	0.037	3.70E-61	-0.331	0.074	6.66E-06	0.281	0.082	6.34E-04
Number of children ever born	Reproductive	0.421	0.051	8.51E-17	0.310	0.094	1.00E-03	0.112	0.106	2.94E-01
Age at Menopause	Reproductive	-0.161	0.042	1.00E-04	-0.129	0.087	1.40E-01	0.032	0.097	7.39E-01
Parents age at death	Aging	-0.376	0.091	3.51E-05	-0.339	0.177	5.59E-02	0.038	0.199	8.50E-01
Rheumatoid Arthritis	Autoimmune	0.162	0.042	1.00E-04	-0.040	0.093	6.67E-01	0.202	0.102	4.88E-02

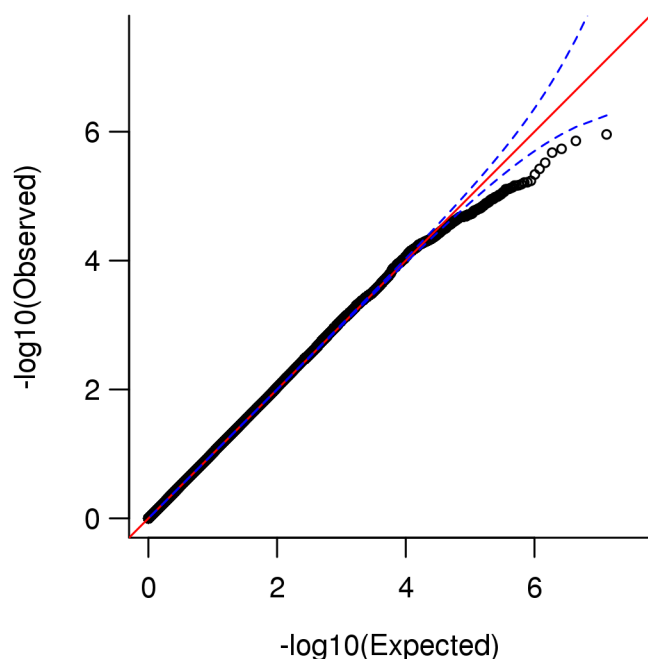
Supplementary Figures



Supplementary Figure 1. Genotyping iPSYCH-ADHD sample, main steps and sample loss

Flowchart demonstrating the main steps and sample loss during the process of obtaining high quality genotypes for the iPSYCH sample.

Detailed description of the Danish registers, DNA generation, genotyping and QC is described under the detailed description of the iPSYCH sample.



Supplementary Figure 2. Q-Q plot from test for heterogeneity between Chinese and European ancestry cohorts in the ADHD GWAS meta-analysis

Quantile-quantile plot of P -values from the 1 degree of freedom test (I^2 statistic (I^2)) of heterogeneity between the Beijing, China cohort (1,012 cases; 925 controls) and all European ancestry cohorts (19,099 cases; 34,194 controls).

Supplementary Figure 3a1 – 3n1. Forest plots for index SNPs in gws loci

Forest plots for the index SNP in each of the gws associated regions in the GWAS meta-analysis (20,183 cases; 35,191 controls). Each plot provides a visualization of the effect size estimates (natural logarithm of the odds ratio ($\ln(OR)$), estimated from logistic regression using relevant covariates, for each wave in the iPSYCH cohort and each PGC sample and for the summary meta-analysis (meta-analysis using an inverse-variance weighted fixed effects model) in addition the 95% confidence

intervals are included for the estimates. Sample size for each wave (w) for cases/controls w1:1373/1016, w2:1171/2633, w3:947/1025, w4:618/1026, w5:779/982, w6:776/971, w7:665/861, w8:817/1083, w9:813/1033, w10:520/747, w11:592/772, w12:425/800, w13:459/810, w14:470/778, w15:581/856, w16:545/827, w17:498/800, w18:416/913, w19:408/915, w20:313/849, w21:443/864, w22:313/931, w23:642/1000.

Supplementary Figure 3a2 – 3n2. Regional association plots for index SNPs in gws loci

Regional association plots of the local association results from the GWAS meta-analysis (20,183 ADHD cases and 35,191 controls). The y-axis represents $-\log(P\text{-values})$ of variant association with ADHD; the P-values are two-sided from meta-analysis using an inverse-variance weighted fixed effects model. The vertical green line represents the threshold for genome-wide significance ($P = 5 \times 10^{-8}$). Each plot includes information about the gws locus, the location and orientation of the genes in the region, LD estimates of surrounding SNPs with the index SNP (r^2 values estimated based on 1KGP3) is indicated by colour (colour bar in upper left corner indicates r^2 values), if multiple index SNPs then different colour scheme for each index SNP. Additionally, the local estimates of recombination rate are indicated in light blue (legend on vertical axis at right). Detailed SNP info in upper right corner (blue letters): SNP name (rsid), P-value (p), odds ratio (or), minor allele frequency (maf), imputation INFO score (info), directions in the analysed samples/waves (risk increasing - decreasing - missing). Gene lists were downloaded from <ftp://hgdownload.cse.ucsc.edu/goldenPath/hg19/database/refGene.txt.gz>. Previously reported gws regions were downloaded from the NHGRI GWAS catalogue available from <http://www.ebi.ac.uk/gwas>.

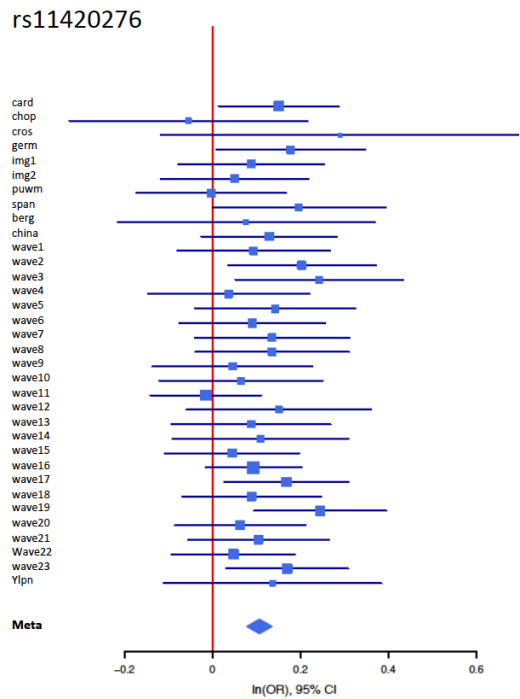


Figure 3a1. Forest plot for rs11420276

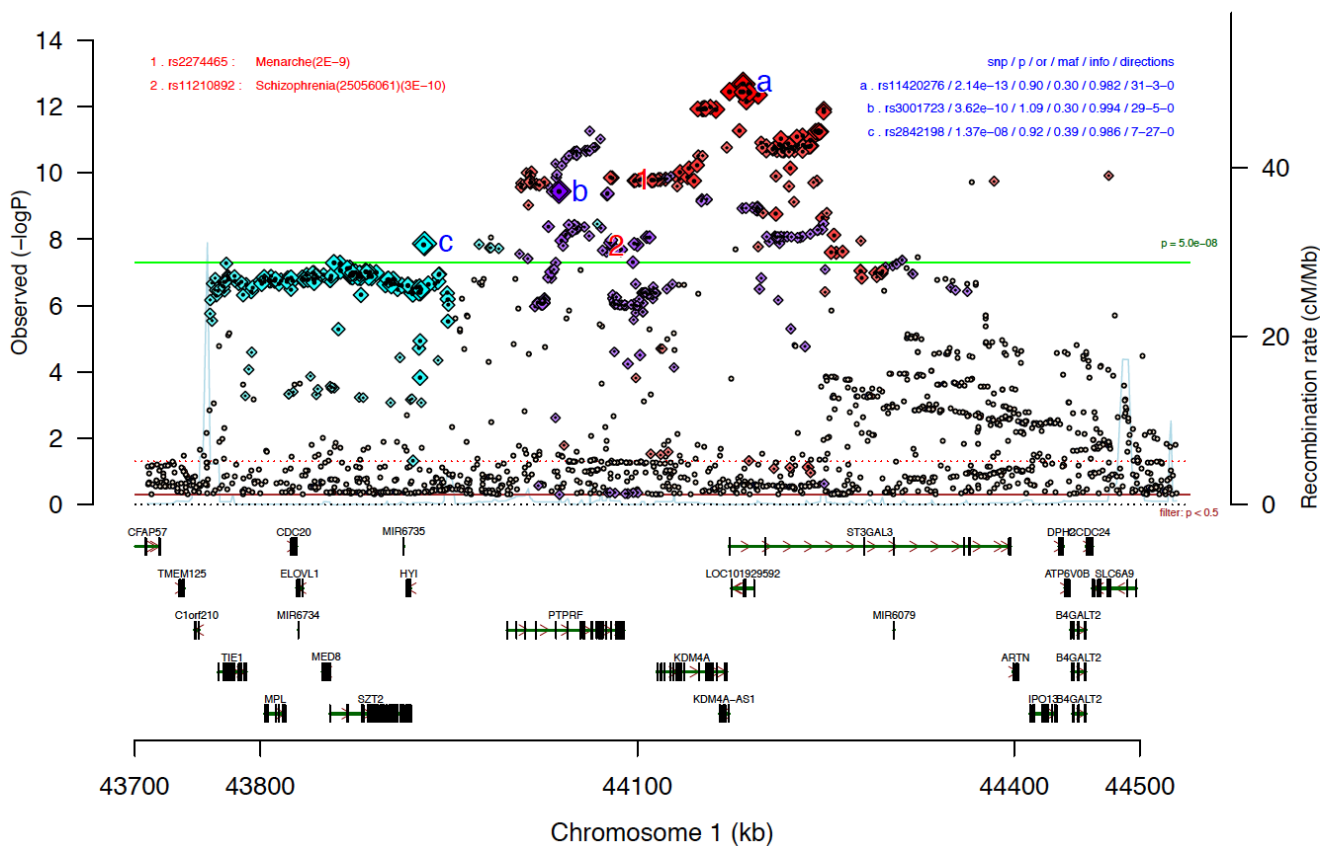


Figure 3a2. Regional association plot for rs11420076

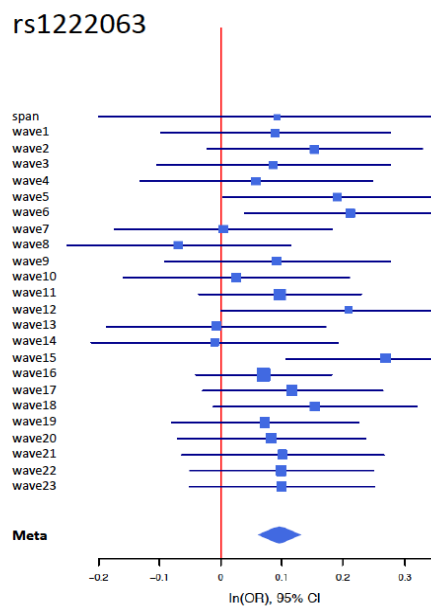


Figure 3b1. Forest plot for rs1222063

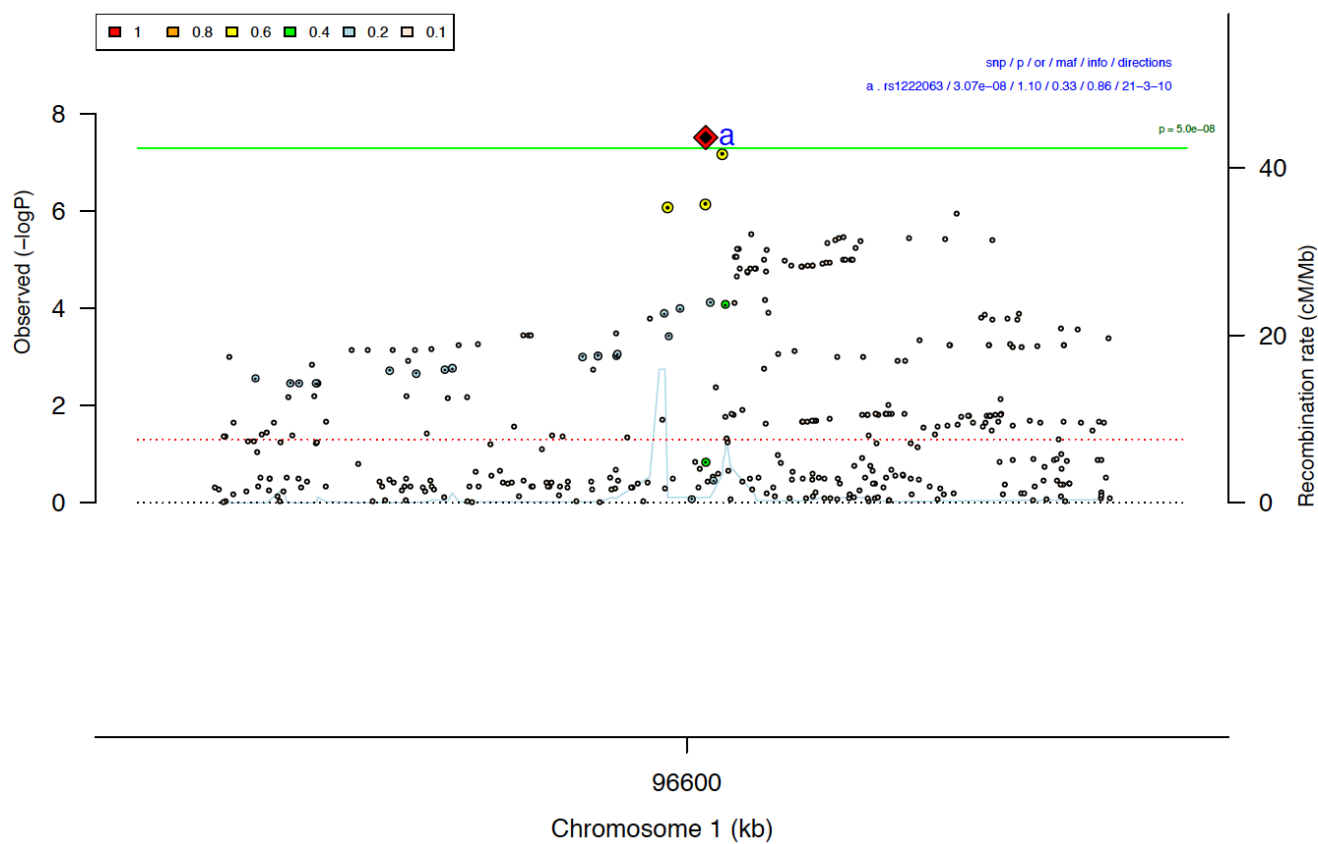


Figure 3b2. Regional association plot for rs1222063

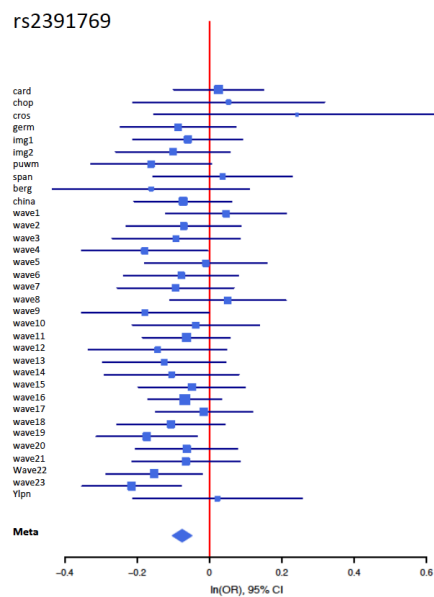


Figure 3c1. Forest plot for rs2391769

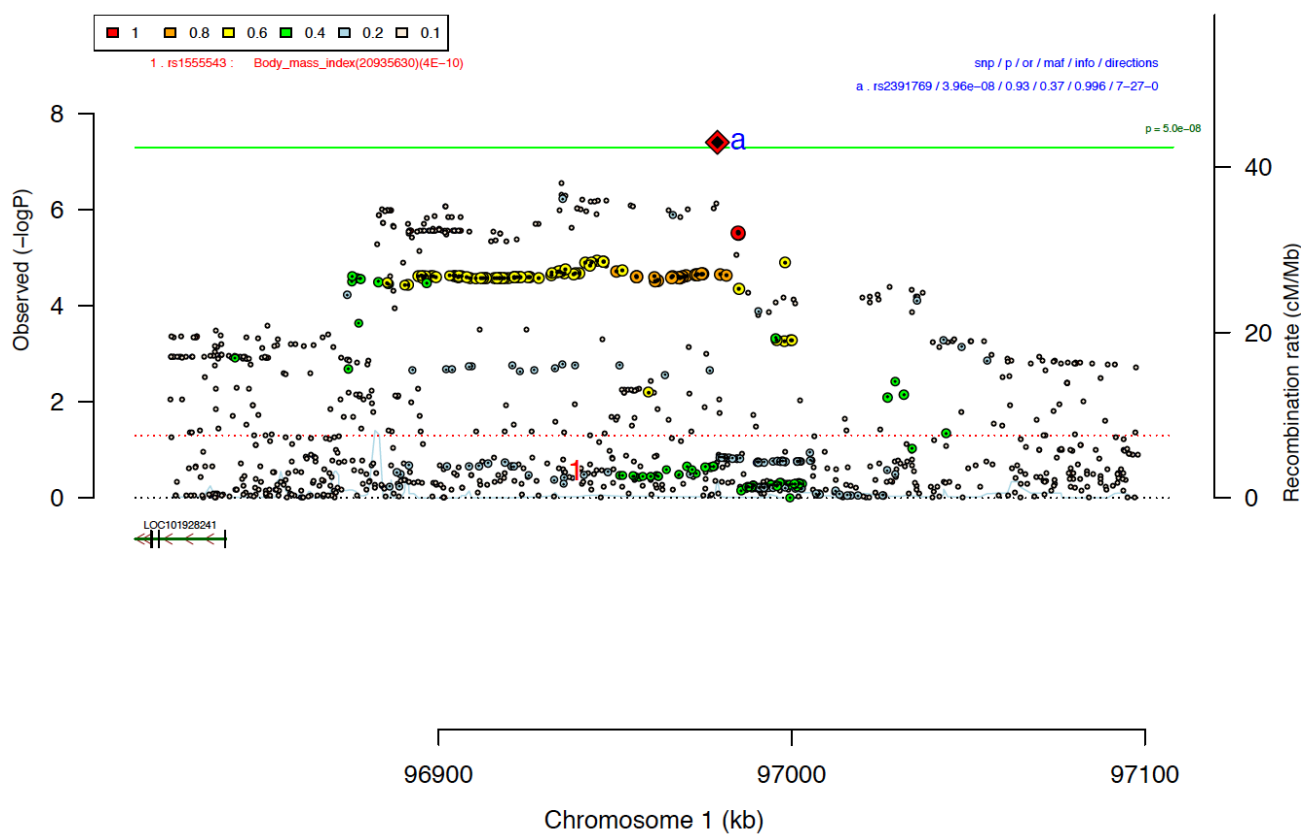


Figure 3c2. Regional association plot for rs2391769

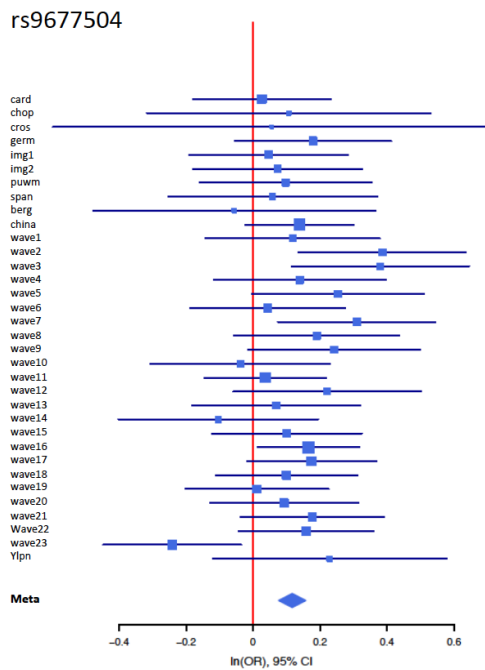


Figure 3d1. Forest plot for rs9677504

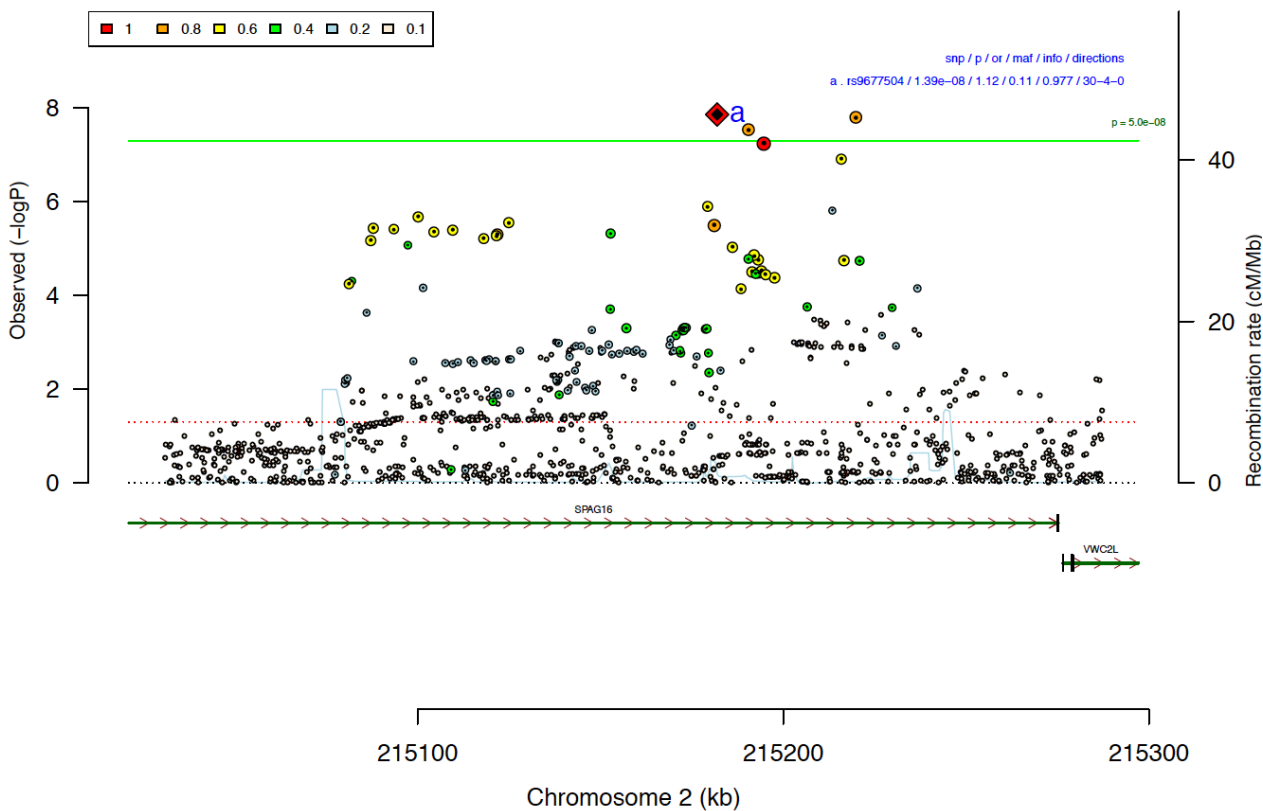


Figure 3d2. Regional association plot for rs9677504

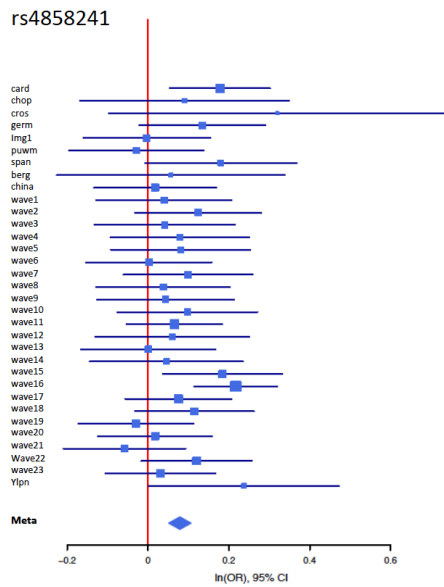


Figure 3e1. Forest plot for rs4858241

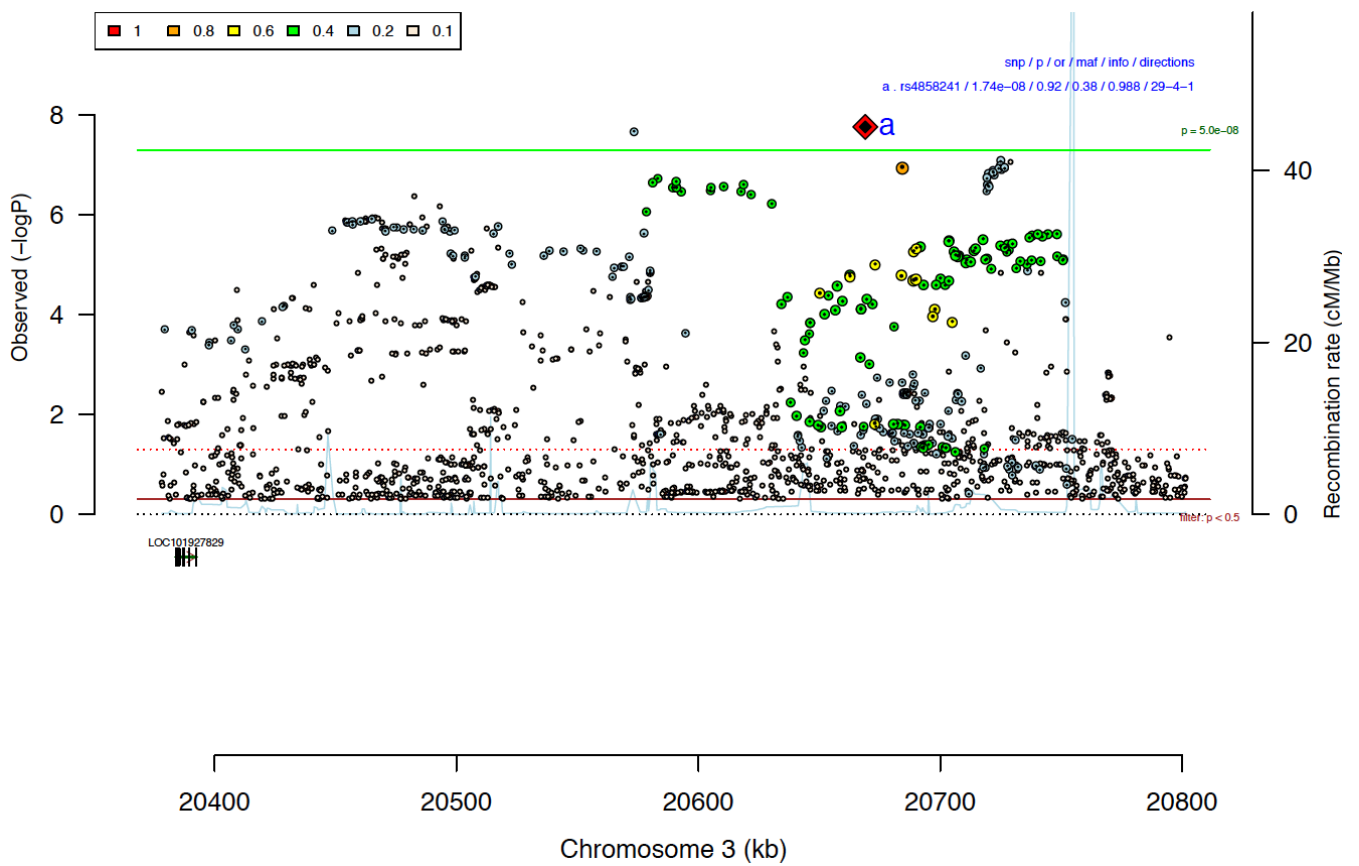


Figure 3e2. Regional association plot for rs4858241

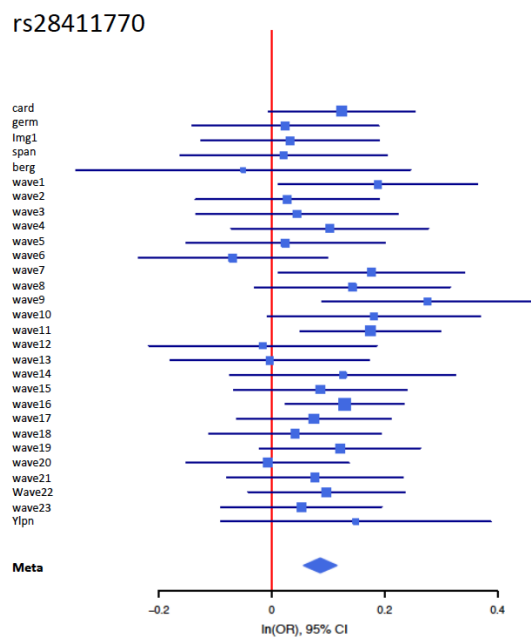


Figure 3f1. Forest plot for rs28411770

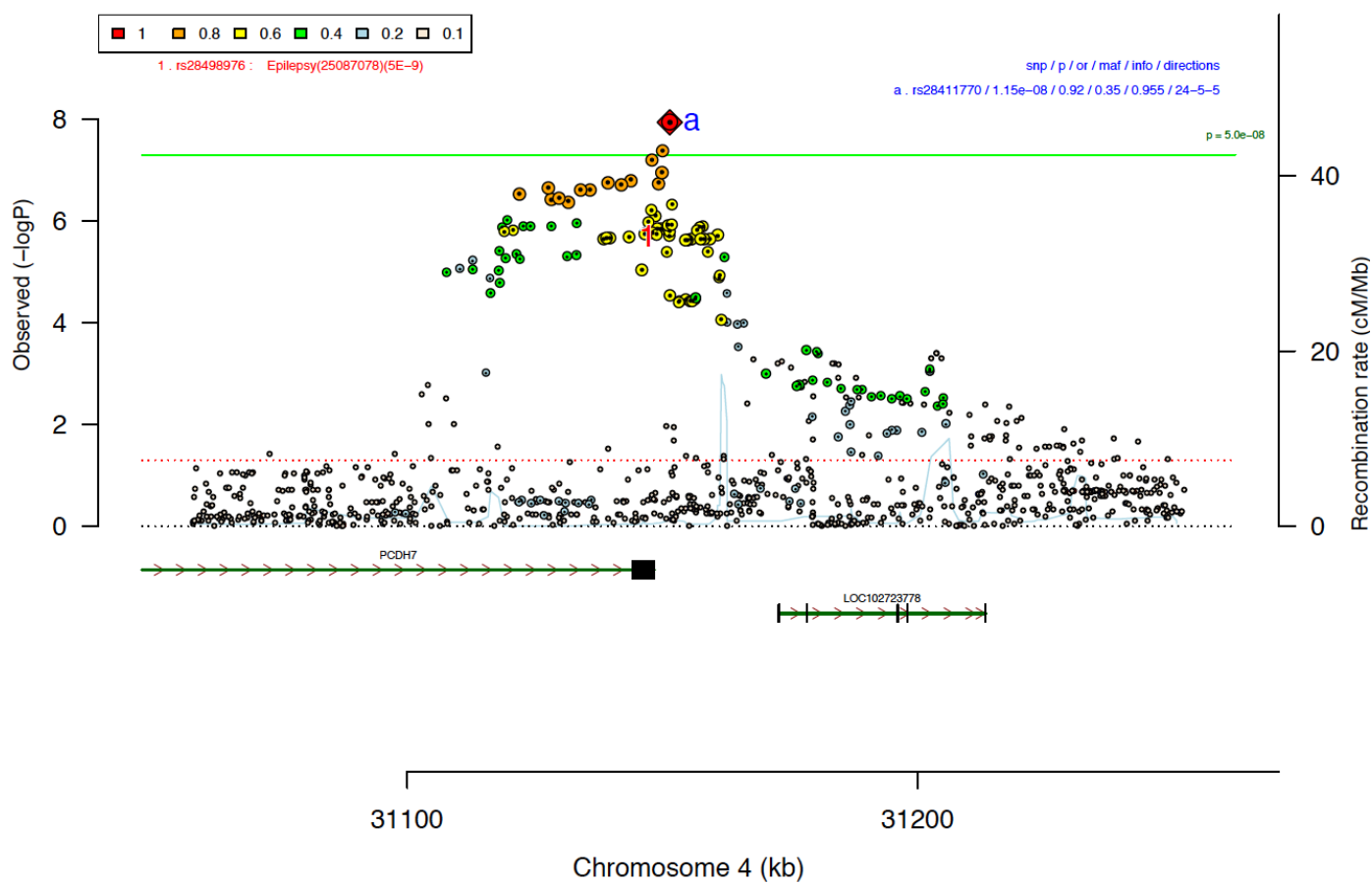


Figure 3f2. Regional association plot for rs2811770

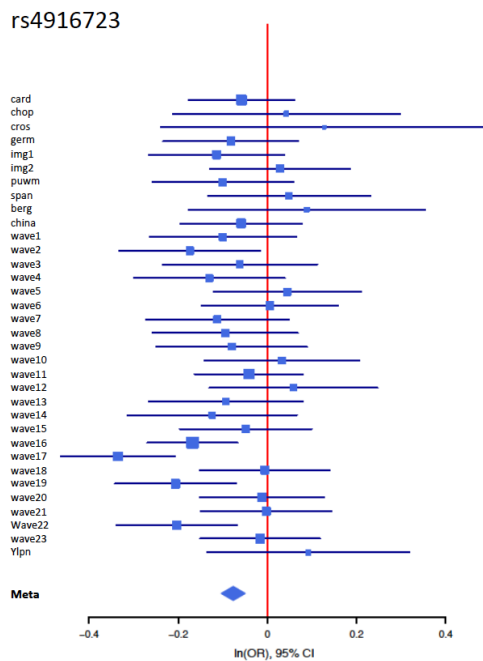


Figure 3g1. Forest plot for rs4916723

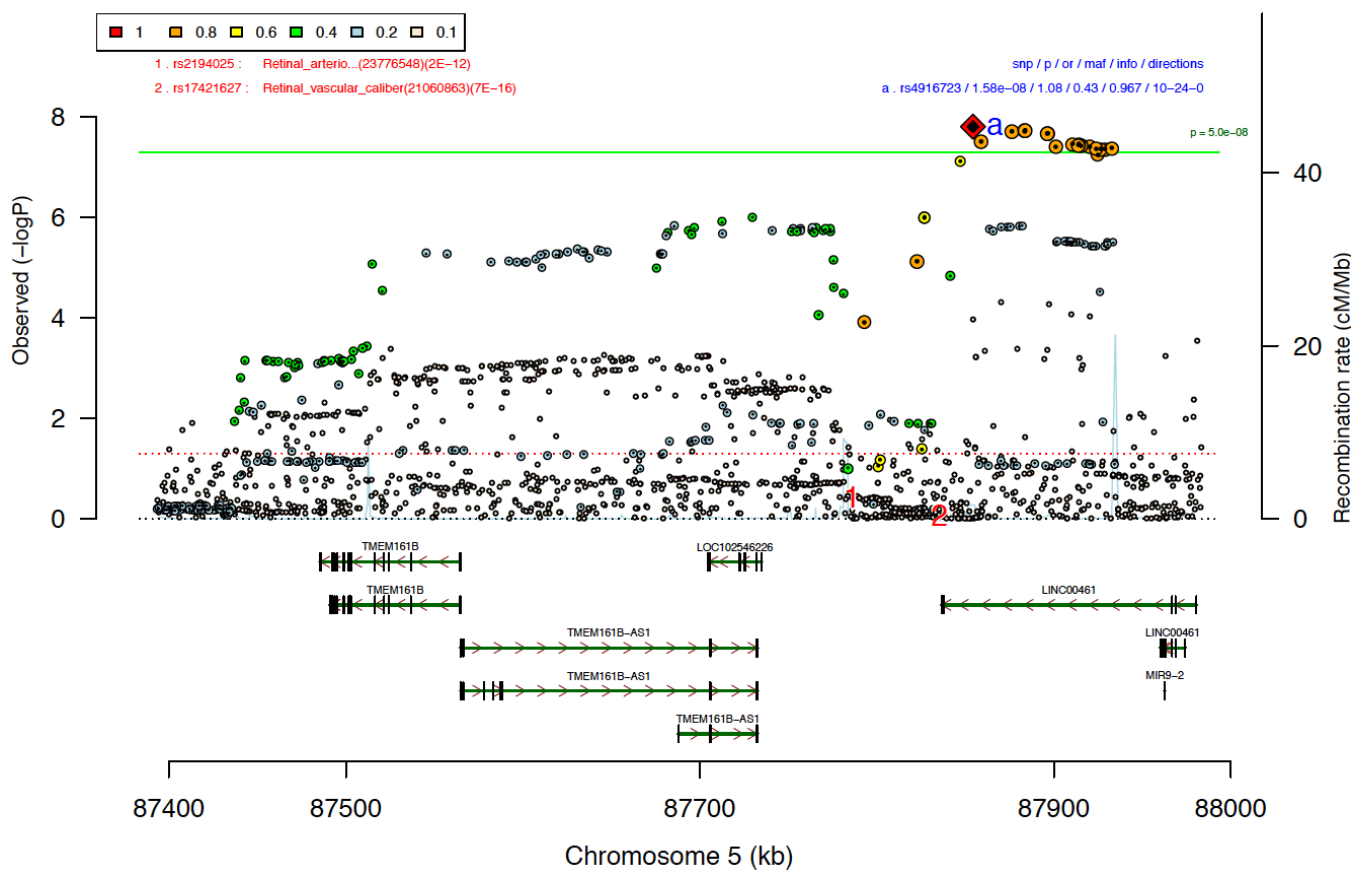


Figure 3g2. Regional association plot for rs4916723

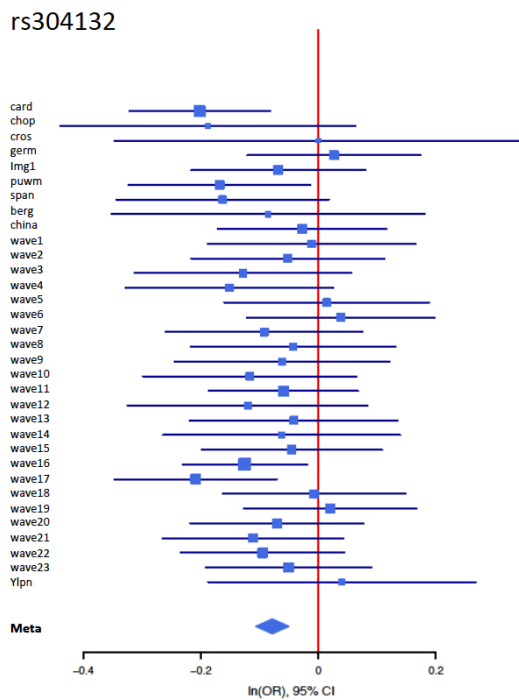


Figure 3h1. Forest plot for rs304132

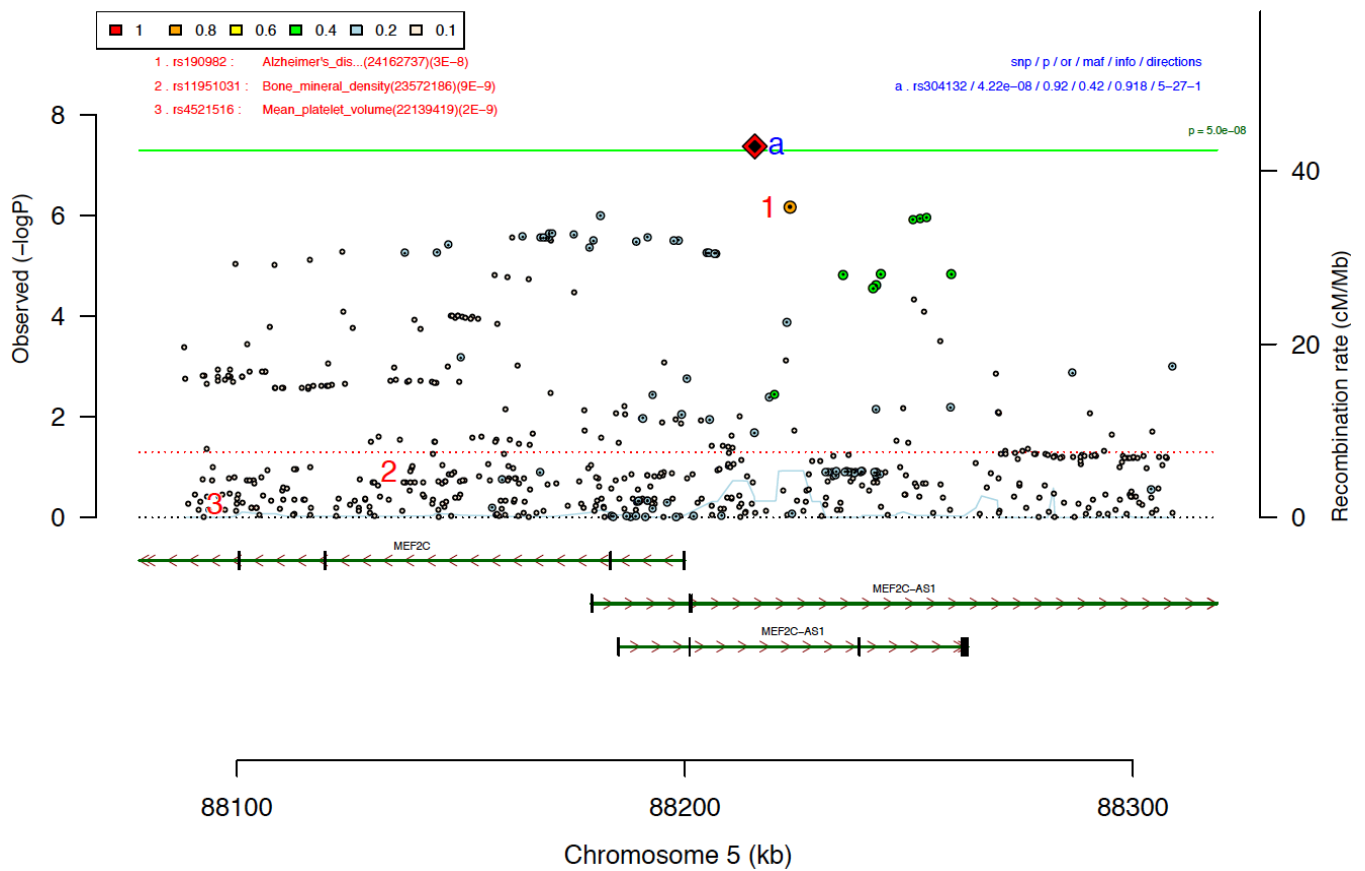


Figure 3h2. Regional association plot for rs304132

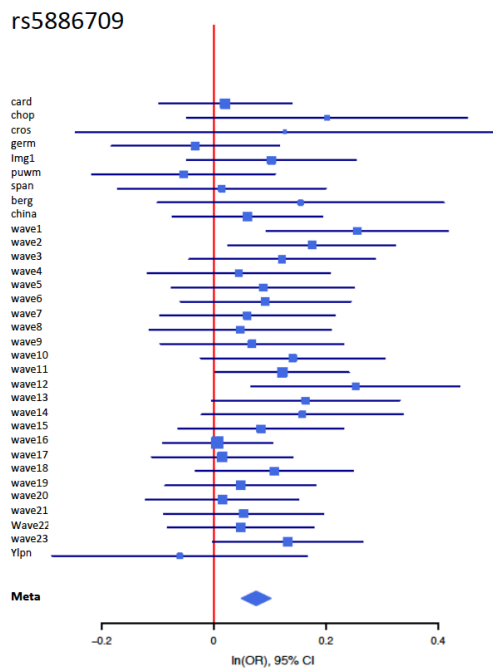


Figure 3i1. Forest plot for rs5886709

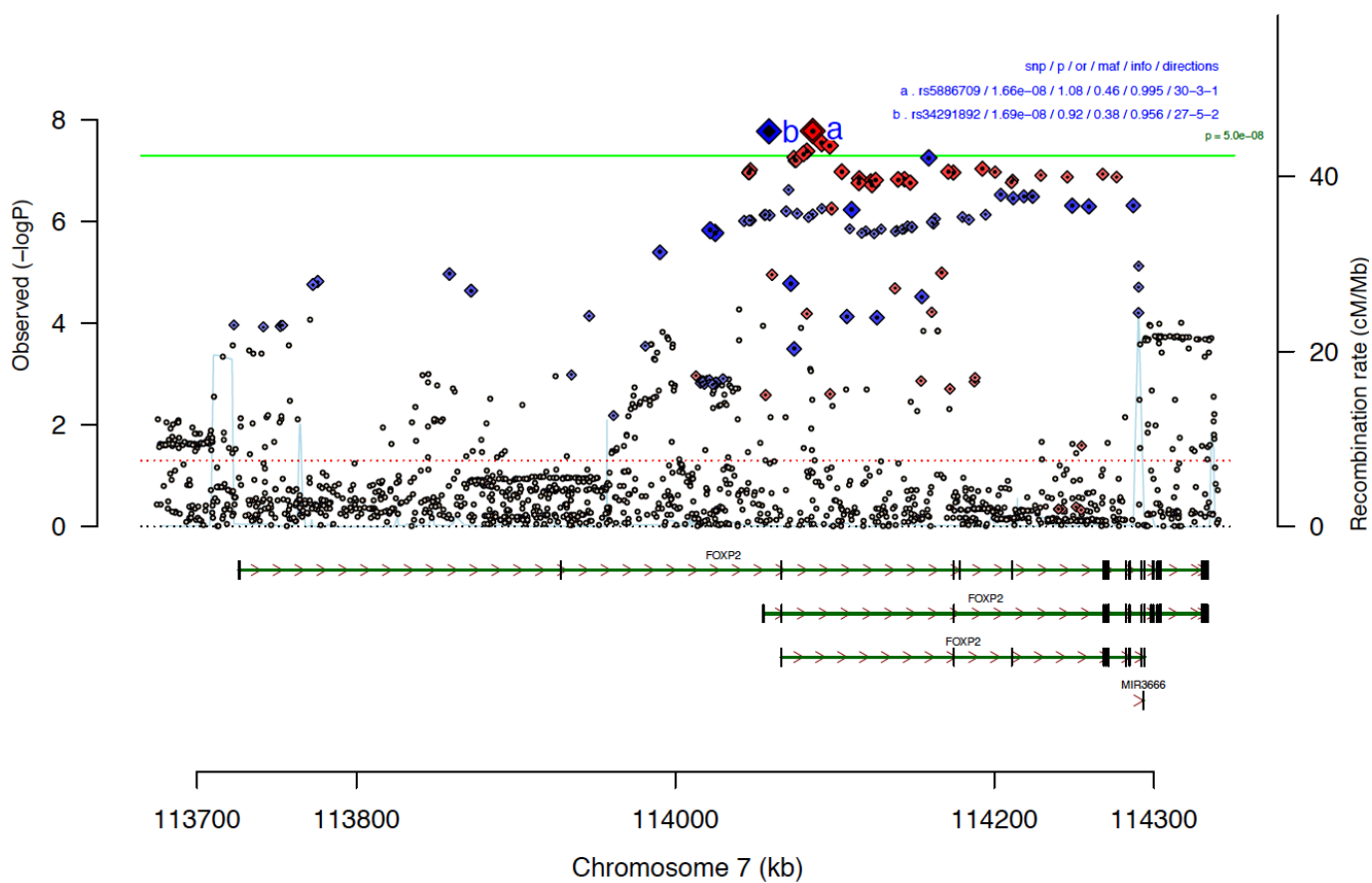


Figure 3i2. Regional association plot for rs5886709

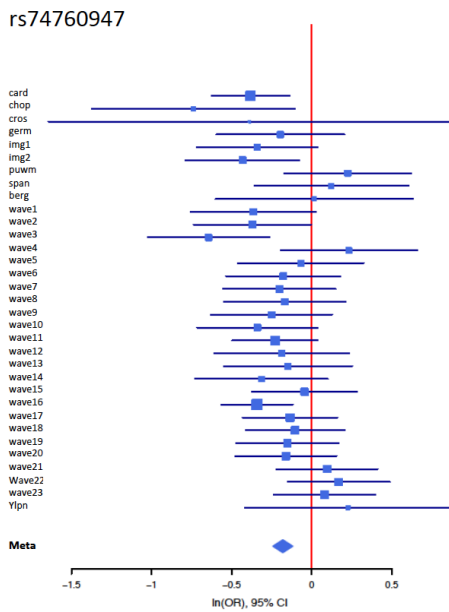


Figure 3j1. Forest plot for rs74760947

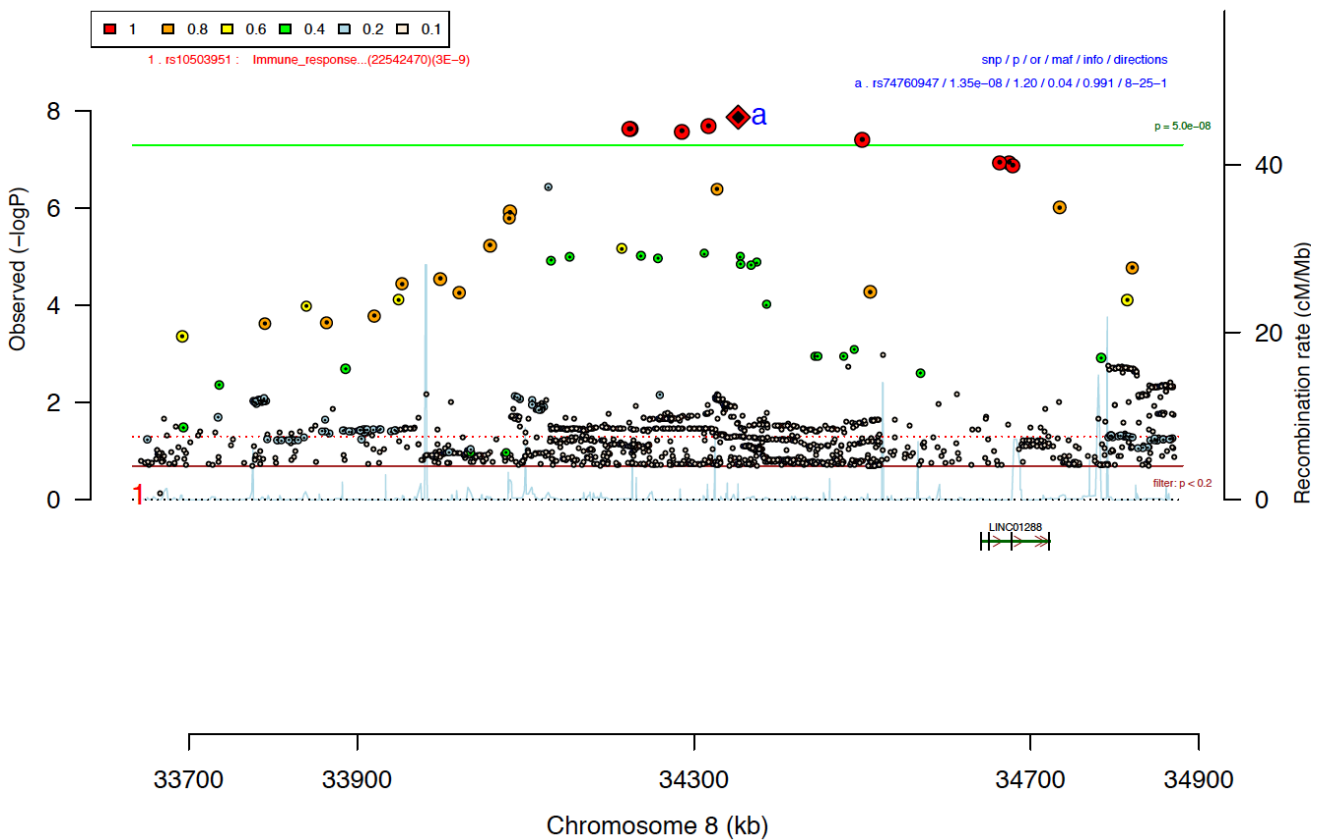


Figure 3j2. Regional association plot for rs74760947

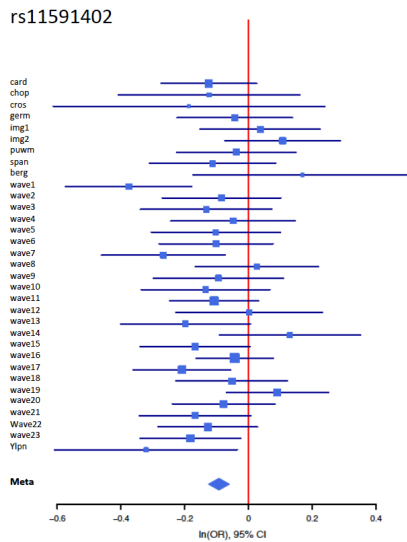


Figure 3k1. Forest plot for rs11591402

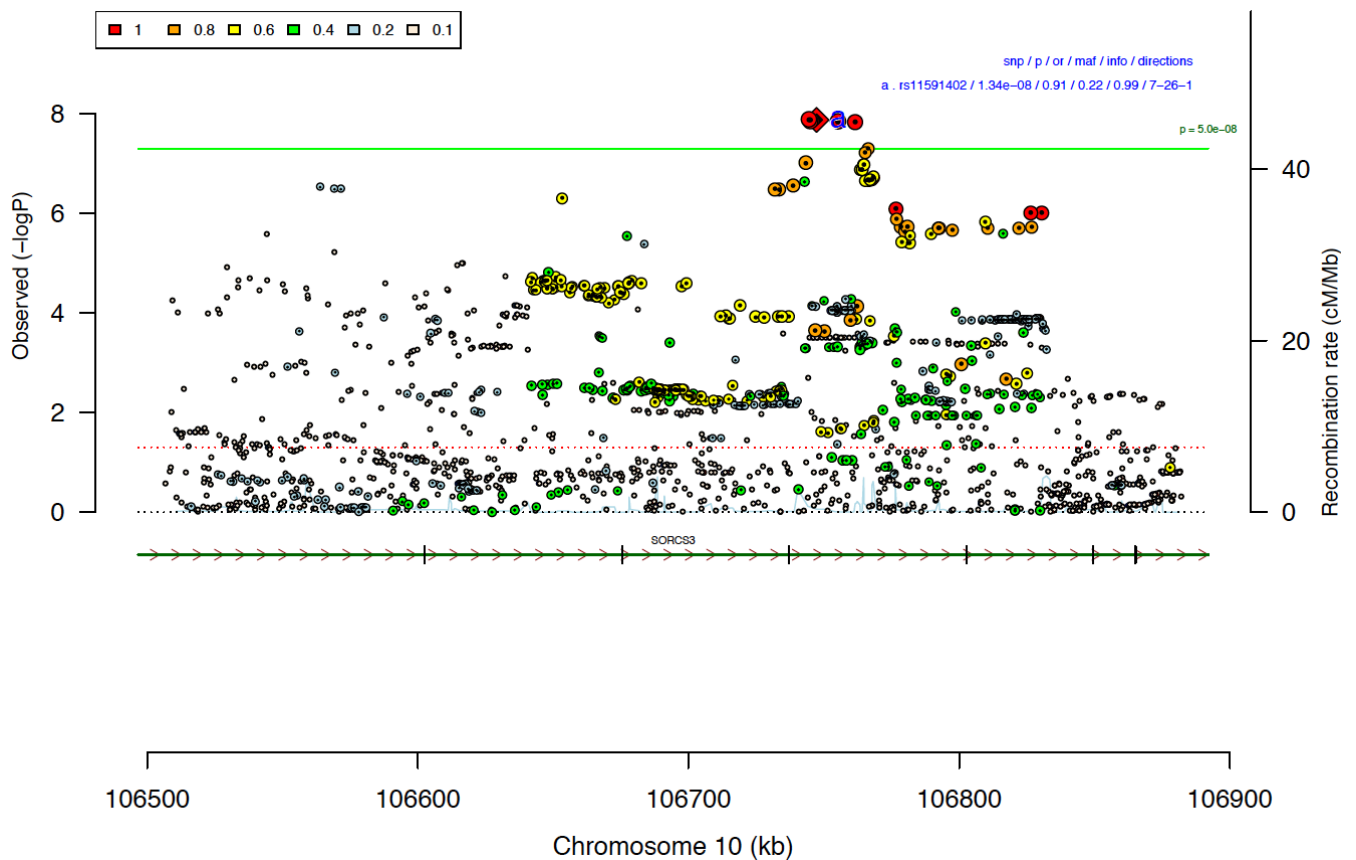


Figure 3k2. Regional association plot for rs11591402

rs1427829

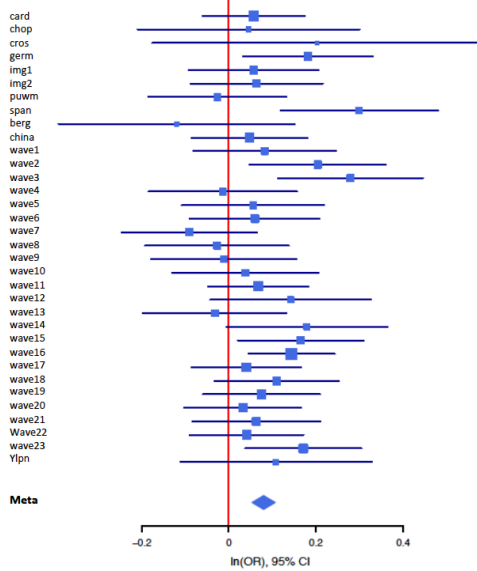


Figure 311. Forest plot for rs1427829

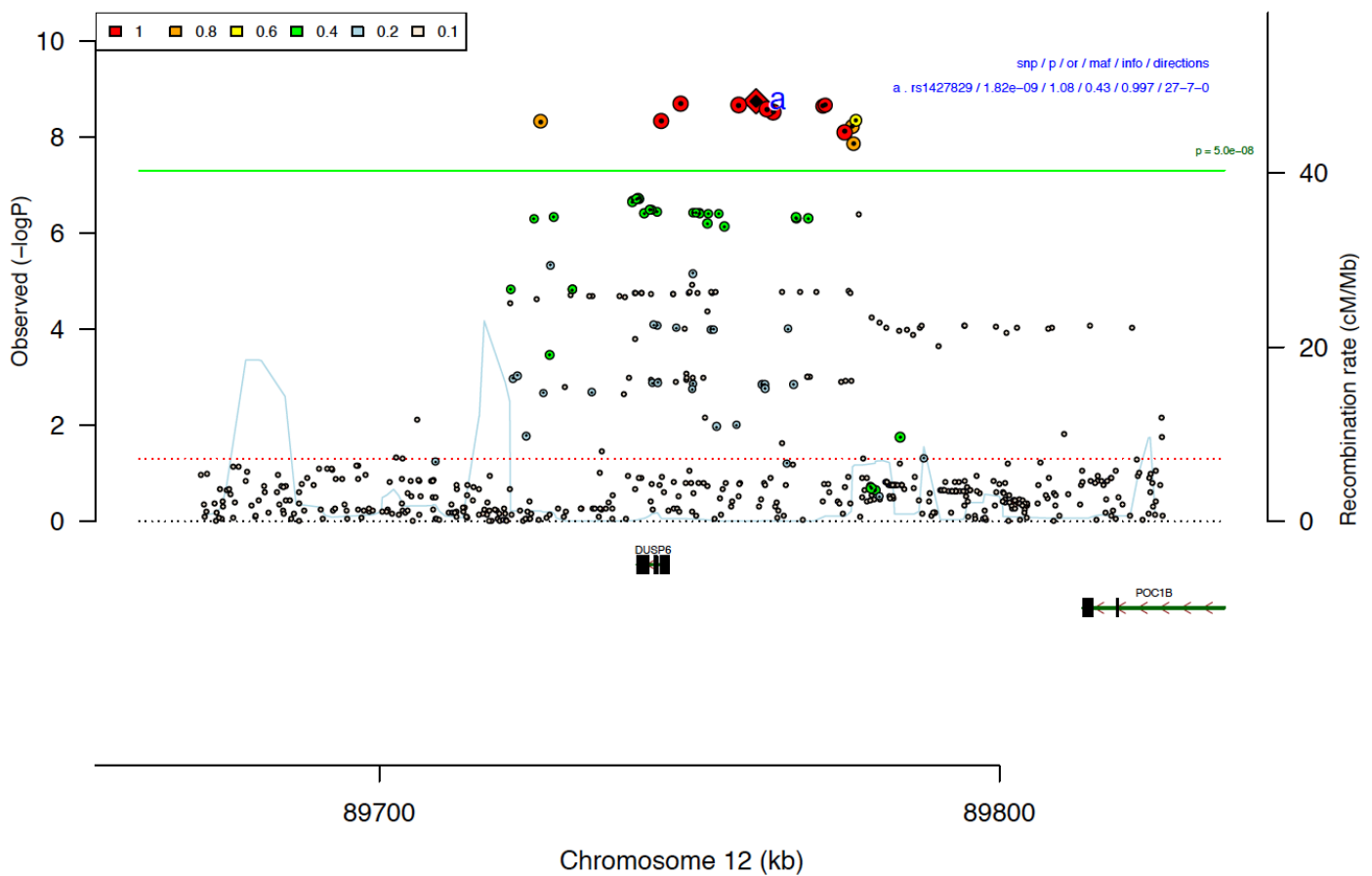


Figure 312. Regional association plot for rs1427829

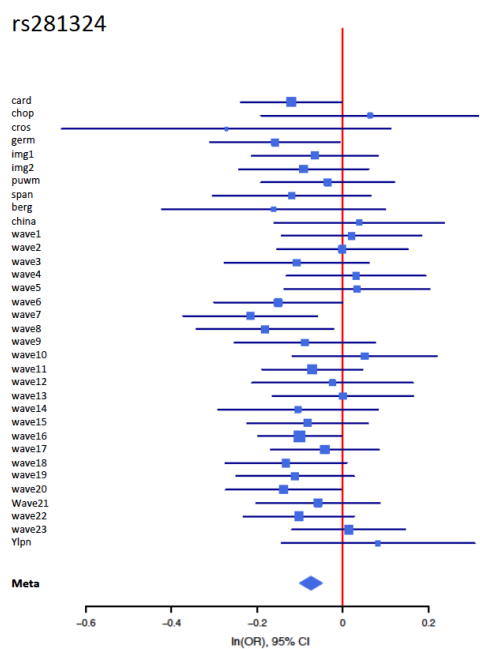


Figure 3m1. Forest plot for rs281324

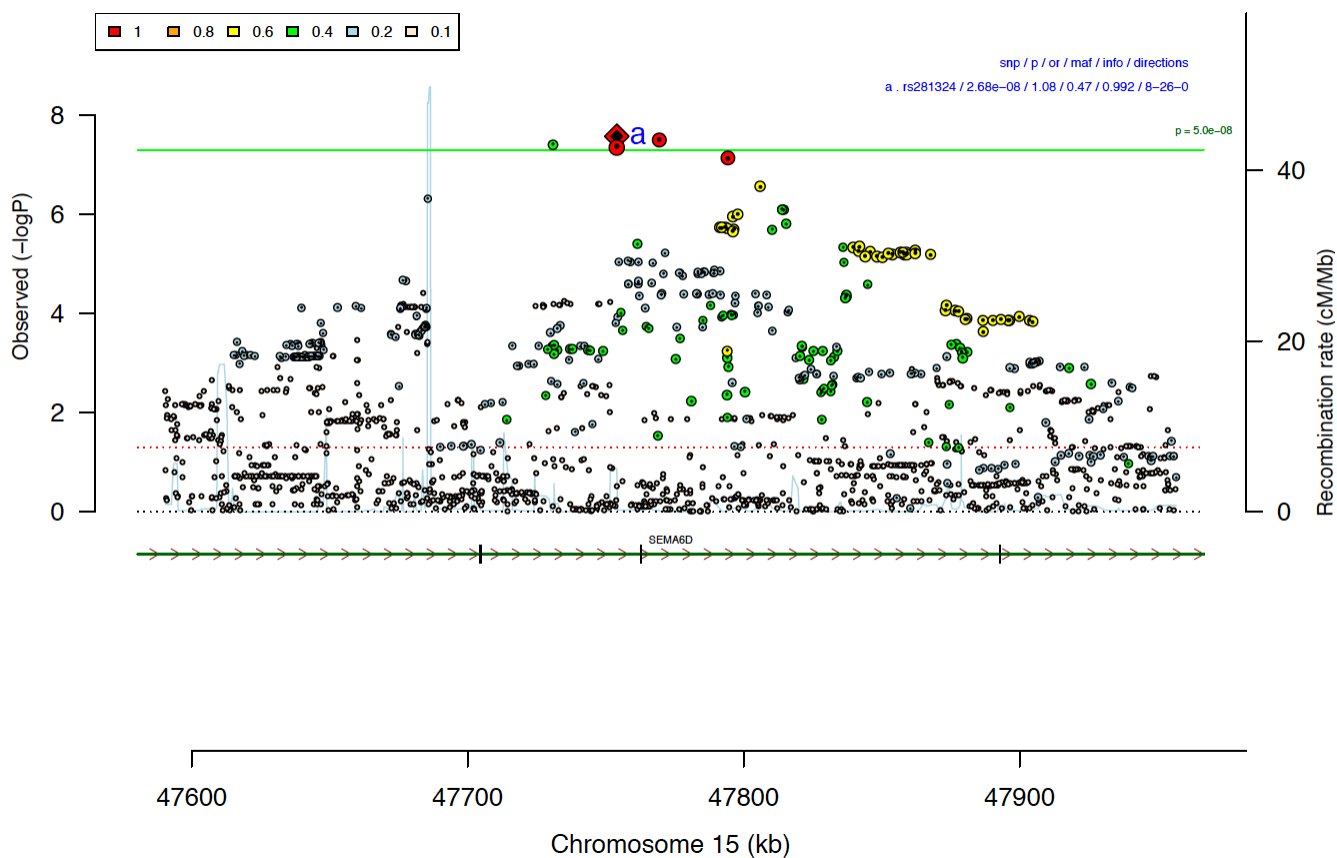


Figure 3m2. Regional association plot for rs281324

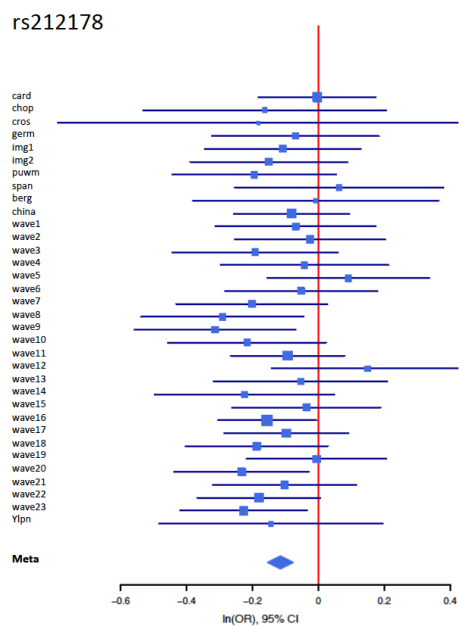


Figure 3n1. Forest plot for rs212178

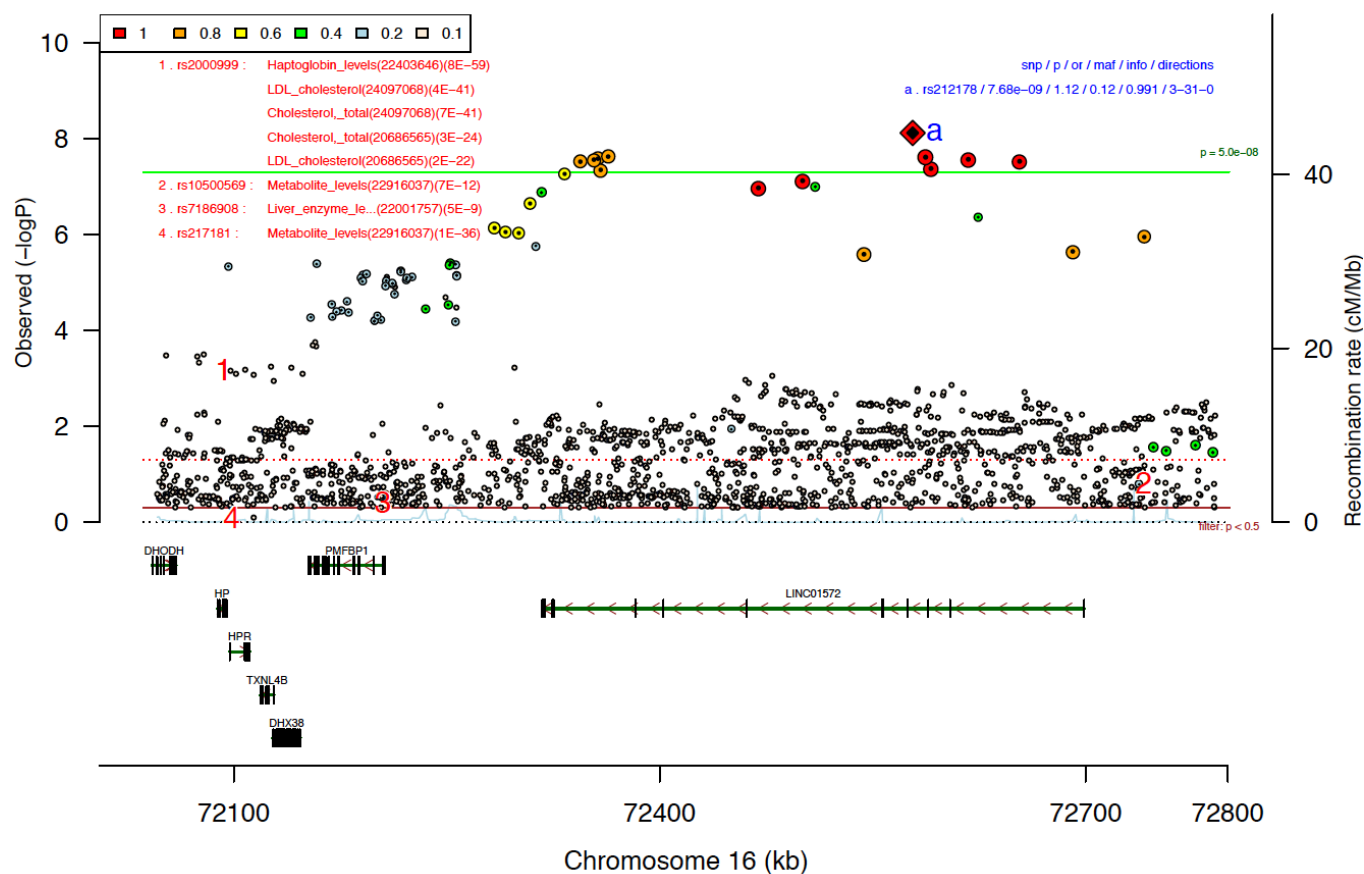
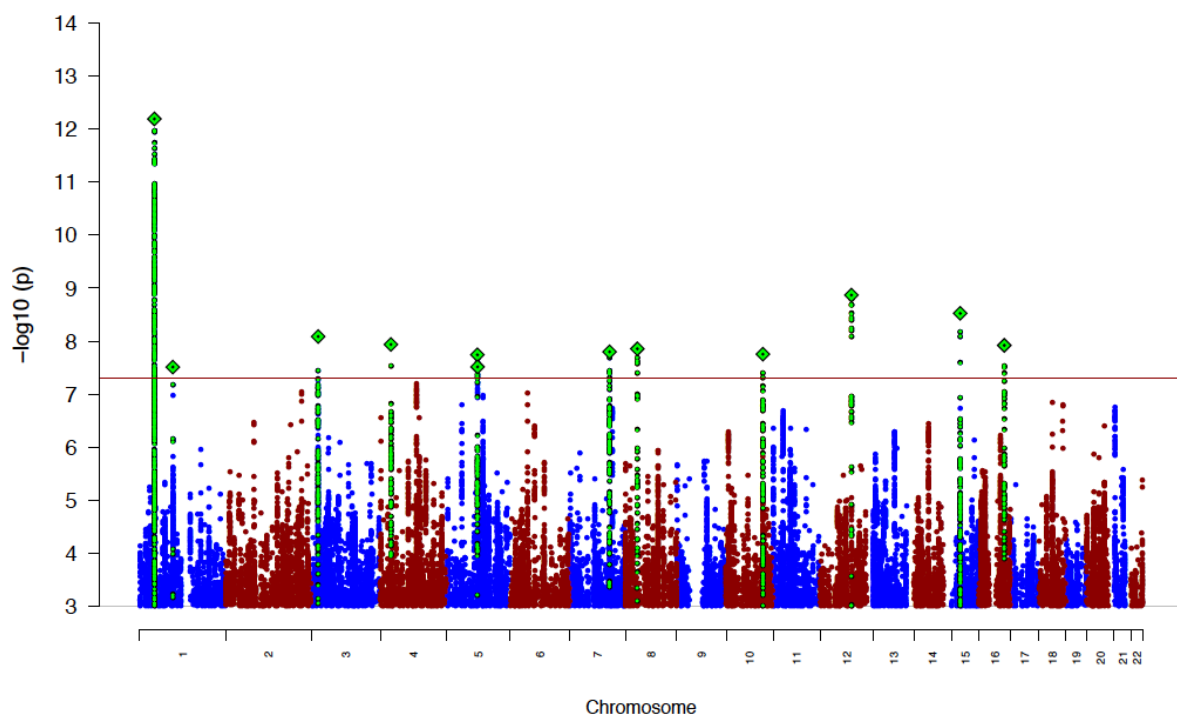
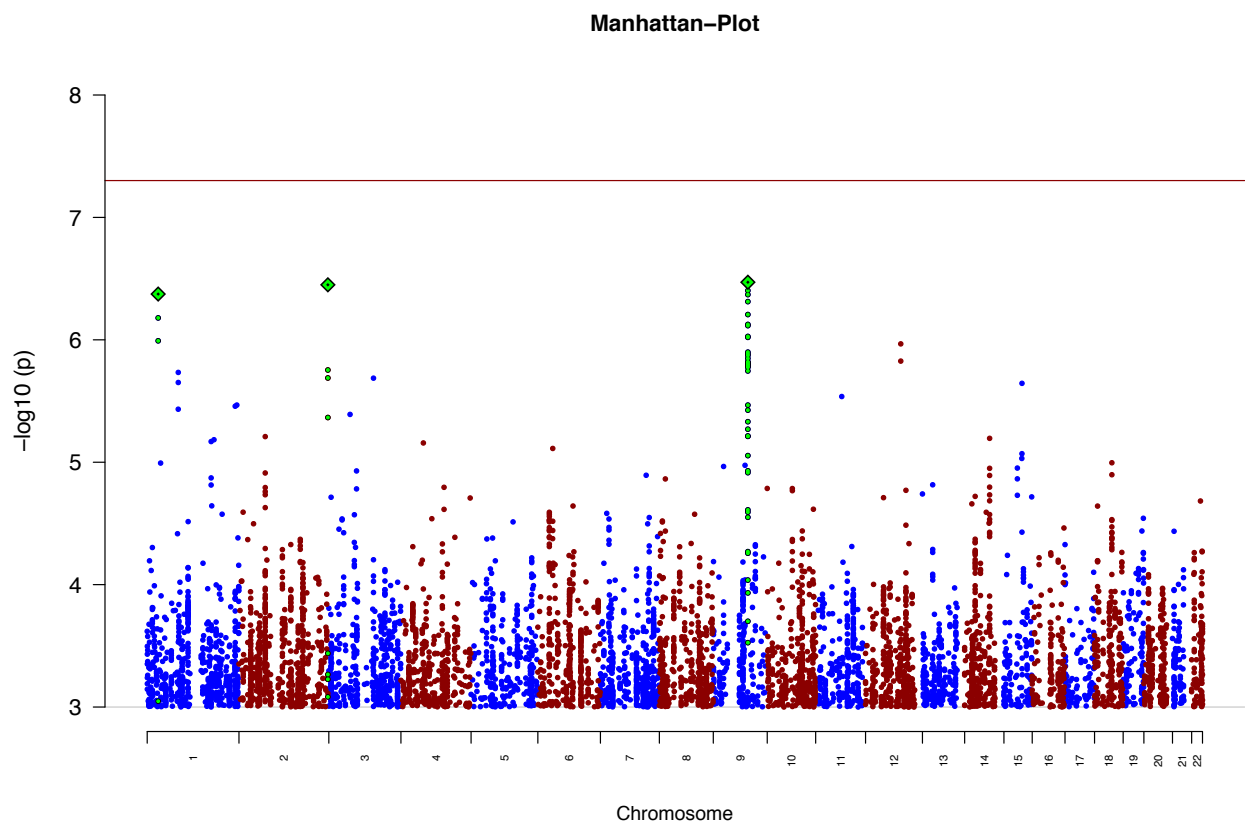


Figure 3n2. Regional association plot for rs212178



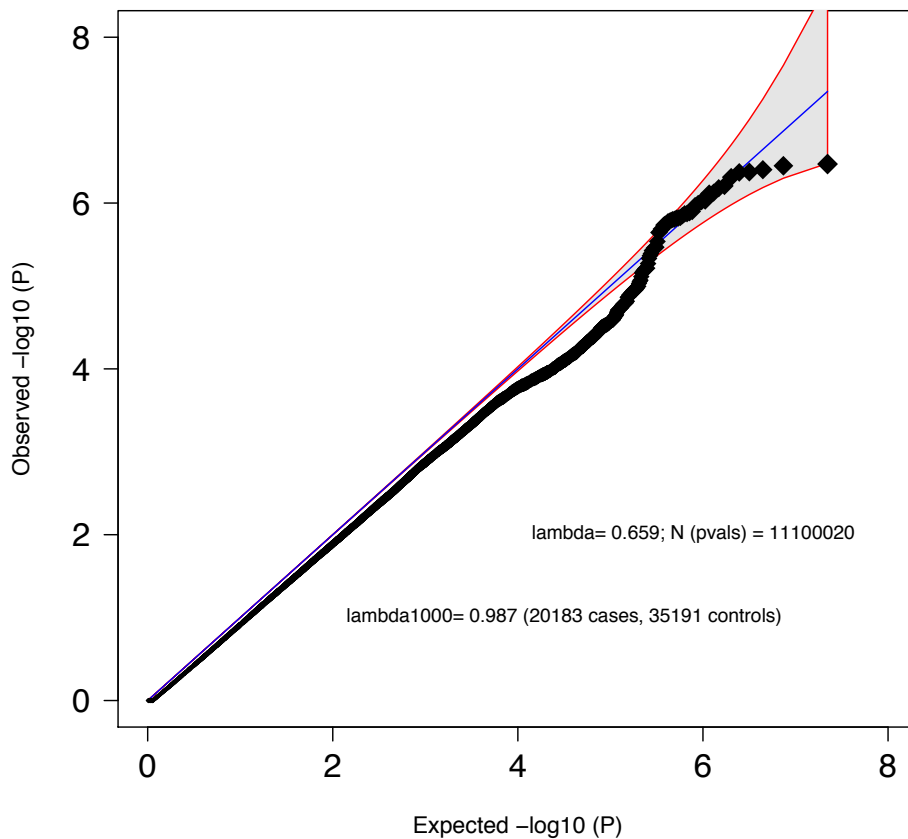
Supplementary Figure 4. Manhattan plot from ADHD European GWAS meta-analysis

Results from GWAS meta-analysis of iPSYCH and PGC European samples. Two-sided P-values from meta-analysis using an inverse-variance weighted fixed effects model, and a sample size of 19,099 cases, 34,194 controls. The red vertical line represents the threshold for genome-wide significant association ($P = 5 \times 10^{-8}$).



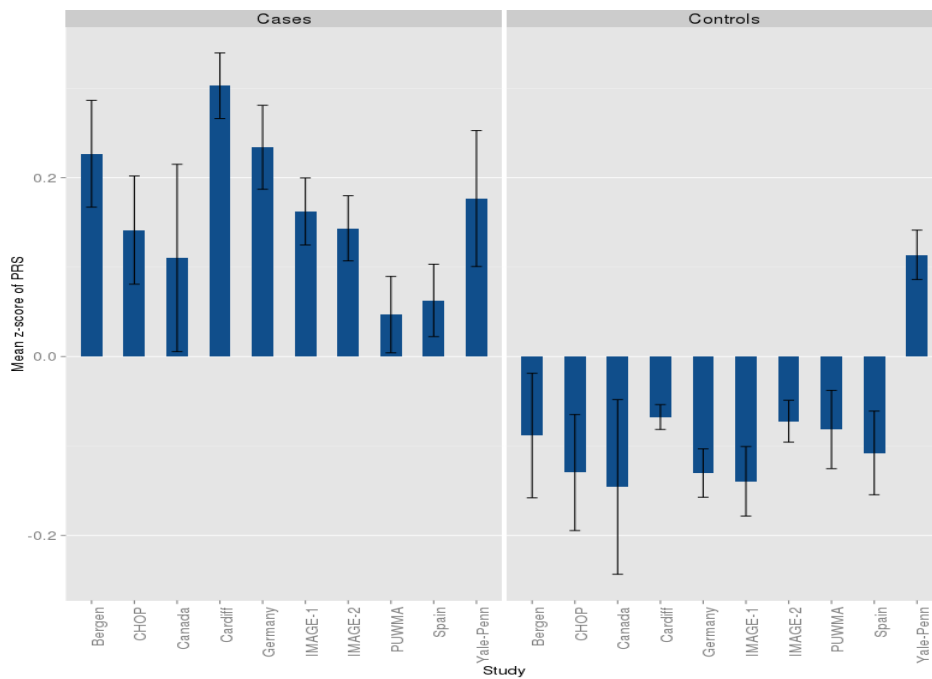
Supplementary Figure 5. Manhattan plot from test for heterogeneity between studies/waves in the ADHD GWAS meta-analysis

Test for heterogeneity across cohorts. The y-axis represents $-\log(P\text{-values})$ from omnibus test of heterogeneity across cohorts/waves (I^2 statistic (I^2)). See Supplementary Table 1 for sample sizes. Red reference line indicates genome-wide significance threshold ($P = 5 \times 10^{-8}$).



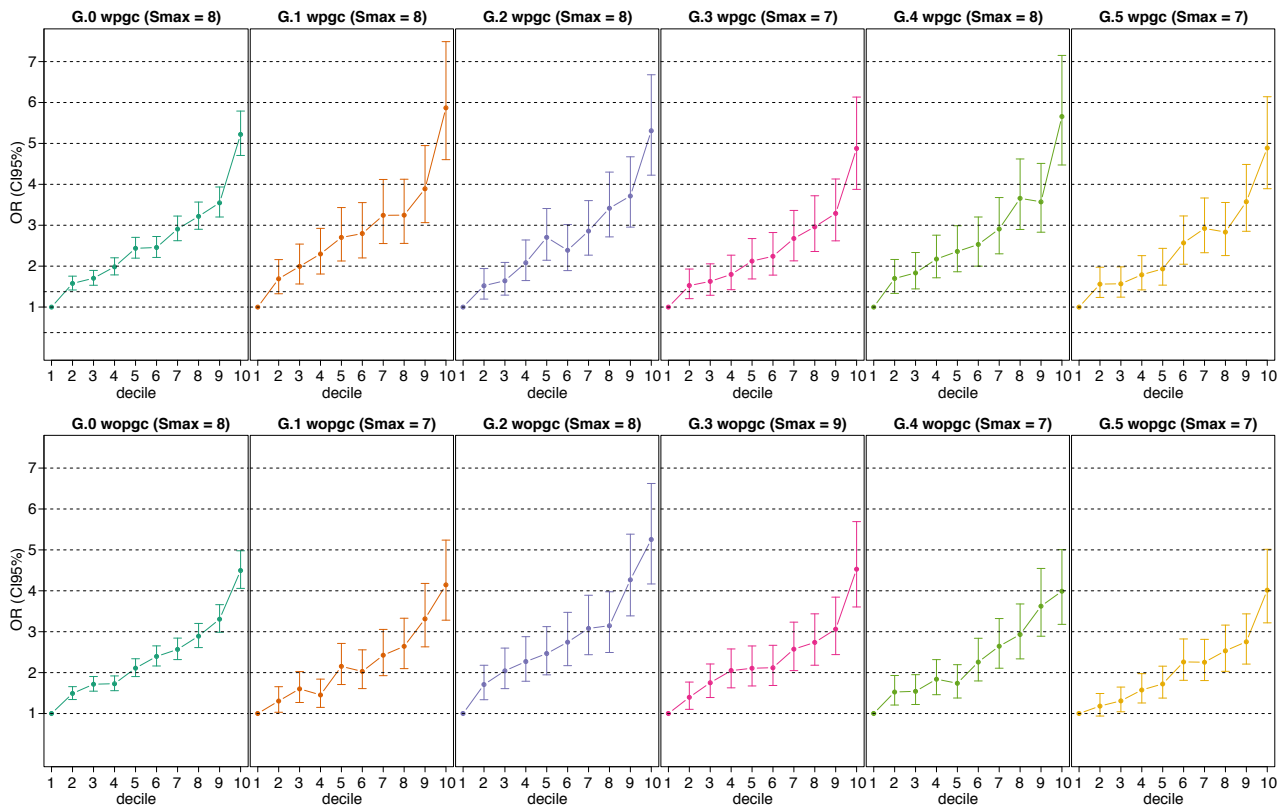
Supplementary Figure 6. Q-Q plot from test for heterogeneity between all samples/waves in the ADHD GWAS meta-analysis

Quantile-quantile plot of P-values from the omnibus test of heterogeneity (I^2) between samples/waves. See Supplementary Table 1 for sample sizes of cohorts and Supplementary Figure 3 legend for wave sample sizes. The blue line indicates the distribution under the null hypothesis and the shaded area indicates the 95% confidence band.



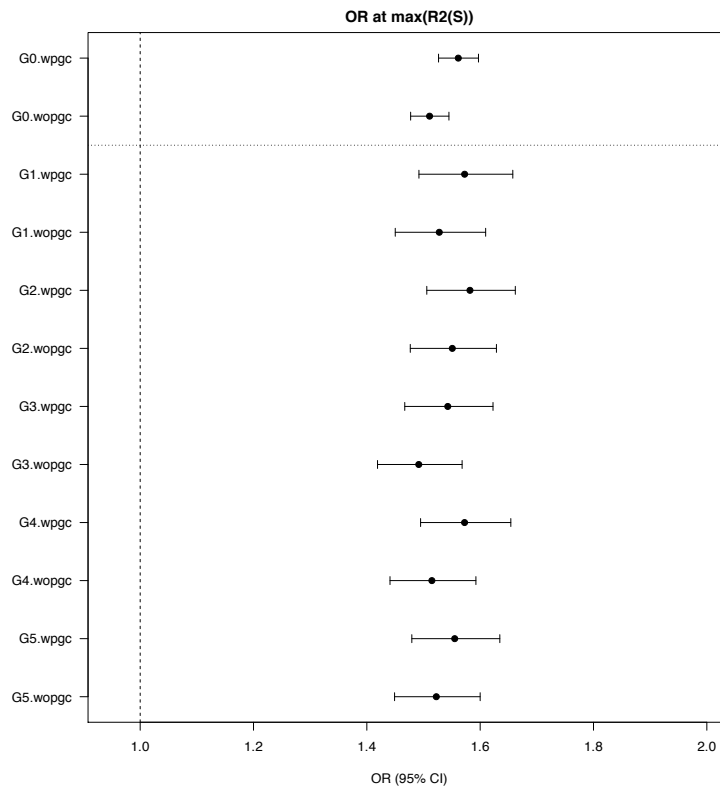
Supplementary Figure 7. ADHD PRS stratified by case-control status and PGC study

The bar represents the mean PRS z-score (+/- standard error) plotted stratified by case/control status and PGC study. See Supplementary Table 1, for sample sizes.



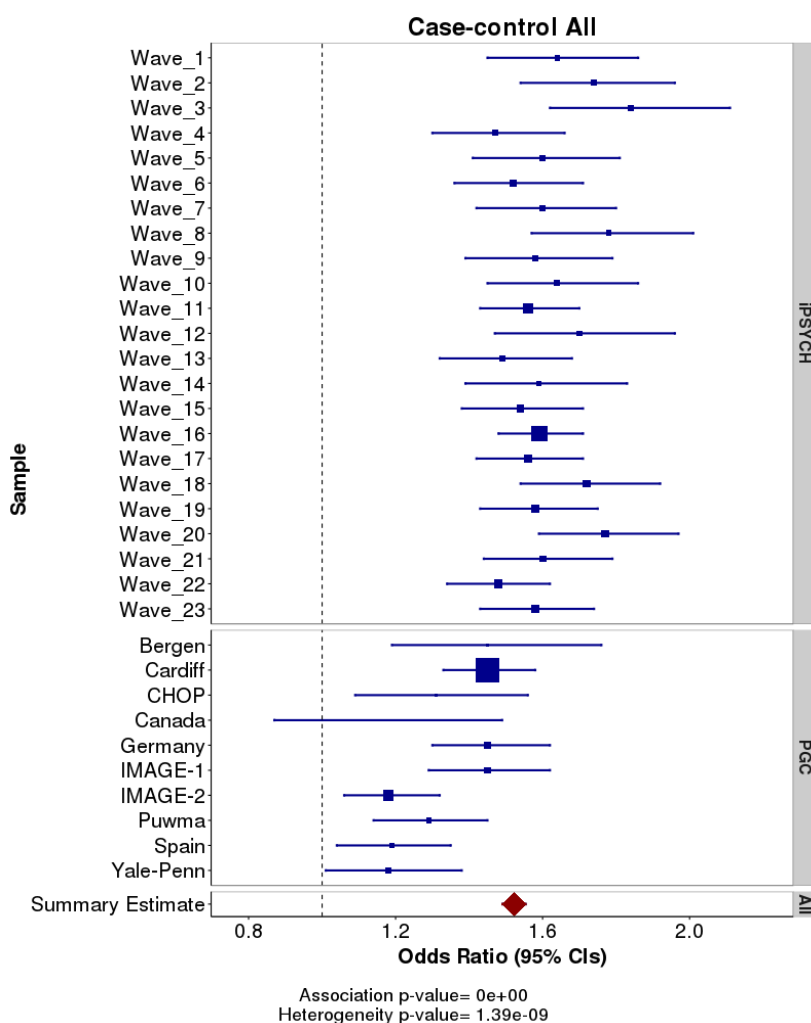
Supplementary Figure 8. Odds ratios by PRS within deciles in target groups

Odds ratios by PRS within deciles for each of the five target groups (G1-G5) and for the pooled (G0) analysis with (upper panels) and without (lower panels) PGC European samples included among the training data sets. Odds Ratios and 95% confidence limits (error bars) were estimated using logistic regression on the continuous scores. The pooled and the five target groups consist of $n_{G0} = 37,076$, $n_{G1} = 6,726$, $n_{G2} = 8,108$, $n_{G3} = 7,339$, $n_{G4} = 7,427$, $n_{G5} = 7,476$ biological independent individuals respectively. Plots are shown for the GWAS P-value threshold for variant inclusion in the training dataset with the highest Nagelkerke's R^2 (Smax).



Supplementary Figure 9. Odds ratios within target groups in iPSYCH

Odds ratios between ADHD cases and controls within target groups in iPSYCH. PRS-based odds ratio and 95% confidence limits (error bars) were obtained from logistic regression of continuous PRS (normalized by target group) for each target group considered separately (G1-G5) and pooled (G0). The pooled (G0) and the five target groups (G1-G5) consist of $n_{G0} = 37,076$, $n_{G1} = 6,726$, $n_{G2} = 8,108$, $n_{G3} = 7,339$, $n_{G4} = 7,427$, $n_{G5} = 7,476$ biological independent individuals. PRS estimated using iPSYCH waves alone as training sample (wopgc) or iPSYCH waves together with PGC European samples (wpgc).



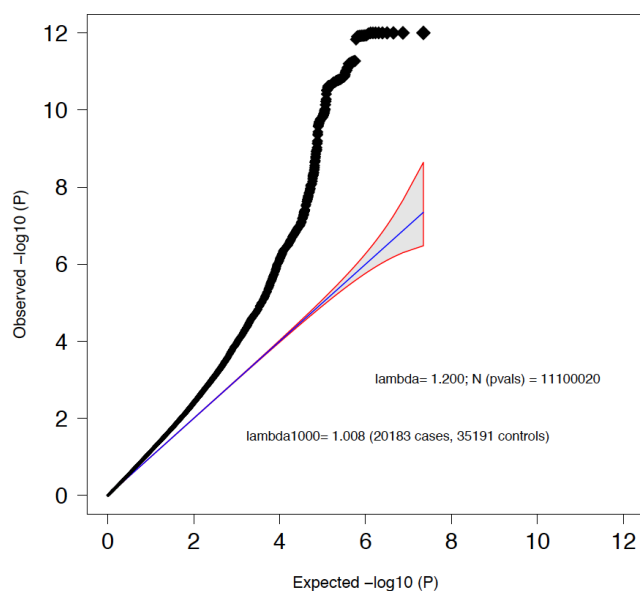
Supplementary Figure 10. PRS-based odds ratios within each study/wave

The dots represent PRS-based odds ratio and 95% confidence limits from logistic regression of standardised PRS for each target study/wave. Across PGC studies and iPSYCH waves, the mean variance explained on the liability scale was 0.0371 (standard error of the mean = 0.0029).

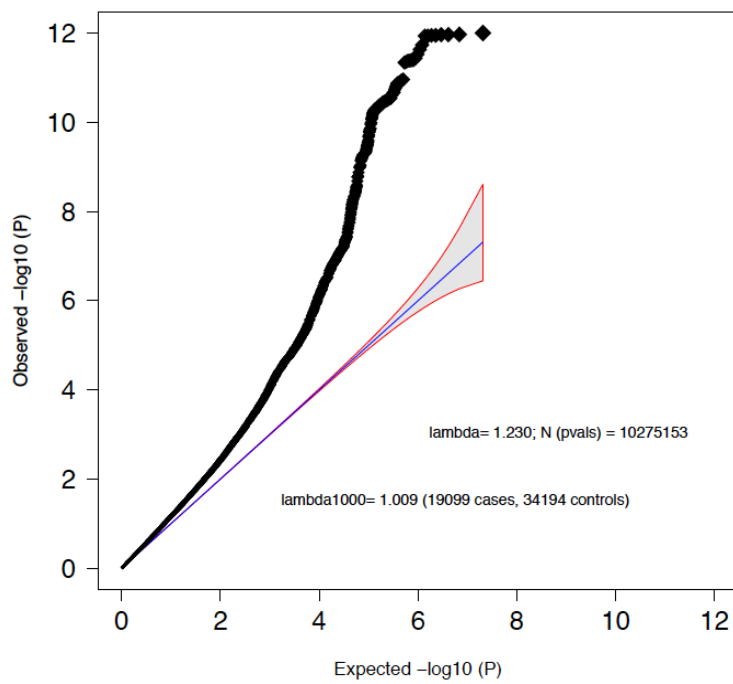
Information about cohort sample size can be found in Supplementary Table 1 and wave sample size is given in the legend of Supplementary Figure 3.A1 - M1.

Supplementary Figure 11a – 11b. Q-Q plot from GWAS meta-analyses

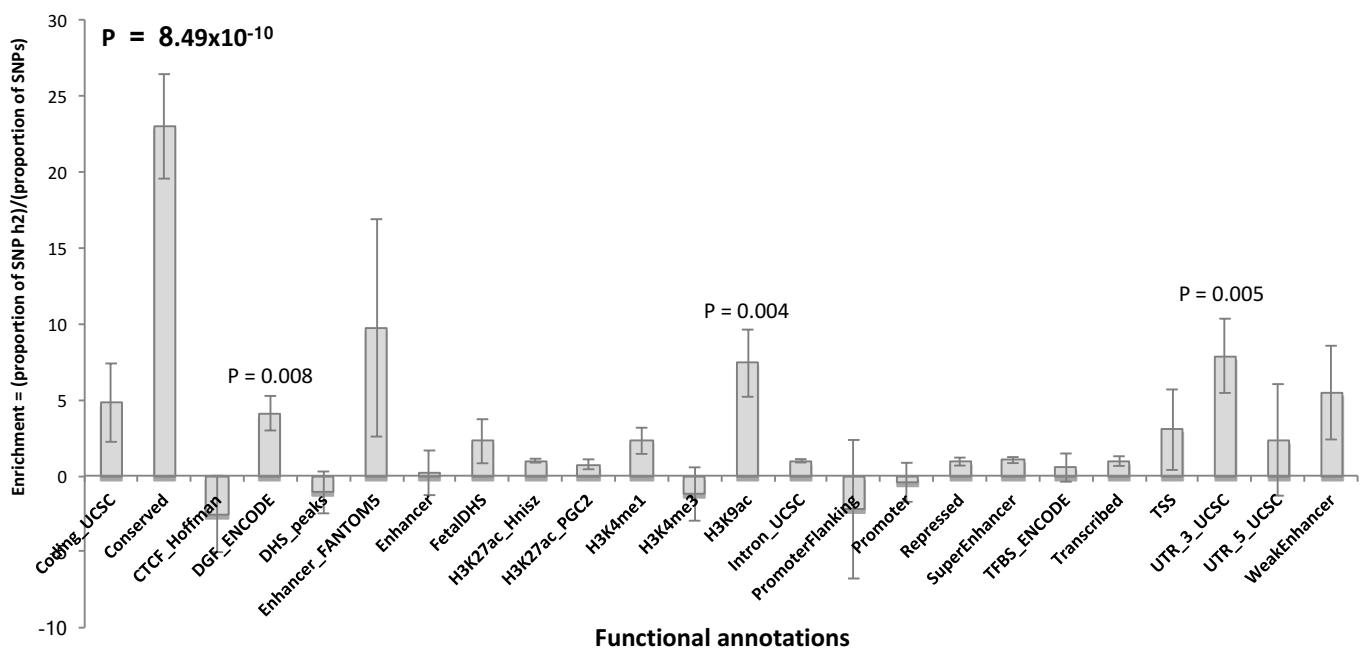
Quantile-quantile plot of the $-\log_{10}$ P-values from GWAS meta-analyses. P-values are two-sided from meta-analysis using an inverse-variance weighted fixed effects model. The blue line indicates the distribution under the null hypothesis and the shaded area indicates the 95% confidence band.



Supplementary Figure 11a. Q-Q plot from GWAS meta-analysis (20,183 cases and 35,191 controls).

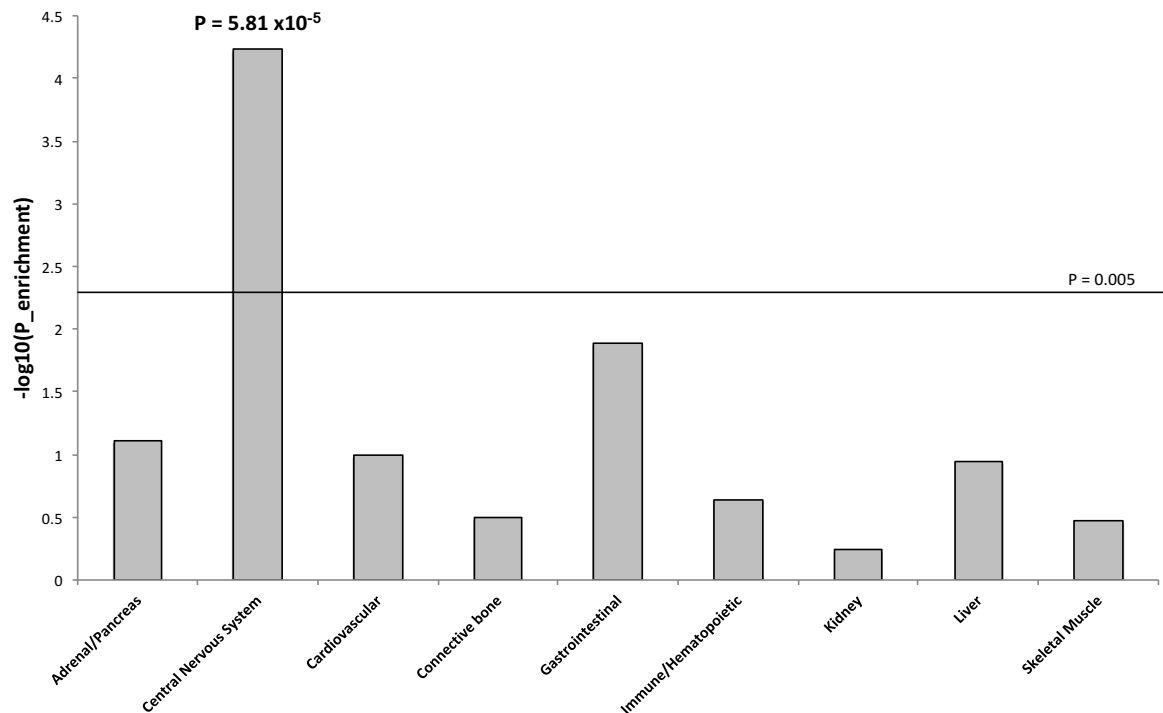


Supplementary Figure 11b. Q-Q plot from European GWAS meta-analysis (19,099 cases, 34,194 controls).



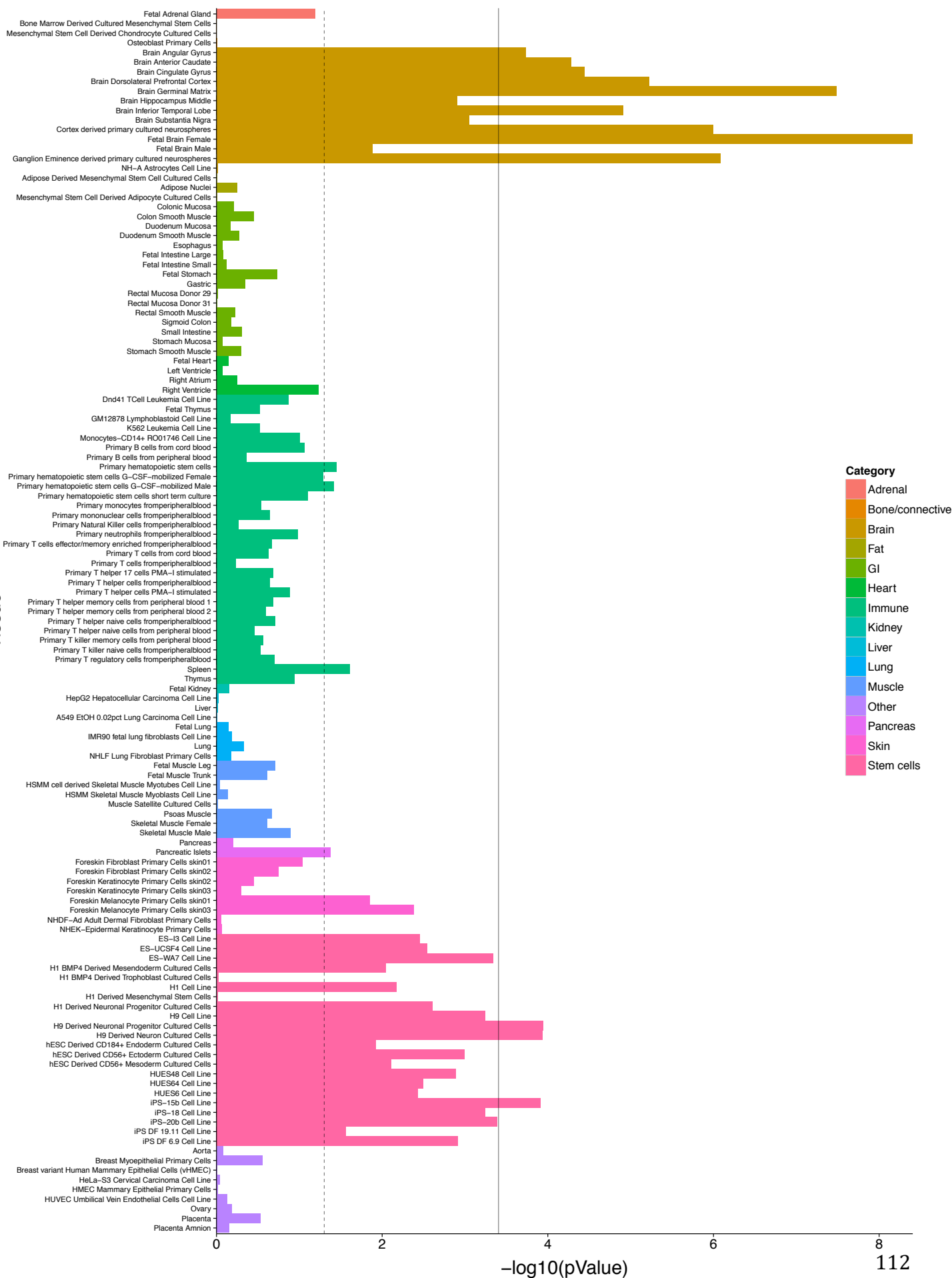
Supplementary Figure 12. Partitioning of h^2 by functional annotations

The bars represent enrichment of heritability per SNP in 24 functional annotations defined by Finucane et al.⁶⁹ The error bars represent jackknife standard errors around the estimates of enrichment. P-values for annotation categories with nominal significant enrichment are shown and values on bold indicate significance after Bonferroni correction (correction for 24 tests). The analysis is based on results from European GWAS meta-analysis (19,099 cases, 34,194 controls).



Supplementary Figure 13. Partitioning of h^2 by tissue-group annotations

Results from partitioning heritability by SNPs located in cell-group specific regulatory elements. The y-axis represents P-values ($-\log(P_{\text{enrichment}})$) from test for enrichment. The line indicate significance after Bonferroni correction ($P = 0.005$; correction for nine tests). The analysis is based on results from European GWAS meta-analysis (19,099 cases, 34,194 controls).

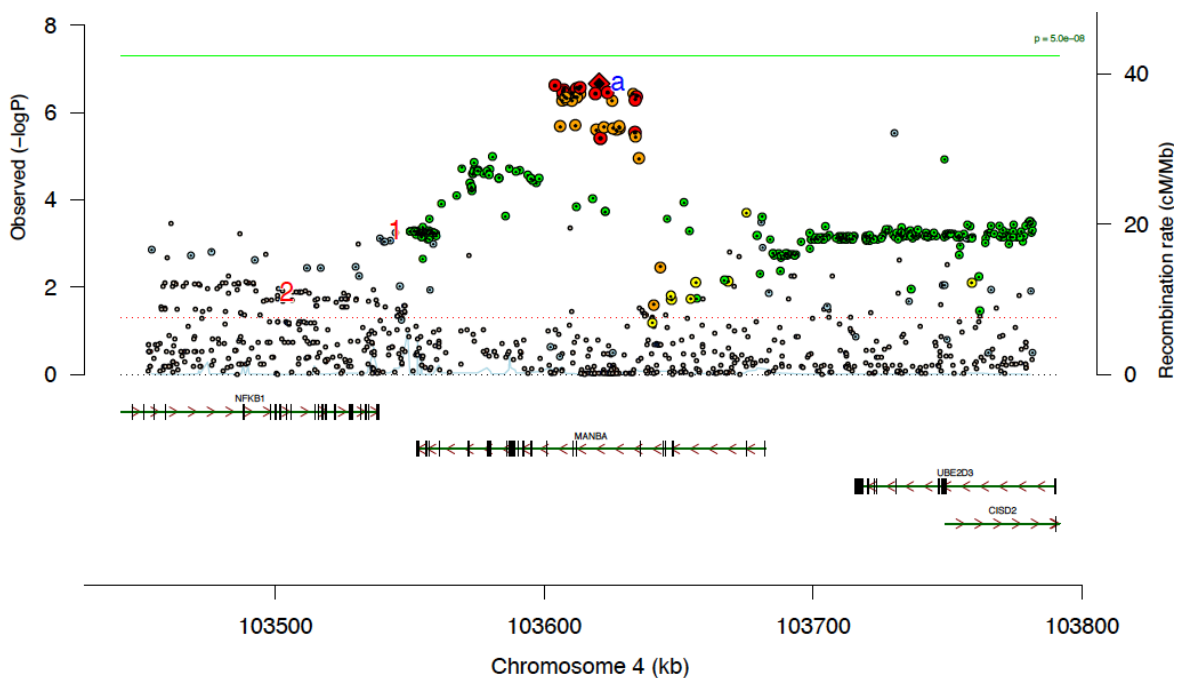


Supplementary Figure 14. Partitioning of h^2 by tissue-specific H3K4Me1 annotations

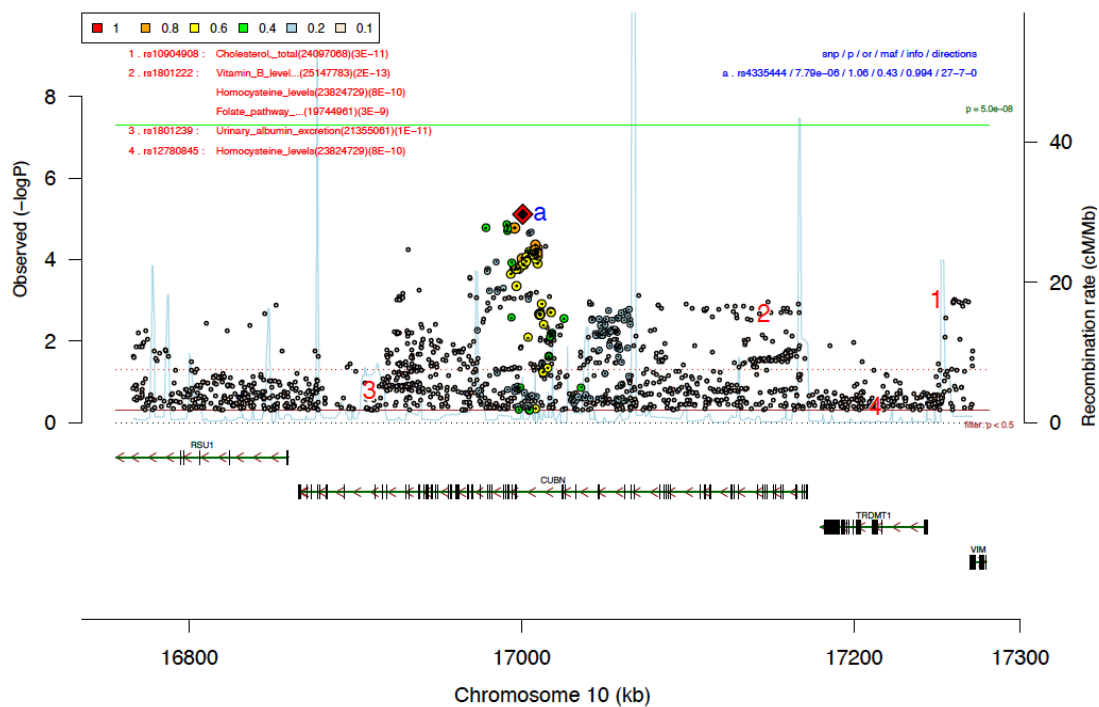
P-values for enrichment in the SNP heritability of ADHD by variants located within regulatory regions (H3K4Me1 peaks) of various cells and tissues (annotations from the Roadmap Epigenomics Mapping Consortium⁷²). Dashed line: threshold for nominal significance. Full line: threshold for significance after Bonferroni correction. The analysis is based on results from European GWAS meta-analysis (19,099 cases, 34,194 controls).

Supplementary Figure 15a – 15d. Gene-based association, regional association plots

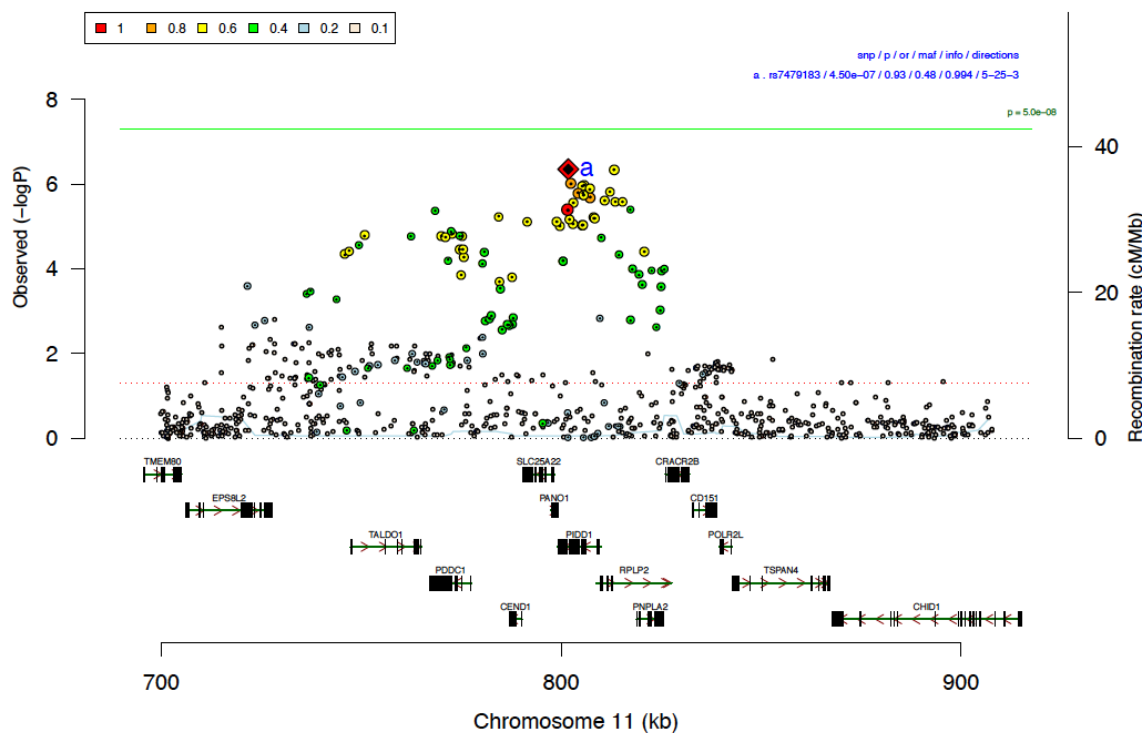
LD structure in the region around the four new genes (genes not overlapping with loci being gws in the single marker GWAS meta-analysis) significantly association with ADHD in the MAGMA gene-based association. The y-axis represents $-\log(P\text{-values})$ of variant association with ADHD; the P-values are two-sided from meta-analysis using an inverse-variance weighted fixed effects model and based on of 20,183 ADHD cases and 35,191 controls. The vertical green line represents the threshold for genome-wide significance ($P = 5 \times 10^{-8}$).



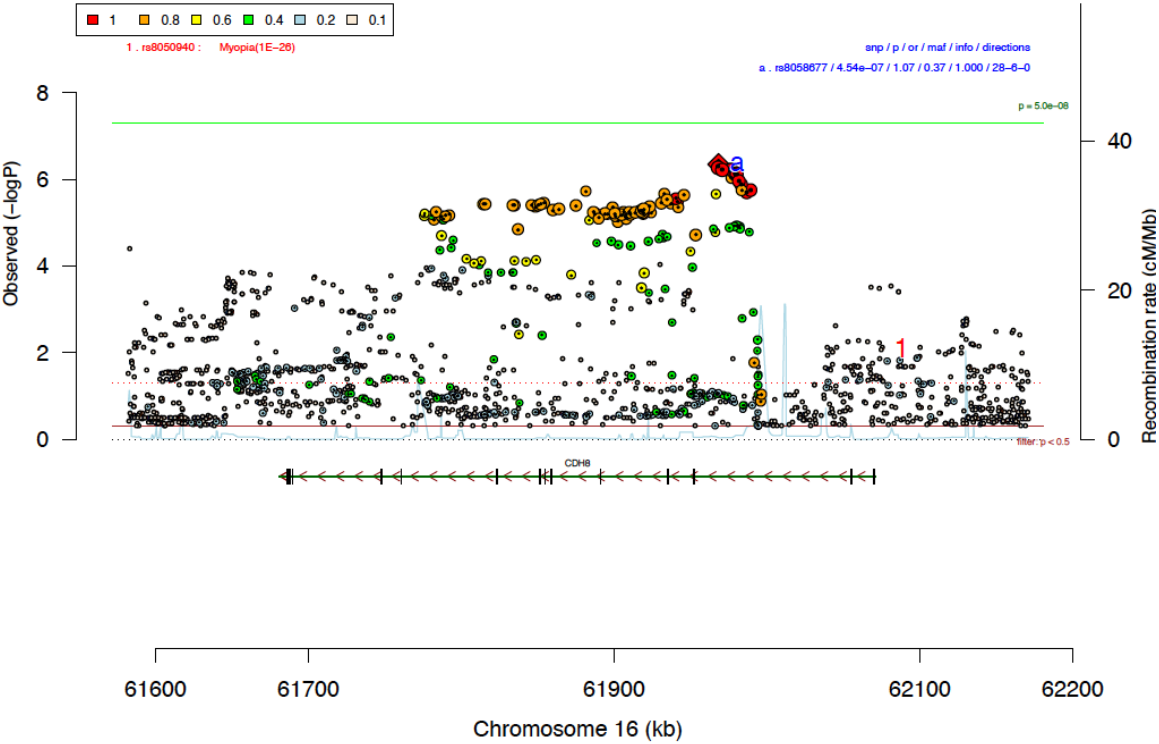
Supplementary Figure 15a. Regional association plot for *MANBA* (+/- 100,000 bp up- and down-stream of the gene).



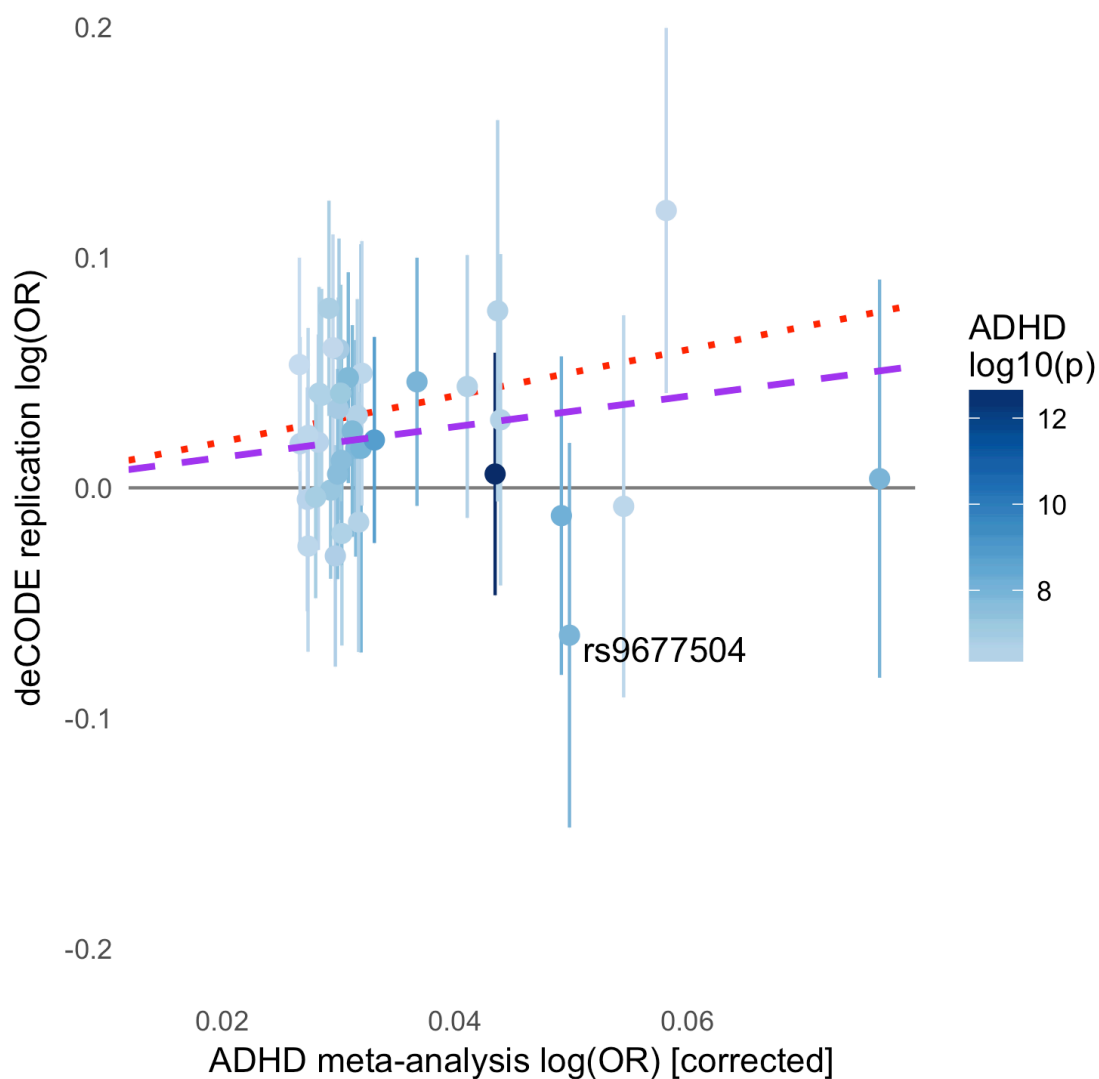
Supplementary Figure 15b. Regional association plot for *CUBN* (+/- 100,000 bp up- and down-stream of the gene).



Supplementary Figure 15c. Regional association plot for *PID1* (+/- 100,000 bp up- and down-stream of the gene).

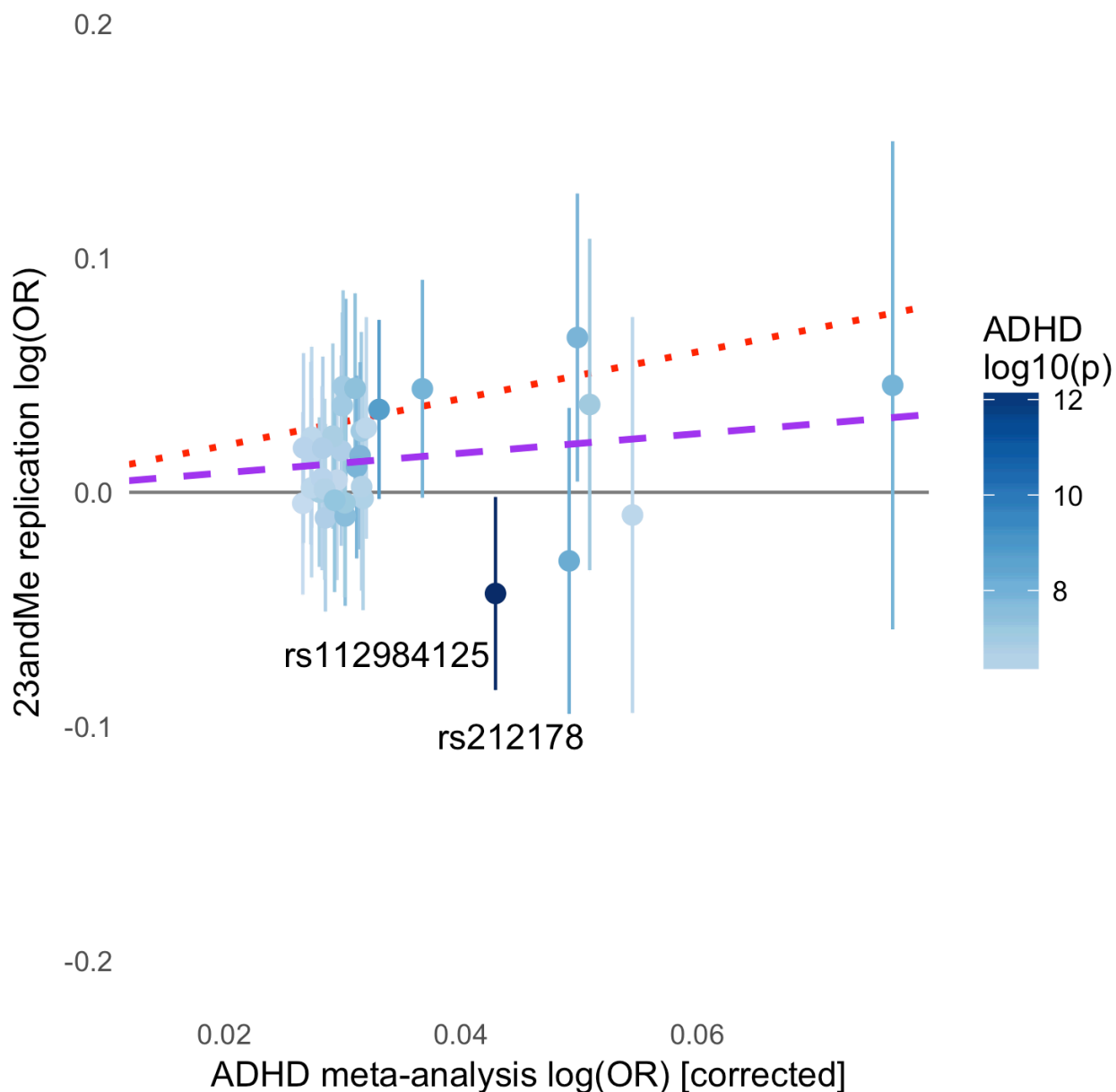


Supplementary Figure 15d. Regional association plot for *CDH8* (+/- 100,000 bp up- and down-stream of the gene).



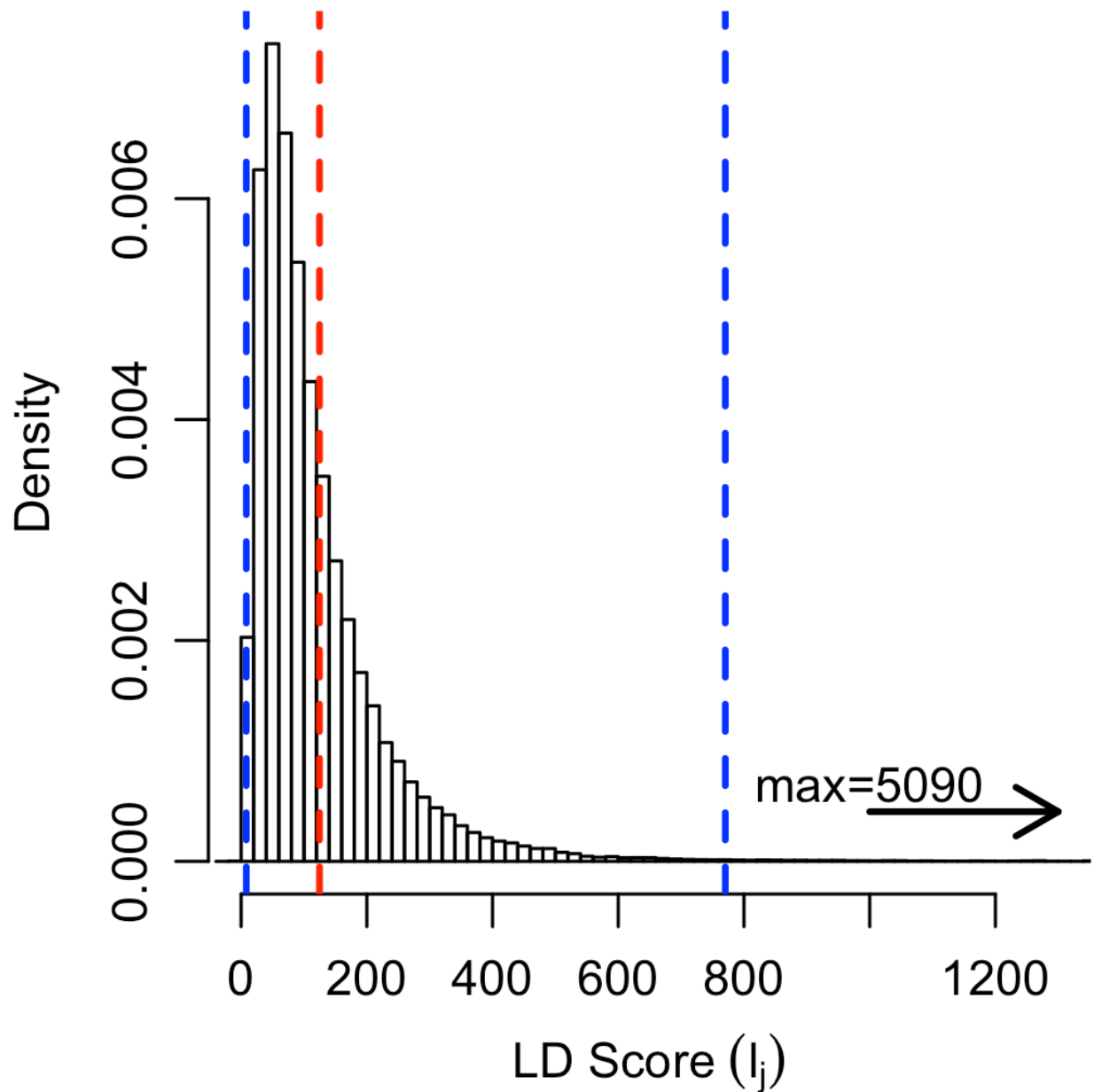
Supplementary Figure 16. Comparison of estimated effect sizes from deCODE

Regression of deCODE effect size estimates (from logistic regression of 5,085 cases, 131,122 controls) on winner's curse-adjusted effect size estimates for top loci ($P < 1 \times 10^{-6}$) in the ADHD GWAS (results from meta-analysis using an inverse-variance weighted fixed effects model including 20,183 ADHD cases and 35,191 controls). All variants oriented to the allele estimated to increase risk in the ADHD GWAS. Dotted red reference line indicates a slope of 1, the target result for an "ideal" replication. Dashed purple line indicates observed slope of linear regression of log odds ratio (OR) weighted by inverse standard error.



Supplementary Figure 17. Comparison of estimated effect sizes from 23andMe

Regression of 23andMe effect size (from meta-analysis using an inverse-variance weighted fixed effects model based on 5,857 cases, 70,393 controls) estimates on winner's curse-adjusted effect size estimates for top loci ($p < 1e-6$) in the ADHD GWAS. All variants oriented to the allele estimated to increase risk in the ADHD GWAS. Dotted red reference line indicates a slope of 1, the target result for an “ideal” replication. Dashed purple line indicates observed slope of linear regression of log odds ratio (OR) weighted by inverse standard error.

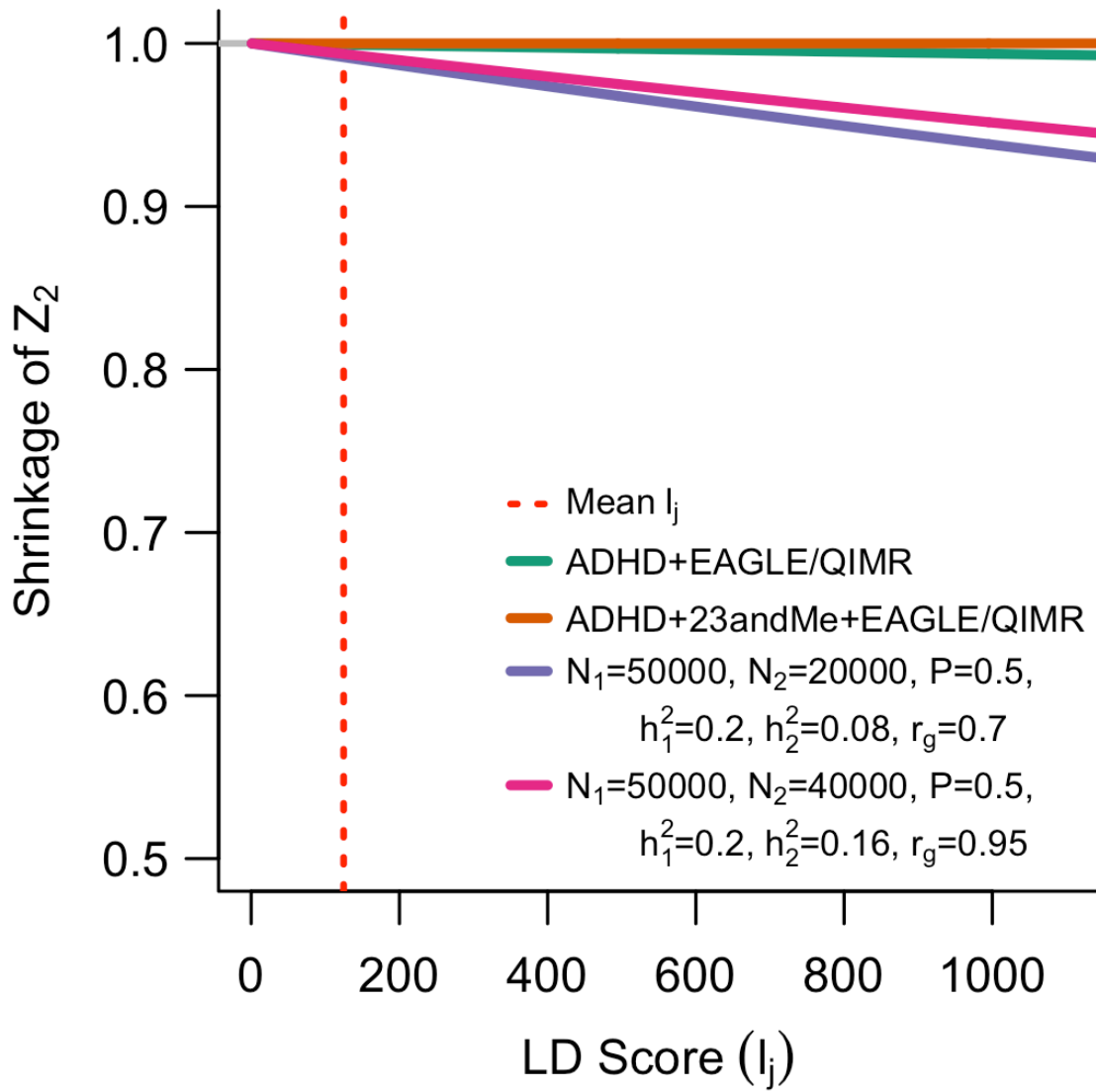


Supplementary Figure 18. Distribution of 1000 Genomes Phase 3 European LD Scores

Distribution of LD scores l_j for common HapMap3 SNPs estimated in 1000 Genomes Phase 3 data using individuals of European ancestry. LD scores downloaded from

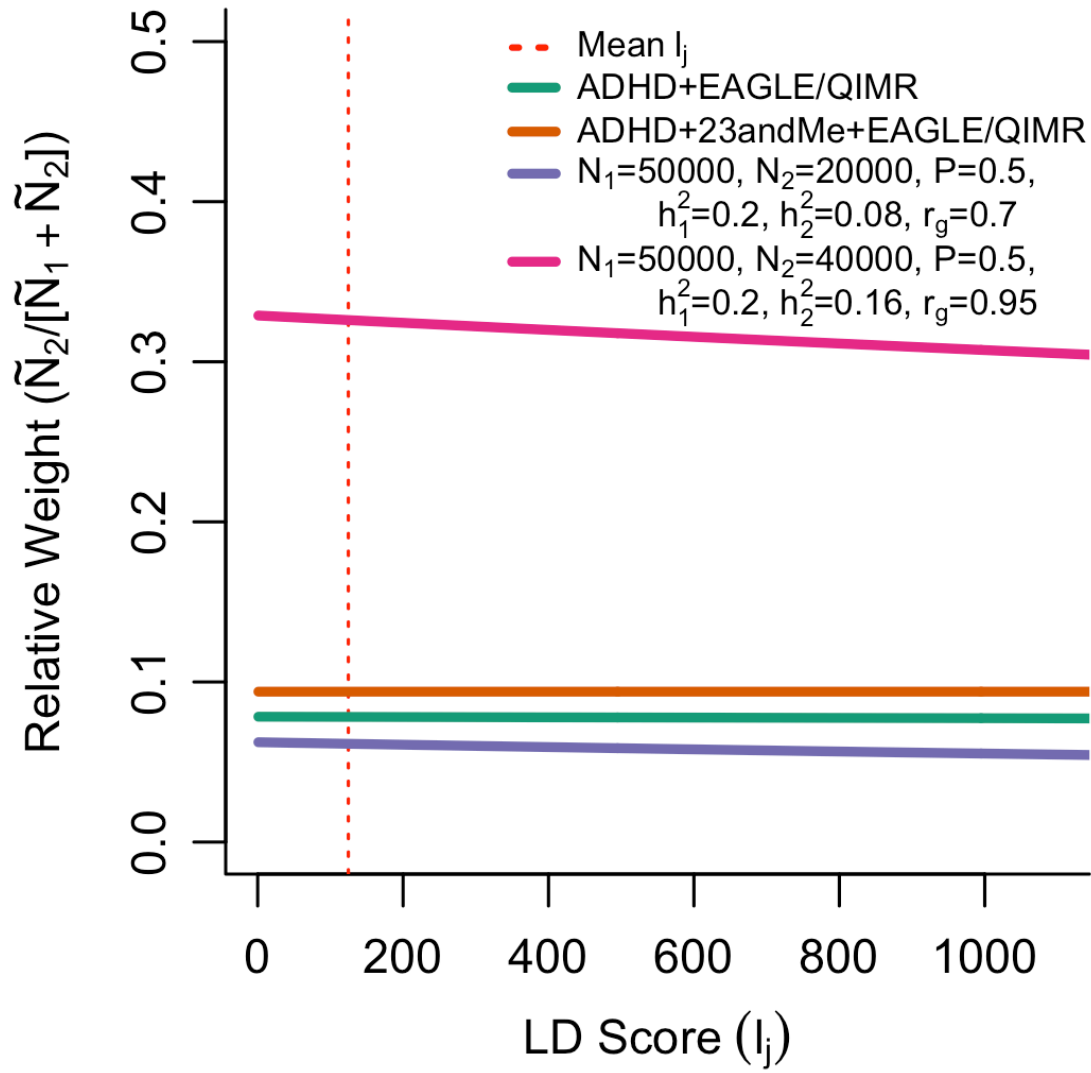
<http://data.broadinstitute.org/alkesgroup/LDSCORE/>. Red reference line indicates mean LD score.

Blue reference lines indicate 0.5% and 99.5% quantiles of the distribution.



Supplementary Figure 19. Shrinkage factor for \tilde{Z}_{2j} with varying l_j

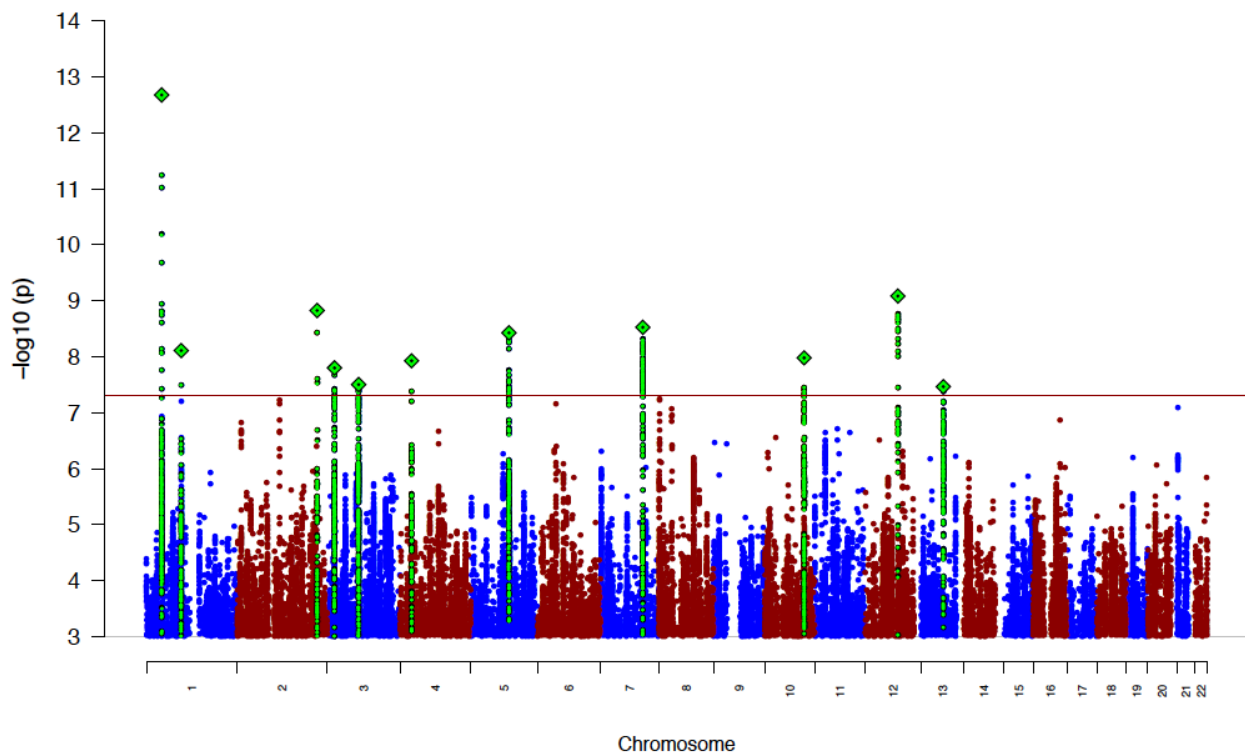
Value of $1/\sqrt{1 + (1 - r_g^2)N_2h_2^2 l_j/M}$, the reduction in Z_{2j} to account for polygenic effects specific to the second phenotype, across the range of observed values for l_j . We compare the value of this term at the estimates of r_g^2 , N_2 , h_2^2 , and M observed in the current study, as well as with example values for scenarios with lower r_g^2 or a more highly powered GWAS of the second phenotype (i.e. increased N_2 and h_2^2). The red reference line indicates the fixed value of $l_j = 124.718$ used for the current study.



Supplementary Figure 20. Relative effective sample size \tilde{N}_{2j} with varying l_j

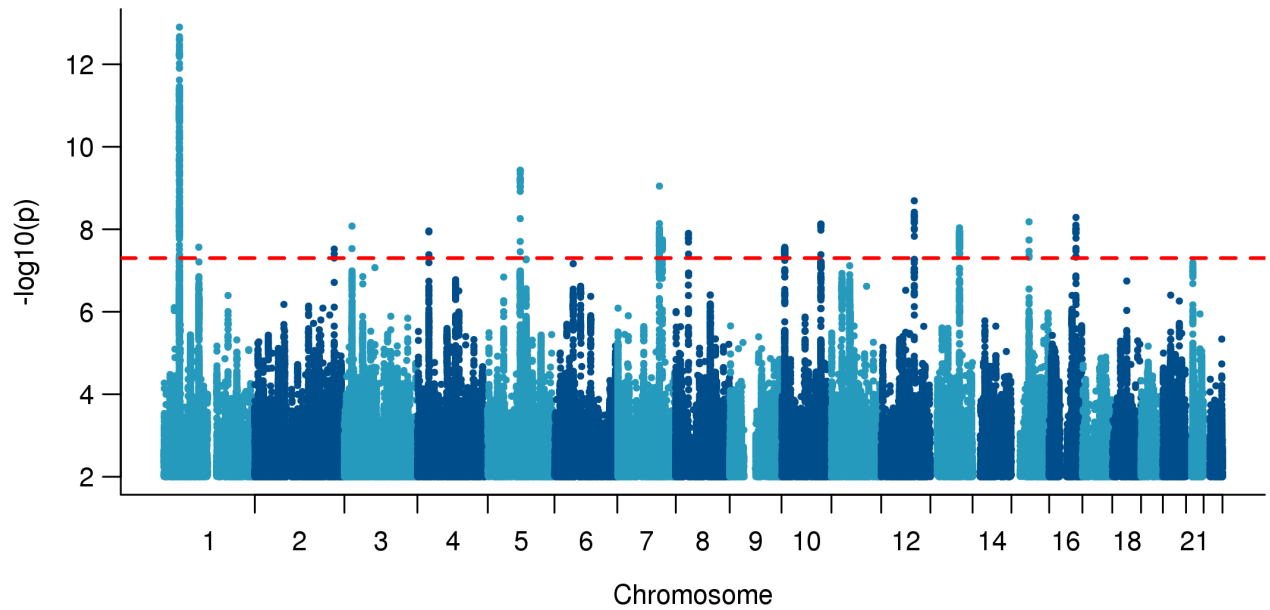
Value of $\tilde{N}_{2j}/(\tilde{N}_{1j} + \tilde{N}_{2j})$, the relative effective sample size for the second phenotype, across the range of observed values for l_j . We compare the value of this term at the estimates of

$N_1, N_2, r_g^2, h_1^2, h_2^2, K, P$, and M observed in the current study, as well as with example values for scenarios with lower r_g^2 or a more highly powered GWAS of the second phenotype (i.e. increased N_2 and h_2^2). The red reference line indicates the fixed value of $l_j = 124.718$ used for the current study.



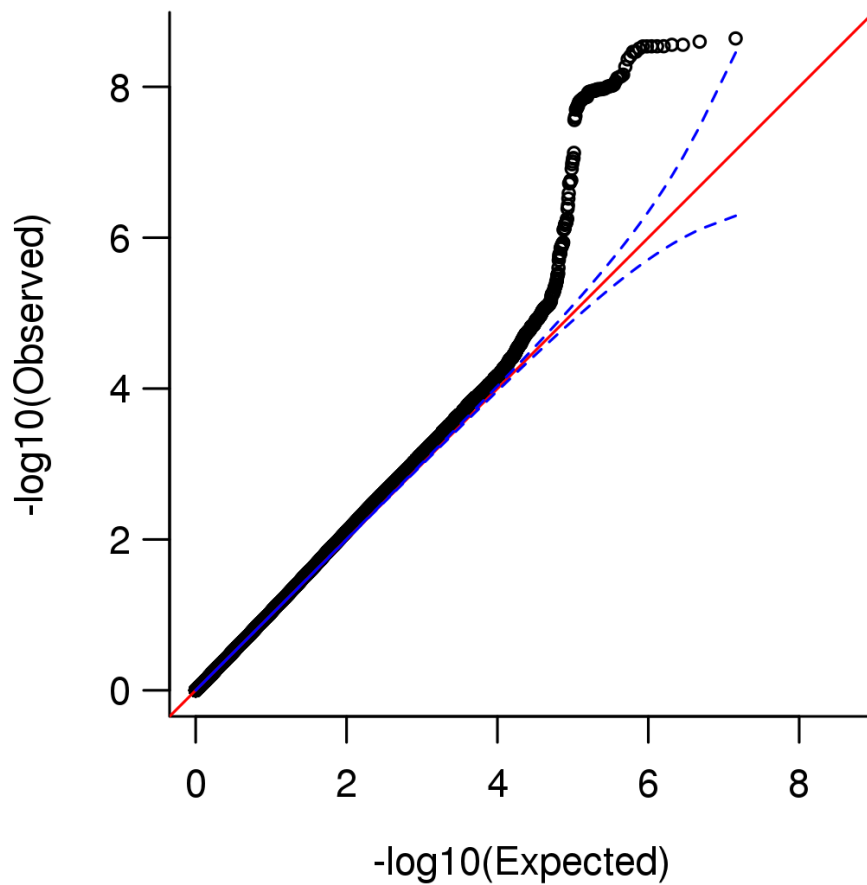
Supplementary Figure 21. Manhattan plot of results from meta-analysis of ADHD+23andMe

Genome-wide association results from the replication meta-analysis of ADHD+23andMe (26,040 cases, 105,584 controls), performed using the inverse-variance weighted fixed effects model. The genome-wide significant locus on chromosome four is only driven by iPSYCH/PGC since there is no information about this locus in 23andMe. The red line indicates the threshold for genome-wide significance ($P=5 \times 10^{-8}$).



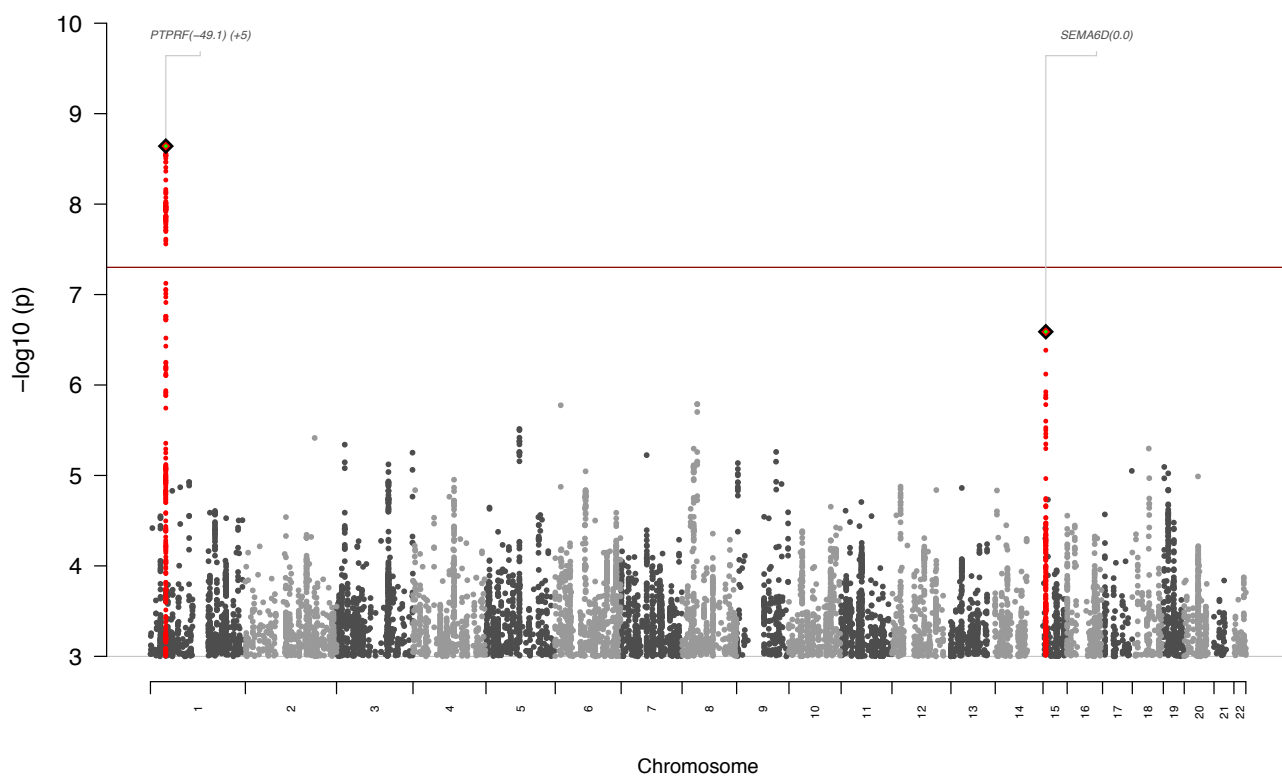
Supplementary Figure 22. Manhattan plot of results from meta-analysis of ADHD+EAGLE/QIMR

Genome-wide results for meta-analysis of the ADHD GWAS (20,183 cases and 35,191 controls) and EAGLE/QIMR (20,464 individuals) using the modified sample size-based weights calibrated by estimates of heritability and genetic correlation. The red line indicates the threshold for genome-wide significance ($P=5 \times 10^{-8}$).



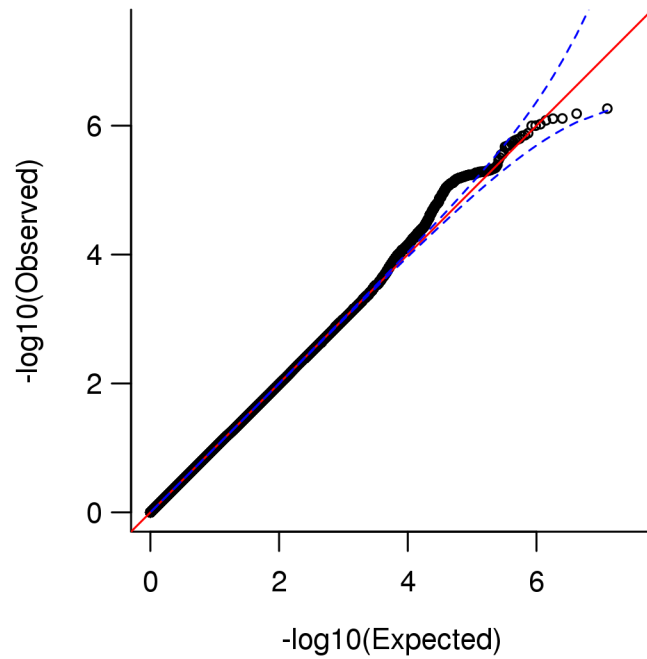
Supplementary Figure 23. Q-Q plot from test for heterogeneity between ADHD GWAS meta-analysis and 23andMe

Quantile-quantile plot of P-values for the 1 degree of freedom test (I squared statistic (I^2)) of heterogeneity between 23andMe (5,857 cases, 70,393 controls) and the ADHD GWAS (20,183 cases and 35,191 controls) for genome-wide variants.



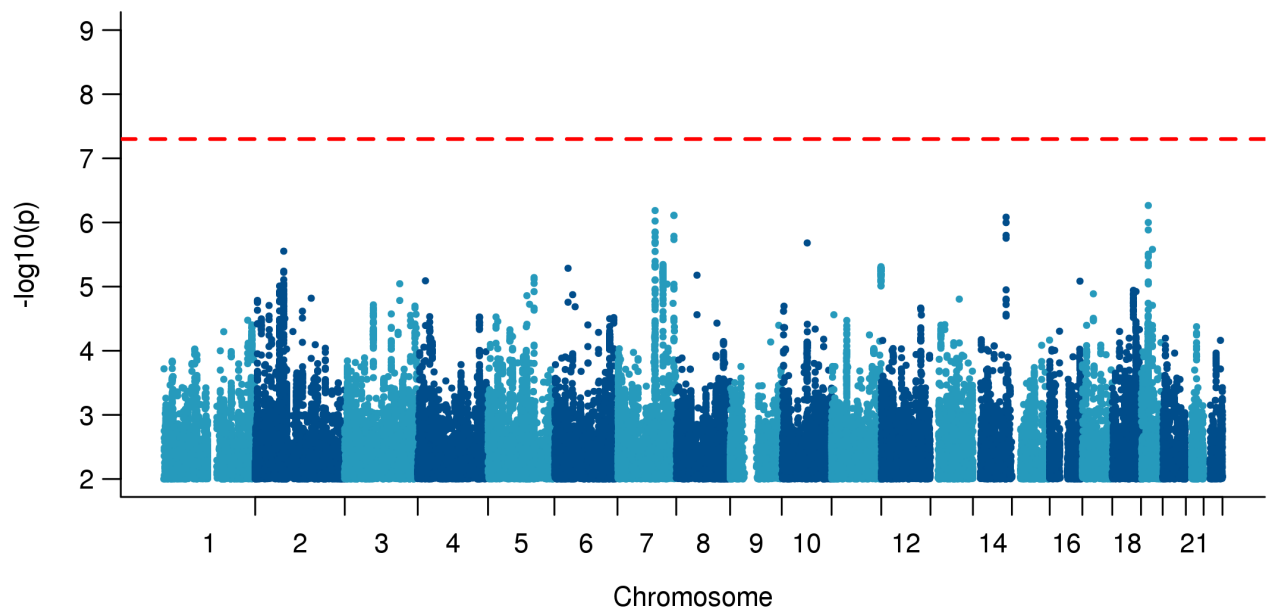
Supplementary Figure 24. Manhattan plot from test for heterogeneity between ADHD GWAS meta-analysis and 23andMe

Genome-wide association results for the 1 degree of freedom test of heterogeneity (I^2 statistic (I^2)) between 23andMe (5,857 cases, 70,393 controls) and the ADHD GWAS (20,183 cases and 35,191 controls). Red reference line indicates genome-wide significance ($P=5 \times 10^{-8}$).



Supplementary Figure 25. Q-Q plot from test for heterogeneity between ADHD GWAS meta-analysis and EAGLE/QIMR

Quantile-quantile plot of P-values for the 1 degree of freedom test of heterogeneity (I^2 statistic) between EAGLE/QIMR (20,464 individuals) and the ADHD GWAS (20,183 cases and 35,191 controls) for genome-wide variants.



Supplementary Figure 26. Manhattan plot from test for heterogeneity between ADHD GWAS meta-analysis and EAGLE/QIMR

Genome-wide association results for the 1 degree of freedom test of heterogeneity (I^2 squared statistic (I^2)) between EAGLE/QIMR (20,464 individuals) and the ADHD GWAS (20,183 cases and 35,191 controls) for genome-wide variants. The dashed red reference line indicates genome-wide significance (5×10^{-8}).

References

- 1 Pedersen, C. B., Gotzsche, H., Moller, J. O. & Mortensen, P. B. The Danish Civil Registration System. A cohort of eight million persons. *Dan Med Bull.* **53**, 441-449 (2006).
- 2 Mors, O., Perto, G. P. & Mortensen, P. B. The Danish Psychiatric Central Research Register. *Scand J Public Health* **39**, 54-57, doi:10.1177/1403494810395825 (2011).
- 3 Borglum, A. D. *et al.* Genome-wide study of association and interaction with maternal cytomegalovirus infection suggests new schizophrenia loci. *Molecular psychiatry* **19**, 325-333, doi:10.1038/mp.2013.2 (2014).
- 4 Hollegaard, M. V. *et al.* Robustness of genome-wide scanning using archived dried blood spot samples as a DNA source. *BMC Genet* **12**, 58, doi:10.1186/1471-2156-12-58 (2011).
- 5 Illumina. illumina GenCall Data Analysis Software. *Illumina Tech Note* (2005).
- 6 Korn, J. M. *et al.* Integrated genotype calling and association analysis of SNPs, common copy number polymorphisms and rare CNVs. *Nat Genet* **40**, 1253-1260, doi:10.1038/ng.237 (2008).
- 7 Goldstein, J. I. *et al.* zCall: a rare variant caller for array-based genotyping: genetics and population analysis. *Bioinformatics* **28**, 2543-2545, doi:10.1093/bioinformatics/bts479 (2012).
- 8 Elia, J. *et al.* Rare structural variants found in attention-deficit hyperactivity disorder are preferentially associated with neurodevelopmental genes. *Molecular psychiatry* **15**, 637-646, doi:10.1038/mp.2009.57 (2010).
- 9 Neale, B. M. *et al.* Genome-wide association scan of attention deficit hyperactivity disorder. *Am J Med Genet B Neuropsychiatr Genet* **147B**, 1337-1344, doi:10.1002/ajmg.b.30866 (2008).
- 10 Neale, B. M. *et al.* Meta-analysis of genome-wide association studies of attention-deficit/hyperactivity disorder. *J Am Acad Child Adolesc Psychiatry* **49**, 884-897, doi:10.1016/j.jaac.2010.06.008 (2010).
- 11 Mick, E. *et al.* Family-based genome-wide association scan of attention-deficit/hyperactivity disorder. *J Am Acad Child Adolesc Psychiatry* **49**, 898-905 e893, doi:10.1016/j.jaac.2010.02.014 (2010).
- 12 Lionel, A. C. *et al.* Rare copy number variation discovery and cross-disorder comparisons identify risk genes for ADHD. *Sci Transl Med* **3**, 95ra75, doi:10.1126/scitranslmed.3002464 (2011).
- 13 Sanchez-Mora, C. *et al.* Case-control genome-wide association study of persistent attention-deficit hyperactivity disorder identifies FBXO33 as a novel susceptibility gene for the disorder. *Neuropsychopharmacology* **40**, 915-926, doi:10.1038/npp.2014.267 (2015).
- 14 Yang, L. *et al.* Polygenic transmission and complex neuro developmental network for attention deficit hyperactivity disorder: genome-wide association study of both common and rare variants. *Am J Med Genet B Neuropsychiatr Genet* **162B**, 419-430, doi:10.1002/ajmg.b.32169 (2013).
- 15 Zayats, T. *et al.* Genome-wide analysis of attention deficit hyperactivity disorder in Norway. *PLoS One* **10**, e0122501, doi:10.1371/journal.pone.0122501 (2015).

- 16 Stergiakouli, E. *et al.* Investigating the contribution of common genetic variants to the risk and pathogenesis of ADHD. *Am J Psychiatry* **169**, 186-194, doi:10.1176/appi.ajp.2011.11040551 (2012).
- 17 Hinney, A. *et al.* Genome-wide association study in German patients with attention deficit/hyperactivity disorder. *Am J Med Genet B Neuropsychiatr Genet* **156B**, 888-897, doi:10.1002/ajmg.b.31246 (2011).
- 18 Neale, B. M. *et al.* Case-control genome-wide association study of attention-deficit/hyperactivity disorder. *J Am Acad Child Adolesc Psychiatry* **49**, 906-920, doi:10.1016/j.jaac.2010.06.007 (2010).
- 19 Bakker, S. C. *et al.* A whole-genome scan in 164 Dutch sib pairs with attention-deficit/hyperactivity disorder: suggestive evidence for linkage on chromosomes 7p and 15q. *Am J Hum Genet* **72**, 1251-1260 (2003).
- 20 Myocardial Infarction Genetics Consortium *et al.* Genome-wide association of early-onset myocardial infarction with single nucleotide polymorphisms and copy number variants. *Nat Genet* **41**, 334-341, doi:10.1038/ng.327 (2009).
- 21 Gelernter, J. *et al.* Genome-wide association study of alcohol dependence: significant findings in African- and European-Americans including novel risk loci. *Molecular psychiatry* **19**, 41-49, doi:10.1038/mp.2013.145 (2014).
- 22 Gelernter, J. *et al.* Genome-wide association study of opioid dependence: multiple associations mapped to calcium and potassium pathways. *Biol Psychiatry* **76**, 66-74, doi:10.1016/j.biopsych.2013.08.034 (2014).
- 23 Gelernter, J. *et al.* Genome-wide association study of cocaine dependence and related traits: FAM53B identified as a risk gene. *Molecular psychiatry* **19**, 717-723, doi:10.1038/mp.2013.99 (2014).
- 24 Gudbjartsson, D. F. *et al.* Large-scale whole-genome sequencing of the Icelandic population. *Nat Genet* **47**, 435-444, doi:10.1038/ng.3247 (2015).
- 25 Pappa, I. *et al.* A genome-wide approach to children's aggressive behavior: The EAGLE consortium. *Am J Med Genet B Neuropsychiatr Genet*, doi:10.1002/ajmg.b.32333 (2015).
- 26 Paternoster, L. *et al.* Meta-analysis of genome-wide association studies identifies three new risk loci for atopic dermatitis. *Nat Genet* **44**, 187-192, doi:10.1038/ng.1017 (2011).
- 27 van der Valk, R. J. *et al.* A novel common variant in DCST2 is associated with length in early life and height in adulthood. *Hum Mol Genet* **24**, 1155-1168, doi:10.1093/hmg/ddu510 (2015).
- 28 Middeldorp, C. M. *et al.* A Genome-Wide Association Meta-Analysis of Attention-Deficit/Hyperactivity Disorder Symptoms in Population-Based Pediatric Cohorts. *J Am Acad Child Adolesc Psychiatry* **55**, 896-905 e896, doi:10.1016/j.jaac.2016.05.025 (2016).
- 29 The 1000 Genomes Project Consortium. An integrated map of genetic variation from 1,092 human genomes. *Nature* **491**, 56-65, doi:10.1038/nature11632 (2012).
- 30 Willer, C. J., Li, Y. & Abecasis, G. R. METAL: fast and efficient meta-analysis of genomewide association scans. *Bioinformatics* **26**, 2190-2191, doi:10.1093/bioinformatics/btq340 (2010).
- 31 Wright, M. J. & Martin, N. G. Brisbane Adolescent Twin Study: Outline of study methods and research projects. *Australian Journal of Psychology* **56**, 65-78, doi:10.1080/00049530410001734865 (2004).

- 32 Swanson, J. M. *et al.* Categorical and Dimensional Definitions and Evaluations of Symptoms of ADHD: History of the SNAP and the SWAN Rating Scales. *Int J Educ Psychol Assess* **10**, 51-70 (2012).
- 33 Das, S. *et al.* Next-generation genotype imputation service and methods. *Nat Genet* **48**, 1284-1287, doi:10.1038/ng.3656 (2016).
- 34 Ebejer, J. L. *et al.* Genome-wide association study of inattention and hyperactivity-impulsivity measured as quantitative traits. *Twin Res Hum Genet* **16**, 560-574, doi:10.1017/thg.2013.12 (2013).
- 35 Schizophrenia Working Group of the Psychiatric Genomics Consortium. Biological insights from 108 schizophrenia-associated genetic loci. *Nature* **511**, 421-427, doi:10.1038/nature13595 (2014).
- 36 Delaneau, O., Marchini, J. & Zagury, J. F. A linear complexity phasing method for thousands of genomes. *Nat Methods* **9**, 179-181, doi:10.1038/nmeth.1785 (2011).
- 37 Howie, B., Marchini, J. & Stephens, M. Genotype imputation with thousands of genomes. *G3* **1**, 457-470, doi:10.1534/g3.111.001198 (2011).
- 38 Sudmant, P. H. *et al.* An integrated map of structural variation in 2,504 human genomes. *Nature* **526**, 75-81, doi:10.1038/nature15394 (2015).
- 39 The 1000 Genomes Project Consortium. A global reference for human genetic variation. *Nature* **526**, 68-74, doi:10.1038/nature15393 (2015).
- 40 Price, A. L. *et al.* Long-range LD can confound genome scans in admixed populations. *Am J Hum Genet* **83**, 132-135; author reply 135-139, doi:10.1016/j.ajhg.2008.06.005 (2008).
- 41 Purcell, S. *et al.* PLINK: a tool set for whole-genome association and population-based linkage analyses. *Am J Hum Genet* **81**, 559-575, doi:10.1086/519795 (2007).
- 42 Chang, C. C. *et al.* Second-generation PLINK: rising to the challenge of larger and richer datasets. *Gigascience* **4**, 7, doi:10.1186/s13742-015-0047-8 (2015).
- 43 Price, A. L. *et al.* Principal components analysis corrects for stratification in genome-wide association studies. *Nat Genet* **38**, 904-909, doi:10.1038/ng1847 (2006).
- 44 Winkler, T. W. *et al.* Quality control and conduct of genome-wide association meta-analyses. *Nat. Protocols* **9**, 1192-1212, doi:10.1038/nprot.2014.071 (2014).
- 45 Bulik-Sullivan, B. K. *et al.* LD Score regression distinguishes confounding from polygenicity in genome-wide association studies. *Nat Genet* **47**, 291-295, doi:10.1038/ng.3211 (2015).
- 46 de Leeuw, C. A., Mooij, J. M., Heskes, T. & Posthuma, D. MAGMA: generalized gene-set analysis of GWAS data. *PLoS Comput Biol* **11**, e1004219, doi:10.1371/journal.pcbi.1004219 (2015).
- 47 Wellcome Trust Case Control Consortium *et al.* Bayesian refinement of association signals for 14 loci in 3 common diseases. *Nat Genet* **44**, 1294-1301, doi:10.1038/ng.2435 (2012).
- 48 Gormley, P. *et al.* Meta-analysis of 375,000 individuals identifies 38 susceptibility loci for migraine. *Nat Genet* **48**, 856-866, doi:10.1038/ng.3598 (2016).
- 49 McLaren, W. *et al.* The Ensembl Variant Effect Predictor. *Genome Biol* **17**, 122, doi:10.1186/s13059-016-0974-4 (2016).
- 50 Harrow, J. *et al.* GENCODE: the reference human genome annotation for The ENCODE Project. *Genome Res* **22**, 1760-1774, doi:10.1101/gr.135350.111 (2012).
- 51 Won, H. *et al.* Chromosome conformation elucidates regulatory relationships in developing human brain. *Nature* **538**, 523-527, doi:10.1038/nature19847 (2016).

- 52 GTEx Consortium. The Genotype-Tissue Expression (GTEx) pilot analysis: multitissue gene regulation in humans. *Science* **348**, 648-660, doi:10.1126/science.1262110 (2015).
- 53 Zhernakova, D. V. *et al.* Identification of context-dependent expression quantitative trait loci in whole blood. *Nat Genet* **49**, 139-145, doi:10.1038/ng.3737 (2017).
- 54 Roadmap Epigenomics Consortium *et al.* Integrative analysis of 111 reference human epigenomes. *Nature* **518**, 317-330, doi:10.1038/nature14248 (2015).
- 55 Kircher, M. *et al.* A general framework for estimating the relative pathogenicity of human genetic variants. *Nat Genet* **46**, 310-315, doi:10.1038/ng.2892 (2014).
- 56 Hou, C. A simple approximation for the distribution of the weighted combination of non-independent or independent probabilities. *Statistics and Probability Letters* **73**, 179-187 (2005).
- 57 Farrell, M. S. *et al.* Evaluating historical candidate genes for schizophrenia. *Molecular psychiatry* **20**, 555-562, doi:10.1038/mp.2015.16 (2015).
- 58 Hawi, Z. *et al.* The molecular genetic architecture of attention deficit hyperactivity disorder. *Molecular psychiatry* **20**, 289-297, doi:10.1038/mp.2014.183 (2015).
- 59 Day, F. R. *et al.* Large-scale genomic analyses link reproductive aging to hypothalamic signaling, breast cancer susceptibility and BRCA1-mediated DNA repair. *Nat Genet* **47**, 1294-1303, doi:10.1038/ng.3412 (2015).
- 60 Subramanian, A. *et al.* Gene set enrichment analysis: a knowledge-based approach for interpreting genome-wide expression profiles. *Proc Natl Acad Sci U S A* **102**, 15545-15550, doi:10.1073/pnas.0506580102 (2005).
- 61 Vernes, S. C. *et al.* Foxp2 regulates gene networks implicated in neurite outgrowth in the developing brain. *PLoS Genet* **7**, e1002145, doi:10.1371/journal.pgen.1002145 (2011).
- 62 Spiteri, E. *et al.* Identification of the transcriptional targets of FOXP2, a gene linked to speech and language, in developing human brain. *Am J Hum Genet* **81**, 1144-1157, doi:10.1086/522237 (2007).
- 63 Lek, M. *et al.* Analysis of protein-coding genetic variation in 60,706 humans. *Nature* **536**, 285-291, doi:10.1038/nature19057 (2016).
- 64 Cross-Disorder Group of the Psychiatric Genomics Consortium *et al.* Genetic relationship between five psychiatric disorders estimated from genome-wide SNPs. *Nat Genet* **45**, 984-994, doi:10.1038/ng.2711 (2013).
- 65 Yang, J., Lee, S. H., Goddard, M. E. & Visscher, P. M. GCTA: a tool for genome-wide complex trait analysis. *Am J Hum Genet* **88**, 76-82, doi:10.1016/j.ajhg.2010.11.011 (2011).
- 66 Purcell, S. M. *et al.* Common polygenic variation contributes to risk of schizophrenia and bipolar disorder. *Nature* **460**, 748-752, doi:10.1038/nature08185 (2009).
- 67 Sherva, R. *et al.* Genome-wide Association Study of Cannabis Dependence Severity, Novel Risk Variants, and Shared Genetic Risks. *JAMA Psychiatry* **73**, 472-480, doi:10.1001/jamapsychiatry.2016.0036 (2016).
- 68 Polanczyk, G., de Lima, M. S., Horta, B. L., Biederman, J. & Rohde, L. A. The worldwide prevalence of ADHD: a systematic review and metaregression analysis. *Am J Psychiatry* **164**, 942-948, doi:10.1176/ajp.2007.164.6.942 (2007).
- 69 Finucane, H. K. *et al.* Partitioning heritability by functional annotation using genome-wide association summary statistics. *Nat Genet* **47**, 1228-1235, doi:10.1038/ng.3404 (2015).

- 70 Finucane, H. K. *et al.* Partitioning heritability by functional annotation using genome-wide association summary statistics. *Nat Genet* **47**, 1228-1235 (2015).
- 71 Trynka, G. *et al.* Chromatin marks identify critical cell types for fine mapping complex trait variants. *Nat Genet* **45**, 124-130, doi:10.1038/ng.2504 (2013).
- 72 Kundaje, A. *et al.* Integrative analysis of 111 reference human epigenomes. *Nature* **518**, 317-330 (2015).
- 73 Ernst, J. & Kellis, M. Large-scale imputation of epigenomic datasets for systematic annotation of diverse human tissues. *Nature biotechnology* **33**, 364-376 (2015).
- 74 Bulik-Sullivan, B. *et al.* An atlas of genetic correlations across human diseases and traits. *Nat Genet* **47**, 1236-1241, doi:10.1038/ng.3406 (2015).
- 75 Sniekers, S. *et al.* Genome-wide association meta-analysis of 78,308 individuals identifies new loci and genes influencing human intelligence. *Nat Genet* **49**, 1107-1112, doi:10.1038/ng.3869 (2017).
- 76 Davies, G. *et al.* Genome-wide association study of cognitive functions and educational attainment in UK Biobank (N=112 151). *Molecular psychiatry* **21**, 758-767, doi:10.1038/mp.2016.45 (2016).
- 77 Hammerschlag, A. R. *et al.* Genome-wide association analysis of insomnia complaints identifies risk genes and genetic overlap with psychiatric and metabolic traits. *Nat Genet* **49**, 1584-1592, doi:10.1038/ng.3888 (2017).
- 78 Duncan, L. *et al.* Significant Locus and Metabolic Genetic Correlations Revealed in Genome-Wide Association Study of Anorexia Nervosa. *Am J Psychiatry* **174**, 850-858, doi:10.1176/appi.ajp.2017.16121402 (2017).
- 79 Wray, N. R. *et al.* Genome-wide association analyses identify 44 risk variants and refine the genetic architecture of major depression. *Nat Genet* **50**, 668-681, doi:10.1101/167577 (2018).
- 80 Yates, F. Contingency Tables Involving Small Numbers and the χ^2 Test. *Supplement to the Journal of the Royal Statistical Society* **1**, 217-235, doi:10.2307/2983604 (1934).
- 81 R Core Team. *R: A language and environment for statistical computing.* , <<http://www.R-project.org/>> (2014).
- 82 Okbay, A. *et al.* Genome-wide association study identifies 74 loci associated with educational attainment. *Nature* **533**, 539-542, doi:10.1038/nature17671 (2016).
- 83 Pearson K., L. A. On the inheritance of characters not capable of exact quantitative measurement. *Philosophical Transactions of the Royal Society of London Series A*, 79-150 (1901).
- 84 Cohen, J. The cost of dichotomization. *Applied Psychological Measurement* **7**, 249-253, doi:10.1177/014662168300700301 (1983).
- 85 Hunter, J. & Schmidt, F. Dichotomization of continuous variables: The implications for meta-analysis. *Journal of Applied Psychology* **75**, 334-349, doi:10.1037/0021-9010.75.3.334 (1990).
- 86 Hsieh, F. Y., Bloch, D. A. & Larsen, M. D. A simple method of sample size calculation for linear and logistic regression. *Stat Med* **17**, 1623-1634 (1998).
- 87 Lee, S. H., Wray, N. R., Goddard, M. E. & Visscher, P. M. Estimating missing heritability for disease from genome-wide association studies. *Am J Hum Genet* **88**, 294-305, doi:10.1016/j.ajhg.2011.02.002 (2011).
- 88 Yang, J. *et al.* Common SNPs explain a large proportion of the heritability for human height. *Nat Genet* **42**, 565-569, doi:10.1038/ng.608 (2010).

- 89 Stouffer, S., DeVinney, L. & Suchmen, E. *The American soldier: Adjustment during army life.*, Vol. 1 (Princeton University Press, 1949).
- 90 Faraone, S. V. *et al.* Attention-deficit/hyperactivity disorder. *Nature Reviews Disease Primers*, 15020, doi:10.1038/nrdp.2015.20 (2015).
- 91 Ribases, M. *et al.* Exploration of 19 serotonergic candidate genes in adults and children with attention-deficit/hyperactivity disorder identifies association for 5HT2A, DDC and MAOB. *Molecular psychiatry* **14**, 71-85, doi:10.1038/sj.mp.4002100 (2009).
- 92 Benyamin, B. *et al.* Childhood intelligence is heritable, highly polygenic and associated with FBNP1L. *Molecular psychiatry* **19**, 253-258, doi:10.1038/mp.2012.184 (2014).
- 93 Rietveld, C. A. *et al.* GWAS of 126,559 individuals identifies genetic variants associated with educational attainment. *Science* **340**, 1467-1471, doi:10.1126/science.1235488 (2013).
- 94 Okbay, A. *et al.* Genetic variants associated with subjective well-being, depressive symptoms, and neuroticism identified through genome-wide analyses. *Nat Genet* **48**, 624-633, doi:10.1038/ng.3552 (2016).
- 95 Cross-Disorder Group of the Psychiatric Genomics Consortium. Identification of risk loci with shared effects on five major psychiatric disorders: a genome-wide analysis. *Lancet* **381**, 1371-1379, doi:10.1016/S0140-6736(12)62129-1 (2013).
- 96 Speliotes, E. K. *et al.* Association analyses of 249,796 individuals reveal 18 new loci associated with body mass index. *Nat Genet* **42**, 937-948, doi:10.1038/ng.686 (2010).
- 97 Berndt, S. I. *et al.* Genome-wide meta-analysis identifies 11 new loci for anthropometric traits and provides insights into genetic architecture. *Nat Genet* **45**, 501-512, doi:10.1038/ng.2606 (2013).
- 98 Shungin, D. *et al.* New genetic loci link adipose and insulin biology to body fat distribution. *Nature* **518**, 187-196, doi:10.1038/nature14132 (2015).
- 99 Bradfield, J. P. *et al.* A genome-wide association meta-analysis identifies new childhood obesity loci. *Nat Genet* **44**, 526-531, doi:10.1038/ng.2247 (2012).
- 100 Morris, A. P. *et al.* Large-scale association analysis provides insights into the genetic architecture and pathophysiology of type 2 diabetes. *Nat Genet* **44**, 981-990, doi:10.1038/ng.2383 (2012).
- 101 Teslovich, T. M. *et al.* Biological, clinical and population relevance of 95 loci for blood lipids. *Nature* **466**, 707-713, doi:10.1038/nature09270 (2010).
- 102 The Tobacco and Genetics Consortium. Genome-wide meta-analyses identify multiple loci associated with smoking behavior. *Nat Genet* **42**, 441-447, doi:10.1038/ng.571 (2010).
- 103 Patel, Y. M. *et al.* Novel Association of Genetic Markers Affecting CYP2A6 Activity and Lung Cancer Risk. *Cancer Res* **76**, 5768-5776, doi:10.1158/0008-5472.CAN-16-0446 (2016).
- 104 Wang, Y. *et al.* Rare variants of large effect in BRCA2 and CHEK2 affect risk of lung cancer. *Nat Genet* **46**, 736-741, doi:10.1038/ng.3002 (2014).
- 105 Barban, N. *et al.* Genome-wide analysis identifies 12 loci influencing human reproductive behavior. *Nat Genet* **48**, 1462-1472, doi:10.1038/ng.3698 (2016).
- 106 Pilling, L. C. *et al.* Human longevity is influenced by many genetic variants: evidence from 75,000 UK Biobank participants. *Aging (Albany NY)* **8**, 547-560, doi:10.18632/aging.100930 (2016).
- 107 Okada, Y. *et al.* Genetics of rheumatoid arthritis contributes to biology and drug discovery. *Nature* **506**, 376-381, doi:10.1038/nature12873 (2014).

- 108 Wang, B. Molecular mechanism underlying sialic acid as an essential nutrient for brain development and cognition. *Adv Nutr* **3**, 465S-472S, doi:10.3945/an.112.001875 (2012).
- 109 Yoo, S. W. *et al.* Sialylation regulates brain structure and function. *FASEB J* **29**, 3040-3053, doi:10.1096/fj.15-270983 (2015).
- 110 Hu, H. *et al.* ST3GAL3 mutations impair the development of higher cognitive functions. *Am J Hum Genet* **89**, 407-414, doi:10.1016/j.ajhg.2011.08.008 (2011).
- 111 Sturgill, E. R. *et al.* Biosynthesis of the major brain gangliosides GD1a and GT1b. *Glycobiology* **22**, 1289-1301, doi:10.1093/glycob/cws103 (2012).
- 112 Ledeen, R. W. & Wu, G. Ganglioside function in calcium homeostasis and signaling. *Neurochem Res* **27**, 637-647 (2002).
- 113 Wu, G., Xie, X., Lu, Z. H. & Ledeen, R. W. Cerebellar neurons lacking complex gangliosides degenerate in the presence of depolarizing levels of potassium. *Proc Natl Acad Sci U S A* **98**, 307-312, doi:10.1073/pnas.011523698 (2001).
- 114 Edvardson, S. *et al.* West syndrome caused by ST3Gal-III deficiency. *Epilepsia* **54**, e24-27, doi:10.1111/epi.12050 (2013).
- 115 Walton, E. *et al.* Epigenetic profiling of ADHD symptoms trajectories: a prospective, methylome-wide study. *Molecular psychiatry*, doi:10.1038/mp.2016.85 (2016).
- 116 Woo, J. *et al.* Trans-synaptic adhesion between NGL-3 and LAR regulates the formation of excitatory synapses. *Nat Neurosci* **12**, 428-437, doi:10.1038/nn.2279 (2009).
- 117 Yang, T., Massa, S. M. & Longo, F. M. LAR protein tyrosine phosphatase receptor associates with TrkB and modulates neurotrophic signaling pathways. *J Neurobiol* **66**, 1420-1436, doi:10.1002/neu.20291 (2006).
- 118 Zabolotny, J. M. *et al.* Overexpression of the LAR (leukocyte antigen-related) protein-tyrosine phosphatase in muscle causes insulin resistance. *Proc Natl Acad Sci U S A* **98**, 5187-5192, doi:10.1073/pnas.071050398 (2001).
- 119 Zhang, Z. *et al.* A heterozygous mutation disrupting the SPAG16 gene results in biochemical instability of central apparatus components of the human sperm axoneme. *Biol Reprod* **77**, 864-871, doi:10.1095/biolreprod.107.063206 (2007).
- 120 Zhang, Z. *et al.* A sperm-associated WD repeat protein orthologous to Chlamydomonas PF20 associates with Spag6, the mammalian orthologue of Chlamydomonas PF16. *Mol Cell Biol* **22**, 7993-8004 (2002).
- 121 Somers, V. *et al.* Autoantibody profiling in multiple sclerosis reveals novel antigenic candidates. *J Immunol* **180**, 3957-3963 (2008).
- 122 de Bock, L. *et al.* Anti-SPAG16 antibodies in primary progressive multiple sclerosis are associated with an elevated progression index. *Eur J Neurol* **23**, 722-728, doi:10.1111/ene.12925 (2016).
- 123 Leung, L. C. *et al.* Coupling of NF-protocadherin signaling to axon guidance by cue-induced translation. *Nat Neurosci* **16**, 166-173, doi:10.1038/nn.3290 (2013).
- 124 Blevins, C. J., Emond, M. R., Biswas, S. & Jontes, J. D. Differential expression, alternative splicing, and adhesive properties of the zebrafish delta1-protocadherins. *Neuroscience* **199**, 523-534, doi:10.1016/j.neuroscience.2011.09.061 (2011).
- 125 Krishna, K. K., Hertel, N. & Redies, C. Cadherin expression in the somatosensory cortex: evidence for a combinatorial molecular code at the single-cell level. *Neuroscience* **175**, 37-48, doi:10.1016/j.neuroscience.2010.11.056 (2011).

- 126 Kim, S. Y., Chung, H. S., Sun, W. & Kim, H. Spatiotemporal expression pattern of non-clustered protocadherin family members in the developing rat brain. *Neuroscience* **147**, 996-1021, doi:10.1016/j.neuroscience.2007.03.052 (2007).
- 127 International League Against Epilepsy Consortium on Complex Epilepsies. Genetic determinants of common epilepsies: a meta-analysis of genome-wide association studies. *Lancet Neurol* **13**, 893-903, doi:10.1016/S1474-4422(14)70171-1 (2014).
- 128 Miyake, K. *et al.* The protocadherins, PCDHB1 and PCDH7, are regulated by MeCP2 in neuronal cells and brain tissues: implication for pathogenesis of Rett syndrome. *BMC Neurosci* **12**, 81, doi:10.1186/1471-2202-12-81 (2011).
- 129 Oliver, P. L. *et al.* Disruption of Visc-2, a Brain-Expressed Conserved Long Noncoding RNA, Does Not Elicit an Overt Anatomical or Behavioral Phenotype. *Cereb Cortex* **25**, 3572-3585, doi:10.1093/cercor/bhu196 (2015).
- 130 Janson, C. G., Chen, Y., Li, Y. & Leifer, D. Functional regulatory regions of human transcription factor MEF2C. *Brain Res Mol Brain Res* **97**, 70-82 (2001).
- 131 Harrington, A. J. *et al.* MEF2C regulates cortical inhibitory and excitatory synapses and behaviors relevant to neurodevelopmental disorders. *Elife* **5**, doi:10.7554/eLife.20059 (2016).
- 132 Adachi, M., Lin, P. Y., Pranav, H. & Monteggia, L. M. Postnatal Loss of Mef2c Results in Dissociation of Effects on Synapse Number and Learning and Memory. *Biol Psychiatry* **80**, 140-148, doi:10.1016/j.biopsych.2015.09.018 (2016).
- 133 Li, H. *et al.* Transcription factor MEF2C influences neural stem/progenitor cell differentiation and maturation in vivo. *Proc Natl Acad Sci U S A* **105**, 9397-9402, doi:10.1073/pnas.0802876105 (2008).
- 134 Barbosa, A. C. *et al.* MEF2C, a transcription factor that facilitates learning and memory by negative regulation of synapse numbers and function. *Proc Natl Acad Sci U S A* **105**, 9391-9396, doi:10.1073/pnas.0802679105 (2008).
- 135 Lambert, J. C. *et al.* Meta-analysis of 74,046 individuals identifies 11 new susceptibility loci for Alzheimer's disease. *Nat Genet* **45**, 1452-1458, doi:10.1038/ng.2802 (2013).
- 136 Hyde, C. L. *et al.* Identification of 15 genetic loci associated with risk of major depression in individuals of European descent. *Nat Genet* **48**, 1031-1036, doi:10.1038/ng.3623 (2016).
- 137 Novara, F. *et al.* Refining the phenotype associated with MEF2C haploinsufficiency. *Clin Genet* **78**, 471-477, doi:10.1111/j.1399-0004.2010.01413.x (2010).
- 138 Mikhail, F. M. *et al.* Clinically relevant single gene or intragenic deletions encompassing critical neurodevelopmental genes in patients with developmental delay, mental retardation, and/or autism spectrum disorders. *Am J Med Genet A* **155A**, 2386-2396, doi:10.1002/ajmg.a.34177 (2011).
- 139 Sia, G. M., Clem, R. L. & Hagan, R. L. The human language-associated gene SRPX2 regulates synapse formation and vocalization in mice. *Science* **342**, 987-991, doi:10.1126/science.1245079 (2013).
- 140 Tsui, D., Vessey, J. P., Tomita, H., Kaplan, D. R. & Miller, F. D. FoxP2 regulates neurogenesis during embryonic cortical development. *J Neurosci* **33**, 244-258, doi:10.1523/JNEUROSCI.1665-12.2013 (2013).
- 141 Schreiwies, C. *et al.* Humanized Foxp2 accelerates learning by enhancing transitions from declarative to procedural performance. *Proc Natl Acad Sci U S A* **111**, 14253-14258, doi:10.1073/pnas.1414542111 (2014).

- 142 Vernes, S. C. *et al.* A functional genetic link between distinct developmental language disorders. *N Engl J Med* **359**, 2337-2345, doi:10.1056/NEJMoa0802828 (2008).
- 143 Lai, C. S., Gerrelli, D., Monaco, A. P., Fisher, S. E. & Copp, A. J. FOXP2 expression during brain development coincides with adult sites of pathology in a severe speech and language disorder. *Brain* **126**, 2455-2462, doi:10.1093/brain/awg247 (2003).
- 144 Wilcke, A. *et al.* Imaging genetics of FOXP2 in dyslexia. *Eur J Hum Genet* **20**, 224-229, doi:10.1038/ejhg.2011.160 (2012).
- 145 Lai, C. S., Fisher, S. E., Hurst, J. A., Vargha-Khadem, F. & Monaco, A. P. A forkhead-domain gene is mutated in a severe speech and language disorder. *Nature* **413**, 519-523, doi:10.1038/35097076 (2001).
- 146 Ribases, M. *et al.* An association study of sequence variants in the forkhead box P2 (FOXP2) gene and adulthood attention-deficit/hyperactivity disorder in two European samples. *Psychiatr Genet* **22**, 155-160, doi:10.1097/YPG.0b013e328353957e (2012).
- 147 Willnow, T. E., Petersen, C. M. & Nykjaer, A. VPS10P-domain receptors - regulators of neuronal viability and function. *Nature reviews. Neuroscience* **9**, 899-909, doi:10.1038/nrn2516 (2008).
- 148 Hermey, G. *et al.* The three sorCS genes are differentially expressed and regulated by synaptic activity. *J Neurochem* **88**, 1470-1476 (2004).
- 149 Breiderhoff, T. *et al.* Sortilin-related receptor SORCS3 is a postsynaptic modulator of synaptic depression and fear extinction. *PLoS One* **8**, e75006, doi:10.1371/journal.pone.0075006 (2013).
- 150 Oetjen, S., Mahlke, C., Hermans-Borgmeyer, I. & Hermey, G. Spatiotemporal expression analysis of the growth factor receptor SorCS3. *J Comp Neurol* **522**, 3386-3402, doi:10.1002/cne.23606 (2014).
- 151 Reitz, C. *et al.* Independent and epistatic effects of variants in VPS10-d receptors on Alzheimer disease risk and processing of the amyloid precursor protein (APP). *Transl Psychiatry* **3**, e256, doi:10.1038/tp.2013.13 (2013).
- 152 Muda, M. *et al.* MKP-3, a novel cytosolic protein-tyrosine phosphatase that exemplifies a new class of mitogen-activated protein kinase phosphatase. *J Biol Chem* **271**, 4319-4326 (1996).
- 153 Caunt, C. J. & Keyse, S. M. Dual-specificity MAP kinase phosphatases (MKPs): shaping the outcome of MAP kinase signalling. *FEBS J* **280**, 489-504, doi:10.1111/j.1742-4658.2012.08716.x (2013).
- 154 Owens, D. M. & Keyse, S. M. Differential regulation of MAP kinase signalling by dual-specificity protein phosphatases. *Oncogene* **26**, 3203-3213, doi:10.1038/sj.onc.1210412 (2007).
- 155 Stewart, A. E., Dowd, S., Keyse, S. M. & McDonald, N. Q. Crystal structure of the MAPK phosphatase Pyst1 catalytic domain and implications for regulated activation. *Nat Struct Biol* **6**, 174-181, doi:10.1038/5861 (1999).
- 156 Bermudez, O., Pages, G. & Gimond, C. The dual-specificity MAP kinase phosphatases: critical roles in development and cancer. *Am J Physiol Cell Physiol* **299**, C189-202, doi:10.1152/ajpcell.00347.2009 (2010).
- 157 Dickinson, R. J., Eblaghie, M. C., Keyse, S. M. & Morriss-Kay, G. M. Expression of the ERK-specific MAP kinase phosphatase PYST1/MKP3 in mouse embryos during morphogenesis and early organogenesis. *Mech Dev* **113**, 193-196 (2002).

- 158 Li, C., Scott, D. A., Hatch, E., Tian, X. & Mansour, S. L. Dusp6 (Mkp3) is a negative feedback regulator of FGF-stimulated ERK signaling during mouse development. *Development* **134**, 167-176, doi:10.1242/dev.02701 (2007).
- 159 Mortensen, O. V. MKP3 eliminates depolarization-dependent neurotransmitter release through downregulation of L-type calcium channel Cav1.2 expression. *Cell Calcium* **53**, 224-230, doi:10.1016/j.ceca.2012.12.004 (2013).
- 160 Mortensen, O. V., Larsen, M. B., Prasad, B. M. & Amara, S. G. Genetic complementation screen identifies a mitogen-activated protein kinase phosphatase, MKP3, as a regulator of dopamine transporter trafficking. *Mol Biol Cell* **19**, 2818-2829, doi:10.1091/mbc.E07-09-0980 (2008).
- 161 Takaki, M. *et al.* Two kinds of mitogen-activated protein kinase phosphatases, MKP-1 and MKP-3, are differentially activated by acute and chronic methamphetamine treatment in the rat brain. *J Neurochem* **79**, 679-688 (2001).
- 162 Miraoui, H. *et al.* Mutations in FGF17, IL17RD, DUSP6, SPRY4, and FLRT3 are identified in individuals with congenital hypogonadotropic hypogonadism. *Am J Hum Genet* **92**, 725-743, doi:10.1016/j.ajhg.2013.04.008 (2013).
- 163 Luo, Y. *et al.* Differential expression of FOXA1, DUSP6, and HA117 in colon segments of Hirschsprung's disease. *Int J Clin Exp Pathol* **8**, 3979-3986 (2015).
- 164 Banzhaf-Strathmann, J. *et al.* MicroRNA-125b induces tau hyperphosphorylation and cognitive deficits in Alzheimer's disease. *EMBO J* **33**, 1667-1680, doi:10.15252/emj.201387576 (2014).
- 165 Keyse, S. M. Dual-specificity MAP kinase phosphatases (MKPs) and cancer. *Cancer Metastasis Rev* **27**, 253-261, doi:10.1007/s10555-008-9123-1 (2008).
- 166 Kidger, A. M. & Keyse, S. M. The regulation of oncogenic Ras/ERK signalling by dual-specificity mitogen activated protein kinase phosphatases (MKPs). *Semin Cell Dev Biol* **50**, 125-132, doi:10.1016/j.semcdb.2016.01.009 (2016).
- 167 Qu, X. *et al.* Identification, characterization, and functional study of the two novel human members of the semaphorin gene family. *J Biol Chem* **277**, 35574-35585, doi:10.1074/jbc.M206451200 (2002).
- 168 Yoshida, Y., Han, B., Mendelsohn, M. & Jessell, T. M. PlexinA1 signaling directs the segregation of proprioceptive sensory axons in the developing spinal cord. *Neuron* **52**, 775-788, doi:10.1016/j.neuron.2006.10.032 (2006).
- 169 Toyofuku, T. *et al.* Dual roles of Sema6D in cardiac morphogenesis through region-specific association of its receptor, Plexin-A1, with off-track and vascular endothelial growth factor receptor type 2. *Genes Dev* **18**, 435-447, doi:10.1101/gad.1167304 (2004).
- 170 Toyofuku, T. *et al.* Guidance of myocardial patterning in cardiac development by Sema6D reverse signalling. *Nat Cell Biol* **6**, 1204-1211, doi:10.1038/ncb1193 (2004).

Supplementary Note

Additional acknowledgements

Philip Asherson is supported by a National Institute of Health Research Senior Investigator Award (NF-SI-0616-10040), and the Biomedical Research Centre for Mental Health

Dr. Kuntsi's research on ADHD is supported by the EC

(grants:643051 MiND, 667302 CoCA and 602805 Aggressotype); Action Medical Research (GN2080 and GN2315); 4 Medical Research Council and SGDP Centre PhD studentships; and by the ECNP Network ADHD Across the Lifespan.

Dr. Langley was funded by Wellcome Trust (grant: 079711)

Dr. Schachar received support from Bank Chair in Child Psychiatry, Canadian Institutes of Health Research (MOP-106573 and MOP – 93696).

Dr. Roussos was supported by the National Institutes of Health (R01AG050986 Roussos and R01MH109677), Brain Behavior Research Foundation (20540), Alzheimer's Association (NIRG-340998) and the Veterans Affairs (Merit grant BX002395).

Statistical analyses that were carried out on the Genetic Cluster Computer (<http://www.geneticcluster.org>) is hosted by SURFsara and financially supported by the Netherlands Scientific Organization (NWO 480-05-003) along with a supplement from the Dutch Brain Foundation and the VU University Amsterdam. The GRAS data collection was supported by the Max Planck Society, the Max-Planck-Förderstiftung, and the DFG Center for Nanoscale Microscopy & Molecular Physiology of the Brain (CNMPB), Göttingen, Germany.

The Yale-Penn site study was supported by National Institutes of Health Grants RC2 DA028909, R01 DA12690, R01 DA12849, R01 DA18432, R01 AA11330, and R01 AA017535 and the Veterans Affairs Connecticut and Philadelphia Veterans Affairs Mental Illness Research, Educational, and Clinical Centers.

Genotyping services for a part of our genome-wide association study were provided by the Center for Inherited Disease Research and Yale University (Center for Genome Analysis). Center for Inherited Disease Research is fully funded through a Federal contract from the National Institutes of Health to The Johns Hopkins University (contract number N01-HG-65403).

We gratefully acknowledge all the studies and databases that made GWAS summary data available:

ADIPOGen (Adiponectin genetics consortium), C4D (Coronary Artery Disease Genetics Consortium), CARDIoGRAM (Coronary ARtery DIsease Genome wide Replication and Meta-analysis), CKDGen (Chronic Kidney Disease Genetics consortium), dbGAP (database of Genotypes and Phenotypes), DIAGRAM (DIAbetes Genetics Replication And Meta-analysis), ENIGMA (Enhancing Neuro Imaging Genetics through Meta Analysis), EAGLE (EARly Genetics & Lifecourse Epidemiology Consortium, excluding 23andMe), EGG (Early Growth Genetics Consortium), GABRIEL (A Multidisciplinary Study to Identify the Genetic and Environmental Causes of Asthma in the European Community), GCAN (Genetic Consortium for Anorexia Nervosa), GEFOS (GENetic Factors for OSteoporosis Consortium), GIANT (Genetic Investigation of ANthropometric Traits), GIS (Genetics of Iron Status consortium), GLGC (Global Lipids Genetics Consortium), GPC (Genetics of Personality Consortium), GUGC (Global Urate and Gout consortium), HaemGen (haematological and platelet traits genetics consortium), HRgene (Heart Rate consortium), IIBDGC (International Inflammatory Bowel Disease Genetics Consortium), ILCCO (International Lung Cancer Consortium), IMSGC (International Multiple Sclerosis Genetic Consortium), MAGIC (Meta-Analyses of Glucose and Insulin-related traits Consortium), MESA (Multi-Ethnic Study of Atherosclerosis), PGC (Psychiatric Genomics Consortium), Project MinE consortium, ReproGen (Reproductive Genetics Consortium), SSGAC (Social Science Genetics Association Consortium) and TAG (Tobacco and Genetics Consortium), TRICL (Transdisciplinary Research in Cancer of the Lung consortium), UK Biobank.

We gratefully acknowledge the contributions of Alkes Price (the systemic lupus erythematosus GWAS and primary biliary cirrhosis GWAS) and Johannes Kettunen (lipids metabolites GWAS).

QIMR studies: We thank the participants for their time and commitment to the longitudinal study; Marlene Grace, Ann Eldridge and Natalie Garden for sample collection; Kerrie McAloney for study co-ordination; Harry Beeby, Daniel Park, and David Smyth for IT support, Grant Montgomery, Anjali Henders and the Molecular Genetics Laboratory for DNA sample preparation, and Scott Gordon for genotyping QC. Professor Jonna Kuntsi has given talks at educational events sponsored by Medice; all funds are received by King's College London and used for studies of ADHD. Dr. Dalsgaard is supported by grants from Aarhus University Research Foundation (AUFF-E-2015-FLS-8-61), National Institute of Health (R01, grant no ES026993), and Novo Nordisk Foundation (grant no 22018). Hyejung Won is supported by NIMH grant K99MH113823.